Title

Notch Mediated Arteriovenous Specification in the Brain Endothelium : Dysregulation in Arteriovenous Malformation

Permalink

https://escholarship.org/uc/item/4525m31v

Author

Murphy, Patrick Andries

Publication Date

2011

Peer reviewed|Thesis/dissertation

Notch Mediated Arteriovenous Specification in the Brain Endothelium :
Dysregulation in Arteriovenous Malformation

by

Patrick A. Murphy

DISSERTATION

Submitted in partial satisfaction of the requirements for the degree of

DOCTOR OF PHILOSOPHY

in

Biomedical Sciences

in the

GRADUATE DIVISION

of the

Dedication

To the memory of my father and to my mother.

Without their hard work and aspirations for their children,

I would never have dared to reach as much as I have.

Acknowledgements

I suspect that Rong's decision to allow me to graduate was influenced by her love of Giants baseball. She knew that immediately after I left Boston, the Red Sox won the World Series for the first time in 86 years. I think she had a sense that my departure might do the same for San Francisco. Indeed, after I left San Francisco, the Giants promptly won their first World Series in 56 years, their first in California after moving from New York. I just hope the other Red Sox fans don't hear about this, and boot me from Boston again.

First, many thanks to Dr. Rong Wang and my thesis committee mentors. I still vividly remember the first writing Rong and I worked on together, a proposal for my graduate course in cell biology. I was astonished by the amount of red ink that covered the pages. Her efforts were exhaustive, typical of her style as I have observed through my graduate career. Rong was always available to drill the key points in any argument, and she was willing to work tirelessly with me with great patience. Although I expected this level of dedication from my earliest days in the lab, I slowly began to appreciate what I would consider Rong's true defining quality during my later years in the lab. This is her desire to extract, by pure force of will, the true potential of her surroundings. This applies not only to each piece of data from the lab, but also each individual member of the lab. As I have observed, this is not an easy process. Taxing anything or anyone to their limit never is. Rong is acutely aware of this, and often mentions that superficial happiness and the pursuit

of excellence are typically at odds. But, as I look back over my graduate career, I am proud of what I have accomplished. Throughout this work, I appreciated the gentle prodding of Deepak Srivastava, Jeremy Reiter, and Tom Kornberg. I returned from these meetings grasping a few golden words of wisdom, which I embarrassingly recall, might sometimes have slipped through my fingers had not Jeremy benevolently deciphered them for me.

Second, none of this work would have been completed without the people who worked with me. Tyson Kim, who joined the lab near the middle of my graduate work, brought with him an exciting engineering perspective. I enjoyed the trips we took together to Biophotonics imaging conferences, and Chris Schaffer's lab at Cornell, during which time he introduced me to the key concepts and figures in the multi-photon imaging field. Tyson is the consummate engineer, seeking through knowledge and careful calculation to improve life. I hope to have learned to approximate, though I can never hope to replicate, the attention to detail and planning that Tyson exhibited in all aspects of life. I look forward to seeing the evolution of his unique perspective on biology. I have had the pleasure of mentoring Gloria Lu in her time in the lab. Exact and diligent, as Gloria has grown in scientific experience and expertise, she has become as confident in her scientific thought as I am in her. I have also enjoyed working with Claudia Tomas-Miranda and Steven Shiah, who have been instrumental in these studies. Finally, Andy Bollen and Chris Schaffer have served as important senior figures in my work. Andy Bollen, in all of my work, has provided a critical clinical perspective, enabling me to achieve to some

extent, my desire to study biology at the interface between the clinic and the lab.

Chris has been a key influence on my latest work, through both our direct

interactions, as well the indirect inheritance of many of imaging techniques and

systems by way of his disciple Tyson.

Third, I am grateful for the wonderful labmates and classmates I have had. In my

first years in the lab, I leaned heavily on Tim Carlson, Michael Lam, Xiaoqin Wu,

Yuankai Lin, Yung Hae Kim and Marie Lee, who showed me the ropes. I am indebted

to them for their kindness, and the solid scientific foundation they provided. Chen

He was always ready with some historical perspective, and exquisitely detailed

scientific insight. I was privileged to work with Shant Vartanian, who patiently

introduced me to animal surgery. Seth Bechis, Oliviera Marjanovic and Maria Costa

were exciting experimentalists to be around. In the most recent times, I have

enjoyed working with Tadayoshi Watanabe, Weiya Jiang, and Eric Jelin. Eric

brought his love of language and science to the table in any discussion, and was as

imaginative with his jokes and alternative sur-names as he was with his science.

Henrik Lindskog was more subtle with his pranks, a reflection of his character. His

machinations were no less intricate, but often appeared to be a natural evolution of

the situation, from which he humbly removed his own presence. A great friend,

Henrik always and "absolutely," puts others around him at ease, with wit as much as

whiskey. Finally, the rocks of the lab, Christin Munkittrick and Hui Hu. Christin at

the desk and Hui at the bench. I am sure that I owe many successful abstract

submissions to Christin's keen editing, and hope that the new lab members can

appease her insatiable quest for new animal protocols to submit. Although Hui has recently left the lab, for many years she performed amazing feats of strength, such as maintaining 200+ cages simultaneously, with a pace that made it appear as though everyone else was moving in slow motion. As I left the lab, Ruchika Srinivasan, Corinne Nielsen, and Henar Cuervo joined – and I will look forward to seeing their own spin on the evolving stories. Throughout the years, I have enjoyed great poker nights and bad beer with my classmates, as we suffered and succeeded together.

Finally, my wife has been magnificent in understanding and accommodating my ridiculous desire to do science. She put up with my hours and my experimental daydreaming. There was no time that I more enjoyed than walking up the stairs late, in the dark, into our home on 9th Avenue to see her standing there in the light with the smell of food wafting down (or, as often was the case, up from the Marnee Thai bag in my hand). The end of our time in San Francisco signals the beginning of a new time for us, now a family with baby Cathleen, and I look forward to wonderful years ahead among friends and family in Massachusetts. I got the adventure I aimed for, and have wonderful memories and friendships from our years in San Francisco and at UCSF.

Abstract

Arteriovenous malformations (AVMs) are dangerous vascular lesions of largely unknown etiology. Those that occur in the brain (BAVMs) are particularly devastating, since they often lead to hemorrhagic stroke. Current treatment strategies are limited and may be as risky as the disease itself. At their core, AVMs are an aberration of normal vascular hierarchy caused by enlarged direct connections between the artery and the vein, which shunt blood past the capillary bed. Influenced by the discovery of a Notch-regulated program of arteriovenous (AV) specification, I hypothesized that disruption of this program could cause BAVM. My thesis work identifies increased endothelial Notch signaling as a candidate lesion in brain AVMs by showing that it is sufficient to cause BAVM-like abnormalities in a mouse model, and that it is upregulated in human BAVM tissue samples. Furthermore, it demonstrates that a sustained increase in Notch signaling is required to maintain the BAVMs in our mouse model, since high-flow AVMs rapidly regress to capillaries once Notch transgene is turned off. This work will be presented as three chapters, the first two of which have been published (PMID: 18667694 and PMID: 19546852), and the third of which is submitted for publication.

Table of contents

Introduction

Arteriovenous Malformations (AVMs) are dangerous vascular lesions of unknown etiology

Human AVMs are described as fast-flow lesions consisting of an abnormal tangle of vessels. The core defect is enlarged connections between the artery and vein which allow arteirovenous (AV) shunting of blood flow past the capillaries.(1) As a result, two threatening vascular conditions arise. First, the shunt "steals" blood from perfusing capillaries, causing local tissue ischemia. Second, the rapid AV shunting of blood exposes the abnormal shunts to extreme hemodynamic forces, often resulting in their hemorrhagic rupture. While AVMs can occur in any tissue, those that occur in the brain are particularly devastating. Brain AVMs (BAVM) contribute to half of the hemorrhagic stroke in children, and about 2% of all stroke.(2) Risk of hemorrhage from BAVM is high, and most AVMs will hemorrhage over the course of a lifetime.(3) To prevent this, BAVMs are generally pre-emptively treated by surgical excision, embolization, radiation or some combination thereof. Treatment of rupture-prone BAVMs within the vulnerable brain parenchyma also has associated risks, which are substantial enough to warrant a clinical trial to determine whether treatment results in better outcomes than the natural course of the disease.(4)

Unfortunately the etiology of human BAVMs remains obscure, preventing rational design of molecular therapy. Theories on AVM formation have been based primarily on skin AVMs, which are most accessible, and can be observed at an early

stage of formation.(5) Small telangectasias in the skin are first visible at a much

smaller size, and presumably earlier stage, than those in internal organs. This is

particularly true since the angiograms that detect internal AVMs are generally

performed only when the AVM has grown large enough to disrupt organ function.

Careful histological analysis of skin AVMs at different timepoints has suggested that

the dilation of the post-capillary venule is the first defect in AVM formation.(5)

However, in contrast to the development of skin telangectasias, which often increase

with age, many of the AVMs in internal organs are believed to be congenital.(3) For

example, brain AVMs are often discovered in young people, before the age of 30, and

similarities between brain AVMs and embryonic vessel patterns has suggested that

they are formed by defects in early vascular development.(2, 6) In the absence of

chronic imaging data on AVM development, these theories remain speculative.

Genetic linkage identifies causal lesions in a subset of hereditary AVMs

Traditional, forward genetic, linkage association studies in hereditary AVM

disease revealed causal mutations in Alk1, endoglin, Smad4, RASA1, and PTEN,

identified as dominant mutations in families with multiple affected members.(7-11)

Hereditary Hemorhagic Telangectasia (HHT)

In HHT, AVMs form throughout the tissues of the body, including brain, but

also liver, lung, gut and skin. The disease has been linked to heterozygous

mutations in the Alk1 and endoglin genes, endothelial TGF-beta receptor and co-

receptor, respectively.(7) Mice completely deficient in Alk1 or endoglin are

embryonic lethal, with impaired vascular remodeling and AVMs. Mice with heterozygous loss-of-function mutations in Alk1 or endoglin are viable, but occasionally develop vascular malformations in later life. Conditional deletion of Alk1 in adult mice results in spontaneous AVM formation in growing mice.(12) Conditional deletion of endoglin also results in AVMs in growing tissues, and as in embryonic studies, the AVMs form between arteries and veins with proper specification.(13, 14)   SMAD4, a downstream mediator of Alk1 and endoglin signaling has also been implicated in AVM development.(8, 15) In mice, deletion of SMAD4 specifically in the endothelium, using Tie2-cre, results in impaired vascular modeling and embryonic lethality.(16) Therefore, multiple components of the TGF-beta signaling cascade result in similar AVM phenotypes.

RASA1

Mutations in RASA1 have been implicated in another subset of AVMs associated with capillary malformations.(9, 17) In the families investigated, RASA1 loss-of-function mutations resulted in small, rounded, red or pink capillary malformations (CM) in the skin, as well as AVMs, leading researchers to designate the newly defined disease as CM-AVM. Penetrance of the CM phenotype was 96.5% in individuals with RASA1 mutations. Frequency of detected AVMs lower but still highly significant, with a penetrance of 32.6% (33/101). AVMs in these individuals formed in a variety of areas, including skin, bone, muscle and brain. Of the AVMs, one third (6/18) were intracranial. Two intracranial AV fistulas were also found.

3

PTEN

AVMs have been associated with Cowden syndrome (CS) and Bannayan-Riley-Ruvalcaba (BRR) syndrome, diseases linked to heterozygous PTEN mutations.(10) In a related disease, Proteus-like Syndrome, a germline PTEN mutation was also identified, and further, that a second hit knocked out the normal copy of PTEN in an AVM that developed.(11) Endothelial deletion of PTEN is embryonic lethal, as embryos fail to remodel the initial vascular plexus.(18) Deletion of one allele of PTEN in mice resulted in increased angiogenesis in tumor and plug implant assays.(18)

However, familial AVMs account for only a small portion of human BAVMs. For example, among a population of 638 BAVM patients, only 14 (~2%) were attributed to HHT mutations, the primary form of familial AVMs (19). Thus, the molecular cause of the overwhelming majority of sporadic AVMs remains unknown.

Notch controls a genetic program of arteriovenous specification

Recent work in developing vertebrate embryos has identified a genetic program of AV specification. Strikingly, disruption of this AV specification program led to failed vascular remodeling and enlarged AV connections reminiscent of the core defect in human AVMs.(20-23) The Notch receptor is a critical mediator of arteriovenous (AV) specification, consistent with conserved roles in developmental lineage decisions throughout metazoans.(24, 25) Notch is activated through direct cell-cell communication with ligand expressing cells.(26) The exquisite sensitivity

of the Notch receptor likely contributes to its utility in amplifying small differences between adjacent cells. In the endothelial cells of the zebrafish, fate-mapping analysis by dye injection revealed that "the vascular fate of an angioblast is determined in the lateral plate mesoderm (LPM). Arterial and venous precursors are spatially mixed within LPM, and an individual angioblast contributes to only one or the other of these vessels."(27) The Notch downsteam gene gridlock, zebrafish homologue to Hey2, was identified as a critical determinant of AV specification on the basis that is was in the right place at the right time (LPM prior to the formation of the dorsal aorta, and later in the dorsal aorta), and was necessary for dorsal aorta formation. These observations led to a model in which high Notch activity in hemangioblasts is necessary for arterial specification, while low levels of Notch activity inhibit arterial specification.(28)

Studies in mouse support a key role for Notch signaling in AV specification. Notch1 and Notch4 are expressed in the endothelium, where expression is arterial specific.(29) Complete deletion of Notch1 is embryonic lethal, and while Notch4 deletion is not, the combination of Notch1 and Notch4 deletion results in a more severe phenotype than Notch1 alone.(30) The endothelial expression pattern of Dll4 suggested that it was the ligand for endothelial Notch receptors, and deletion of Dll4 confirmed that it was necessary for vascular development.(22, 31, 32) Interestingly, Dll4 is haploinsufficient, suggesting that the activation of Notch receptors by Dll4 is dose-dependent. In Dll4 mutants, arterial markers ephrin-B2, connexin37, connexin40 and neuropilin-1 are lost, and EphB4 is ectopically expressed in the arterial endothelium.(31, 33) Complete endothelial deletion of

RBPJ-kappa, a critical downstream mediator of Notch signaling, causes similar vascular defects with loss of arterial markers ephrin-B2 and CD44.(22) Conversely, endothelial specific expression of constitutively-active Notch4 is sufficient to induce arterial markers ephrin-B2 and Dll4 in venous endothelium, with a concomitant reduction in venous marker EphB4.(21) Over-expression of Dll4 in the endothelium triggers increased Notch activation, as evidenced by increased expression of the Notch responsive gene Hey1.(34) In these Dll4 GOF embryos, arterial markers Notch1 and connexin37 are expressed ectopically in the venous endothelium, as EphB4 is suppressed.(34) Notch responsive basic helix-loop-helix transcription factors Hey1 and Hey2 are likely mediators of the effects of Notch signaling, since their combined deletion results in a vascular phenotype which resembles Notch1 null mice, and is accompanied by a similar reduction in ephrin-B2, CD44 and neuropilin-1.(33)

In mouse, as in zebrafish, VEGF acts upstream of Notch. *In vitro* experiments with mouse ES cells show that VEGF signaling is important in the development of the endothelial cell lineage from undifferentiated cells, and in the induction of arterial identity. Presented with increasing concentrations of VEGF, ES cells upregulate Notch receptors and ligands.(35) Similar findings have been reported with already differentiated endothelial cells *in vitro*.(36, 37) *In vivo* experiments showed that the induction of Dll4 at the sprouting front of the retinal vasculature following oxygen induced vaso-obliteration is dependent on VEGF signaling, which could be disrupted by the injection of VEGF-binding protein, and increased through the injection of soluble VEGF.(38) In the heart, overexpression of VEGF increases

the proportion of ephrin-B2+ endothelial cells.(39) Although the specific pathways

downstream of VEGF receptor activation which induce the expression of Dll4 are

not entirely clear, Pi3K and ERK kinases, and the Foxc1 and Foxc2 transcription

factors are involved. Both Pi3K and ERK kinases can be activated by VEGFR

stimulation, but they have divergent downstream effects. Zebrafish embryos

deficient in phospholipase C gamma-1, in the ERK pathway downstream of VEGF,

are impaired in their ability to induce the expression of arterial markers Notch5 and

ephrin-B2.(40) However, inhibition of Pi3K can partially rescue vascular defects in

gridlock mutant zebrafish, caused by low levels of Notch activity, suggesting that

Pi3K opposes ERK mediated induction of arterial specification.(41) Consistent with

this, cells with loss of Pi3K signaling preferentially contribute to the artery in

chimeric zebrafish, while cells with gain of Pi3K signaling preferentially contribute

to the vein.(41) Foxc1/Foxc2 are necessary for expression of arterial markers

Notch1, Notch4, Dll4, and ephrin-B2, but not venous marker EphB4 in mouse

embryos.(42) It is not yet entirely clear how Foxc1/Foxc2 are regulated in

endothelial cell development, but there is some evidence for a connection with VEGF

signaling.(43)

    While a long list of proteins are specifically expressed in arteries, vein-

specific markers are rare. This led to the perception that venous specification is the

default pathway. However, the discovery that Coup-TFII expression is necessary

and sufficient for venous specification has altered that perception.(44) Embryos

with complete loss of Coup-TFII develop an enlarged DA, with some areas of the

developing CV completely absent.(45) A similar phenotype, though not quite as

severe is observed in upon endothelial specific deletion of Coup-TFII.(44) Markers

of arterial specification, Hey1, ephrin-B2 and neuropilin1 were increased in the

venous endothelium, showing that Coup-TFII normally suppresses the expression of

these arterial markers in the vein, acting upstream of Notch target genes Hey1 and

ephrin-B2.(44)   Conversely, overexpression of Coup-TFII throughout the

endothelium resulted in the formation of a massive vessel in the embryo, in the

location of the DA, but which did not express the arterial markers neuropilin1 and

Jag1, but did express the venous marker EphB4.(44)   Strikingly, absence of Coup-

TFII in selected cells of chimeric embryos prevented these cells from contributing to

the endothelium of the developing vein, although they could still contribute to the

artery.(44)

Arteriovenous specification may regulate the establishment of vascular

hierarchy

One of the first questions that arose in the study of AV specification is

whether the genes involved are "markers" or "makers."(46) That is, do they merely

show the identity of the vessels which become artery or vein, or do they have a

requisite functions in the development of vascular structure. Of particular interest

is whether these molecules help to establish AV hierarchy, the highly stereotyped

refinement of vessel diameters between the arteries and the veins. The experiments

which identified the arterial expression pattern of ephrin-B2 and the venous

expression pattern of EphB4 answered provided a partial answer to this question

almost immediately. Knock-out of either of these receptors disrupted the

remodeling of the initial vascular plexus, suggesting a role as "makers."(47)

However there were some caveats to these experiments. Given the important

function of blood flow in remodeling of these plexi (in the head and in the yolk sac)

and the defects in flow predicted by the AV shunts that form within large vessels

surrounding the heart in these mutants, the role of the receptors in remodeling the

vasculature is confounded by flow effects.(20)

Notch is thought to regulate the specification of arterial and venous fates, and

ephrin-B2 and EphB4 are believed to mediate the functional consequences of this

specification on the cellular organization of the vasculature. The reason is that, just

as Notch has conserved functions as a mediator of cell fate decisions, ephrin/Eph

interactions function in many systems to regulate the spatial organization of cells

through repulsive and attractive signaling. The best examples of this are the in the

neuronal system, in which these molecules were first discovered.(48) Prior to their

discovery of complimentary EphB4/ephrin-B2 expression in the vasculature, Wang

and Anderson described repulsive signaling initiated by ephrin-B1 and -B2 ligands

to cells with EphB receptors.(49) They found that when neural crest cells were

induced to grow through a grid with alternating stripes coated or not with ephrin-B

ligands, they selectively grew on the stripes not coated with ephrin-B2. Therefore,

the immediate thought, once the pattern and requirement for EphB4/ephrin-B2 in

the vasculature had been described, was that they might function to maintain the

separation of arterial and venous cells.

Eph/ephrin repulsive signaling in the neuronal system prompted

experimenters to examine repulsion in the endothelium. *In vitro* experiments

showed that EphB4+ cells were repelled from ephrin-B2+ substrate, but that

ephrin-B2+ cell were not repelled from EphB4+ substrate, demonstrating that

repulsion could be triggered by activation of the EphB4 receptor by ephrin-B2, and

not vice versa.(50, 51) *In vivo* experiments support the hypothesis that the major

function of ephrin-B2 ligand in vascular development is the activation of EphB

receptors, since vascular development proceeds without obvious abnormalities in

mice in which the ephrin-B2 intracellular domain is replaced by beta-

galactosidase.(52) In contrast to the embryonic lethality caused by global or

endothelial specific deletion of ephrin-B2, these mice are born live with apparently

normal vascular remodeling, but die soon after, likely from heart valve defects.

These results imply that the extracellular domain, but not the intracellular domain,

of ephrin-B2 is essential for vascular remodeling, consistent with a requirement for

forward EphB4 activation, but not reverese ephrin-B2 activation.

Although less is known about the specific downstream effects of ephrin-B2

and EphB4 signaling in the endothelium, other studies have shed light on general

Eph/ephrin signaling as a class. Downstream of Eph receptor activation,

metalloproteinase cleavage allows the separation of the Eph/ephrin complex.(53)

Activation of the Eph receptor then causes actin cytoskeletal rearrangments, which

are controlled by Rho family GTPases bound to the Eph receptor.(54, 55) Detailed

proteomic analysis of tyrosine phosphorylation downstream of EphB2 receptor

activation, combined with computational analysis of the kinases involved, provided

a high-resolution map of the relevant kinase signaling, touching upon signaling

involved in cytoskeletal rearrangment, polarity and migration.(56) When EphB2+

and ephrinB1+ cells are mixed, they spontaneously reorganize into EphB2 and ephrinB1 clusters, though repulsive cues. Clustering was used a readout in an siRNA screen of the critical kinases and phosphylation targets, which revealed significant overlap with the phosphoylated proteins and predicated kinase pathways identified by mass spectrometry.(56)

Many of the predictions about the role of AV specification, repulsive signaling and the separation of arteries and veins have been derived from *in vitro* cell culture experiments, in which the behavior and repulsion of individual endothelial cells can be monitored in real time. However, the critical question is how such repulsive behavior contributes to the shaping of the vascular system *in vivo*. The separation of the first artery and vein, the dorsal aorta (DA) and the cardinal vein (CV), in the mouse embryo in the Wang lab has provided a platform for understanding this. In embryonic development, a lumenized DA forms first, and a developing venous plexus subsequently gives rise to the lumenized CV. It was observed that loss-of-function in either EphB4 or ephrin-B2 resulted in an increase in the number of endothelial cells in the DA at the expense of the cardinal vein.(21) However, the total number of cells in the two vessels combined was not altered, indicating that the enlarged DA was caused by defective allocation of ECs, and not increased proliferation.(21) Furthermore, in the absence of ephrin-B2, EphB4+ cells were retained within the DA.(21) This data suggested that a heterogenous mixture of arterial and venous endothelial cells were contained within the DA, and that EphB4/ephrin-B2 signaling was required to expel the EphB4+ venous cells, prompting their contribution to the CV. Indeed, in early embryonic development,

capillary bridges can be observed between these two vessels, suggesting a path for their migration.(21) Time-lapse imaging in the more accessible zebrafish embryo supported this hypothesis, by directly showing the migration of endothelial cells from the DA to the developing CV.(57)

Although the general conclusions that are drawn from both the mouse and zebrafish models are similar, i.e. that EphB4/ephrin-B2 repulsive signaling results in segregation of arterial and venous fated cells to the developing DA and CA, there are also some notable differences. In contrast to the mouse, where disruption of EphB4/ephrin-B2 causes venous cells to be retained in the arterial position,(21) in zebrafish, morpholino suppression of EphB4 or ephrin-B2 causes endothelial cells to be retained in a large vessel with venous characteristics.(57) Furthermore, zebrafish data suggests that ephrin-B2 mediated reverse signaling plays an important role in maintaining ECs in the DA, since knockdown of ephrin-B2 or expression of a dominant negative version, missing the intracellular domain (ΔC-ephrin-B2), causes transplanted endothelial cells to contribute to the CV rather than DA.(57) In mouse, repulsive signals generated by EphB4 activation seem much more likely to be important, since the intracellular domain of ephrin-B2 is not required for vascular development.(52)

The differences between mouse and zebrafish are not necessarily contradictory. The close proximity of DA and CV in zebrafish, relative to the mouse, make it more difficult to assign arterial or venous specification by location. Given this ambiguity, vein identity was assigned by the enclosure of GATA+ erythrocytes, which occurs in the fish vein and not artery.(57) However, it is possible that mixed

arterial and venous cells would still encircle the GATA+ cells. A reconciliatory

proposition is that, following disruption of EphB4/ephrin-B2 mediated repulsion,

the large vessel that forms in mouse and zebrafish may not be completely either

arterial or venous, but a precursor to both. Likewise, the finding that ephrin-B2

reverse signaling plays an important role in zebrafish, but not in mouse, may be an

artifact of the techniques used. In the mouse mutant, ΔC-ephrin-B2 is still expressed

from the endogenous promoter.(52) In the zebrafish chimera, the all of the

transplanted cells (a mixture of endothelial and non-endothelial) contain RNA

expressing ΔC-ephrin-B2.(57) One consequence is that ΔC-ephrin-B2 expression is

no longer regulated in the zebrafish experiment, meaning that ephrin-B2 may be

expressed at unphysiologically high levels, and from venous cells that do not

typically express it. Another difference is that in zebrafish, the grafted cells compete

with wild-type cells, whereas in the mouse, there is no such competition, since all

cells express ΔC-ephrin-B2. Many reasons that might explain why zebrafish ΔC-

ephrin-B2 cells preferentially contribute to the CV, such increased cis-activation of

the repulsive EphB4 receptor, would not be replicated in the mouse experiment.

A reverse genetic approach to understanding arteriovenous malformations

Thus, embryonic studies have uncovered a program of AV specification that

is essential for vascular remodeling. (58) Most of the knowledge of the molecular

mechanisms of brain AVM has been gained through a forward genetics approach, in

which the phenotype was linked to genetic lesions. Mutations in Alk1, endoglin,

Smad4, RASA1 and PTEN have all been linked to human AVMs in studies of familial

inheritance.(7-11) However, mutations in these genes have been identified in only a small portion of the human disease, and most BAVMs are sporadic, which has limited genetic understanding through studies of inheritance.(2) Moreover, Alk1, endoglin, Smad4, RASA1 and PTEN do not yet have a well-understood function in the vasculature, and thus the mechanism through which they cause the formation of AVMs remains unclear. To gain new insight into the molecular etiology of human brain AVMs, I hypothesize that disruption of the AV specification program may be an unappreciated cause of AVMs. I use a reverse genetic approach to determine whether disruption of the AV specification program, by upregulation of endothelial Notch signaling, is sufficient to induce BAVM-like lesions in an animal model. I then use immunofluorescent histology to test whether Notch signaling is upregulated in human BAVMs. Finally, I use our animal model to examine the cellular and molecular mechanisms underlying the astonishing regression of AVMs and normalization vascular hierarchy, once constitutive Notch signaling is turned off.

Endothelial Notch4 signaling induces hallmarks of brain arteriovenous malformations in mice

Patrick A. Murphy*, Michael T. Y. Lam*†, Xiaoqing Wu*‡, Tyson N. Kim*, Shant M. Vartanian*, Andrew W. Bollen§, Timothy R. Carlson*¶, and Rong A. Wang*‖

*Pacific Vascular Research Laboratory, Division of Vascular Surgery, Department of Surgery, and Department of Anatomy and §Department of Pathology, University of California, San Francisco, CA 94143

Brain arteriovenous malformations (BAVMs) can cause devastating stroke in young people and contribute to half of all hemorrhagic stroke in children. Unfortunately, the pathogenesis of BAVMs is unknown. In this article we show that activation of Notch signaling in the endothelium during brain development causes BAVM in mice. We turned on constitutively active Notch4 (*int3*) expression in endothelial cells from birth by using the tetracycline-regulatable system. All mutants developed hallmarks of BAVMs, including cerebral arteriovenous shunting and vessel enlargement, by 3 weeks of age and died by 5 weeks of age. Twenty-five percent of the mutants showed signs of neurological dysfunction, including ataxia and seizure. Affected mice exhibited hemorrhage and neuronal cell death within the cerebral cortex and cerebellum. Strikingly, *int3* repression resolved ataxia and reversed the disease progression, demonstrating that *int3* is not only sufficient to induce, but also required to sustain the disease. We show that *int3* expression results in widespread enlargement of the microvasculature, which coincided with a reduction in capillary density, linking vessel enlargement to Notch's known function of inhibiting vessel sprouting. Our data suggest that the Notch pathway is a molecular regulator of BAVM pathogenesis in mice, and offer hope that their regression might be possible by targeting the causal molecular lesion.

angiogenesis | cell signaling | endothelial cell | stroke | cerebrovascular

Approximately 600,000 people worldwide harbor brain arteriovenous malformations (BAVMs) that can potentially rupture, leading to stroke and death. Historically, 50% of BAVMs first present with hemorrhage (1). Development of noninvasive imaging methods has increased BAVM detection before hemorrhage, but the efficacy of current treatments, primarily surgical resection, is questionable. Accompanying risk of mortality (3%) and morbidity (9%) may outweigh the risk of rupture itself (2). An ongoing clinical trial (ARUBA) is testing the hypothesis that invasive treatment may not provide a significant improvement over the natural course of the disease (2).

BAVMs disrupt normal vessel hierarchy and are caused by the replacement of capillary beds, which separate arteries from veins, with enlarged and tangled vessels. The retention of characteristics of embryonic brain vasculature in BAVMs has led to the speculation that they form during early brain development (3). Studies of a more accessible skin arteriovenous malformation (AVM) in human beings suggests that enlargement of postcapillary venules precedes AVM formation (4), but experimental evidence is required to validate such mechanisms. An animal model that mimics the characteristics of human BAVMs, principally arteriovenous shunting, would open avenues to understanding their cellular and molecular pathogenesis.

The primary factors regulating vessel hierarchy were once thought to be hemodynamic forces (5). It is now known that genetic programs contribute to the development of vascular hierarchy by specifying arteries and veins (6). Notch signaling has emerged as a critical genetic mediator in the differentiation of arteries and veins. Originally discovered in *Drosophila*, the transmembrane Notch receptor is conserved throughout the animal kingdom and is best known for its function in dichotomous cell fate decisions through cell–cell communication (7). Ligand binding to its extracellular domain results in sequential cleavage events and release of an active intracellular domain (ICD), which then translocates to the nucleus and initiates transcription of downstream genes (7). Thus, nuclear localization of Notch-ICD is a hallmark of Notch activation.

In the vascular system, Notch receptors and ligands are expressed in arteries but not veins (8) and are necessary and sufficient to induce ephrin-B2, a faithful marker of arterial identity (9–11). Notch loss-of-function mutations impair vascular development, resulting in arteriovenous shunting in both zebrafish and mouse embryos (10, 12). Notch gain-of-function also results in abnormal vascular remodeling in embryos, demonstrating that proper spatial and temporal patterns of Notch activity are critical for this process (13). Because BAVMs are thought to occur during brain development (3), we hypothesized that expression of constitutively active Notch4 would induce BAVMs during the neonatal period, when areas of the brain, such as the neocortex and cerebellum, expand by nearly 10-fold (14).

Results

Expression of Constitutively Active Notch4 (int3) in the Endothelium Results in Hemorrhage, Neurological Damage, and Death in Neonates. To test our hypothesis that Notch4 activation in the endothelium of the developing brain would cause BAVM, we expressed int3 specifically in the endothelium from birth in tetracycline-regulated mice (*Tie2-tTA;TRE-int3*) (11). Endothelial-specific expression was demonstrated by a *TRE-LacZ* reporter (11, 15) [supporting information (SI) Fig. S1]. In addition, Notch4-ICD was detected in the nuclei of a subset of mutant but not control endothelial cells (ECs) (Fig. 1*A* and *B*). Because int3 is a portion of Notch4, the anti-Notch4-ICD staining could not distinguish int3 from endogenous Notch4. However, the staining did not detect endogenous levels of Notch4 in the control, suggesting that staining in the mutant represents int3 expression. The nuclear accumulation of Notch4-ICD indicates increased Notch4 activity specifically in ECs of mutant mice.
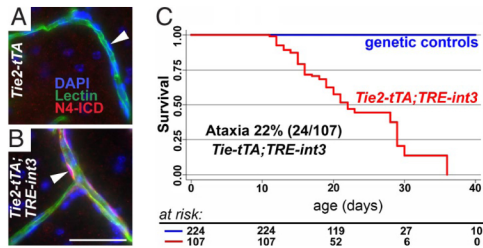
MEDICAL SCIENCES

15

Fig. 1. Endothelial expression of *int3* causes ataxia and death in neonatal mice. (*A* and *B*) Increased Notch4 activation specifically in the ECs lining lectin-perfused vessels of P29 mutant brain was revealed by nuclear staining of Notch4 intracellular domain (N4-ICD). DAPI-labeled EC nuclei (white arrowheads). (*C*) Kaplan–Meier survival curve shows that all mutants died by P36. (Scale bar, 50 μm.)

Mutant mice died between 2 and 5 weeks of age (Fig. 1*C*). Signs of neurological dysfunction, including ataxia and seizure, were evident in 27 of 107 mutant mice. Ataxia ranged in severity, from mice unable to right themselves to those with splayed rear legs. We occasionally noticed seizure episodes in which the mice ran wildly before collapsing. All but one of the cases of ataxia (23/24) and seizure (5/6) occurred before P22, suggesting that younger mice are more susceptible to these phenotypes.

To investigate potential causes for the neurological dysfunction, we examined mutant brains and found prominent hemorrhage by gross inspection (Fig. 2*B*) and by histology (Fig. 2 *C–F*). Hemorrhage occurred most often in the cerebellum, followed by the neocortex, but never in brainstem. We examined six of the ataxic mice and found hemorrhage in the cerebellum (see Fig. 2 *C* and *D*). Hemorrhage appeared more widespread than the neurological phenotype, because we also observed hemorrhage in all ill mutant mice without detectable ataxia (13 of 13; see Fig.
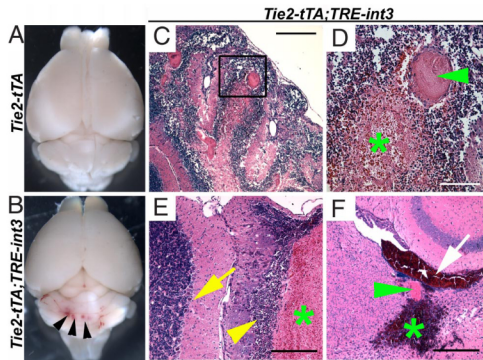

Fig. 2. Brain hemorrhage occurred in all mutant mice. (*A* and *B*) Multifocal hemorrhage (arrowheads) revealed in mutants after vascular perfusion. (*C* and *D*) H&E stained sagittal sections of perfusion fixed cerebellum from a mutant with ataxia show hemorrhage (green asterisk) and thrombosis (green arrowhead). (*E*) H&E stained sagittal section of cerebellar folia from a mutant without ataxia shows hemorrhage (green asterisk) and adjacent dropout of granular and Purkinje neurons (yellow arrowhead). Normal neuronal architecture (yellow arrow) is away from the hemorrhage. (*F*) H&E stained axial section of a severely affected mutant shows intraventricular hemorrhage (white arrow) immediately adjacent to a large, thrombosed vessel (green arrowhead) and parenchymal hemorrhage (green asterisk) in the cerebrum. (Scale bars: *C* and *F*, 400 μm; *D*, 100 μm; *E*, 200 μm.)
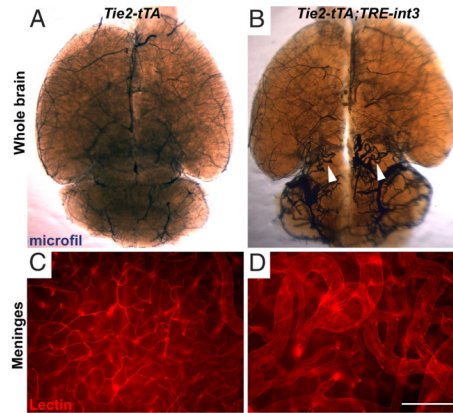
Fig. 3. Enlarged and tangled blood vessels developed in all mutant mice. Vessel enlargement occurred within the parenchyma and on the surface of the brain. Large tangled vessels were shown in the parenchyma of the cerebellum and midbrain by vascular casting at P27 (*B*; white arrowheads) and in the lateral meninges by whole mount imaging of Cy3-labeled lectin perfusion (*D*). (*A* and *C*) Abnormal vessels were not observed in littermate controls. (Scale bar, 200 μm.)

2*E*) and none in their littermate controls. Thrombosis, often a consequence of hemorrhage (16), was seen in hemorrhagic areas (see Fig. 2 *D* and *F*). As with the neurological phenotype, hemorrhage was most severe in mice ill before P22. Blood was found in the ventricle of 4 of 11 ill mice before P21 (see Fig. 2*F*). Neuronal cell death consistently occurred adjacent to hemorrhage (see Fig. 2*E*), suggesting that hemorrhage led to neuronal damage. Foci of pyknotic and karyorectic nuclei, often associated with macrophage infiltrations, were detected in the Purkinje and granular layers of the cerebellum, as well as areas of the neocortex and midbrain (see Fig. 2*E*). Signs of calcification, an indication of earlier cerebral damage, occurred in multiple cases (data not shown). Therefore, increased endothelial Notch4 activation results in hemorrhage, which likely causes neuronal damage and ataxia in the mutant mice.

Vessel Enlargement and Hallmarks of BAVMs in Mutants Before Hemorrhage. Because increased Notch4 activation was targeted to ECs specifically, we investigated lesions underlying hemorrhage and found vascular abnormalities resembling BAVMs. Vascular perfusion with casting agents (Fig. 3*B*) or fluorescent lectins (Fig. 3*D* and Fig. S2) revealed enlarged and tangled vessels, hallmarks of BAVMs (1, 17). We verified that arteries, veins, and intervening vessels were all enlarged, by examining the arterial and venous branches of the middle-cerebral vessels (see Fig. S2). To determine whether the enlarged vessels had smooth muscle coverage, we performed immunofluorescence with anti-smooth muscle α-actin (SMA) and found strong staining in these vessels (Fig. S3). Vessel enlargement occurred before hemorrhage, neuronal cell death, or signs of neurological dysfunction (Fig. S4), suggesting that it is a primary defect.

Because hemorrhage occurred primarily in the cerebellum, followed by the neocortex, and never in brainstem, we tested whether vessel enlargement correlated with hemorrhage. A decrease in the proportion of small vessels and an increase in the proportion of larger vessels were most significant in the cerebellum, followed by the neocortex, and least in brainstem (Fig. 4). Therefore, regional enlargement correlated with hemor-
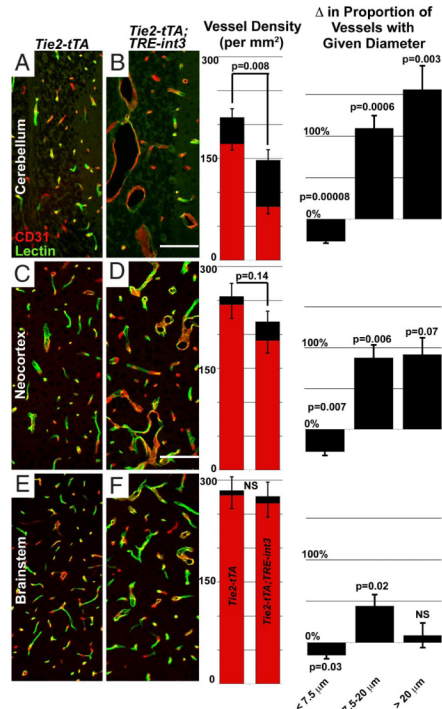
16

Fig. 4. Increased vessel size and decreased vessel density correlated with the frequency of hemorrhage. Shown is immunofluorescence in sagittal sections of brain regions. Density graphs represent FITC-lectin perfused (red) and total CD31 immunostained (black) vessels in each region (per squared millimeter). Δ Proportion of vessel with given diameter represents the percent change in the proportion of small (<7.5 μm), medium (7.5–20 μm), and large (>20 μm) diameter vessels in each region, relative to average controls. (*A* and *B*) *Tie2-tTA* (*n* = 6) and *Tie2-tTA;TRE-int3* (*n* = 3); (*C*, *D*, *E*, and *F*), *Tie2-tTA* (*n* = 6) and *Tie2-tTA;TRE-int3* (*n* = 5). Values represent mean ± SEM. (Scale bars, 200 μm.)

Fig. 5. All mutants developed shunting and arteriovenous malformations. (*A*) Increased carotid blood flow was detected by P21. Maximal (systolic) carotid blood velocity was measured by pulsed-wave Doppler ultrasound. *Tie2-tTA* and *Tie2-tTA;TRE-int3* (*n* = 9 and *n* = 6) at P15; (*n* = 12 and *n* = 14) at P17; (*n* = 16 and *n* = 26) at P21; (*n* = 18 and *n* = 12) at P23; (*n* = 14 and *n* = 9) at P29; values represent mean ± SEM. Changes were highly significant from P21 (***, *P* < 0.00005). Typical Doppler traces from mice at P21 (*A Right*). (*B*) Brain arteriovenous shunts developed by P19 as shown by fluorescent microsphere passage. The microspheres bypassed the brain and lodged in the lung in the mutants but not controls. BF, Bright-field; FITC, green fluorescent images.

rhage, supporting the hypothesis that vessel enlargement contributes to hemorrhage.

Endothelial Notch activity decreases vessel density by inhibiting sprouting angiogenesis (18). To investigate vessel density, we quantified CD31 positive vessels. Vessel density was decreased significantly in the cerebellum, and progressively less so in the neocortex and brainstem (see Fig. 4). Vessel density was inversely correlated with the proportion of large vessels (>50 μm) across all of these regions (Fig. S5), suggesting that vessel enlargement is linked to the reduction in vessel density.

Arteriovenous Shunting Occurs in all Mutants. The fundamental defect in human BAVMs is high-flow arteriovenous shunting. Blood velocity in carotid arteries can double in BAVM patients, a clinical indication of arteriovenous shunting (19). We measured carotid blood velocity with high-resolution ultrasound and found increased carotid blood velocity in all mutants by 3 weeks of age (Fig. 5*A*). This noninvasive approach allowed for progressive measurements in the same animal, demonstrating that carotid blood velocity increased in a short time window between
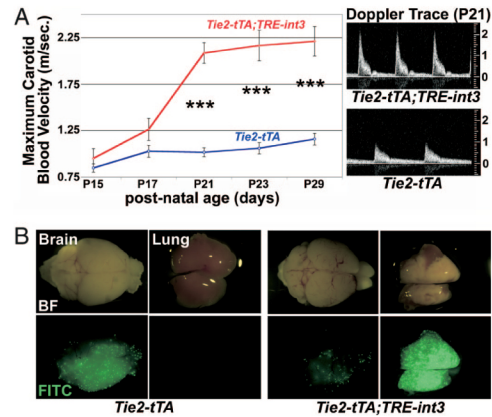
P17 and P21 (see Fig. 5*A*). Furthermore, at P21, velocity in mutants with neurological dysfunction was significantly higher than those without neurological dysfunction (2.6 ± 0.5 m/sec; *n* = 6 versus 1.9 ± 0.5 *n* = 20, respectively; *P* = 0.007). Because of limitations of this assay, we were unable to examine sick mutants before this age, and they often exhibited severe neurological defects. As a result, the cohort of mice examined did not display severe neurological defects, which may contribute to the minimal increase at P15.

To more directly test for arteriovenous shunts, we performed a microsphere passage assay (11). Microspheres lodged within the control brain (Fig. 5*B*) but bypassed the mutant brain and lodged in the downstream lung (*Tie2-tTA n* = 6; *Tie2-tTA;TRE-int3 n* = 5). This result demonstrates the existence of arteriovenous shunts in the brain, mimicking the principal defect of human BAVMs.

To directly visualize arteriovenous shunts, we distinguished arterial from venous branches with the arterial marker ephrin-B2. Expression of the reporter in *ephrin-B2*[+/tLacZ] mice (6) was strong in the middle cerebral arteries and weak in the middle cerebral veins (Fig. 6*A*). In mutants, direct connections between the arteries and veins were prominent at P21 (Fig. 6*B*). Similar arteriovenous connections within the cerebellum were detected by using a nuclear GFP reporter in *ephrin-B2*[+/GFP] mice (20). Cerebellar interfolial arteries (GFP+) in the control follow a typical pattern of branching and ramifying into a fine capillary bed within the granular layer before coalescing into the draining veins (GFP−) (Fig. 6*C*) (21). However, in mutants there were enlarged vascular connections, replacing normal capillaries, between the interfolial arteries and veins (Fig. 6*D*). Therefore, direct arteriovenous shunts were visible in the surface and deep cerebellar vasculature of mutant mice.

Repression of *int3* Rescues Moribund Mice. Taking advantage of the tetracycline-regulated expression system, we tested whether
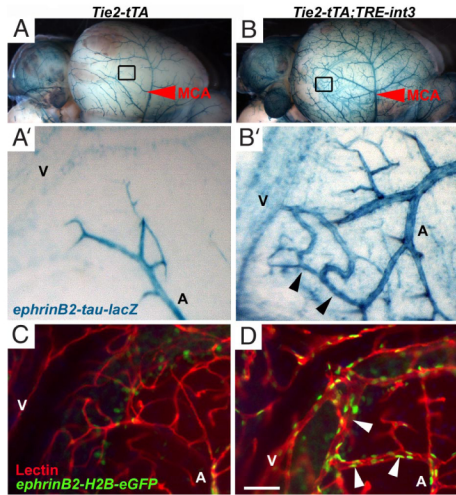
MEDICAL SCIENCES

Fig. 6. Enlarged arteriovenous connections developed on the meningial surface and in the parenchyma of mutant brains. (*A* and *B*) X-gal staining of *ephrin-B2⁺/ltLacZ* brains revealed the middle cerebral artery (MCA, red arrowheads) on the lateral side of the brain. High magnification image of the boxed area in *B* shows direct arteriovenous connections (black arrowheads) between arterial branches of the MCA (A) and venous vessels (V) in *Tie2-tTA;TRE-int3;ephrin-B2⁺/ltLacZ* mice (*B′*). (*C* and *D*) Fluorescent images of sagittal cerebellar 100-μm thick sections show enlarged connections (white arrowheads) between GFP-labeled interfolial arteries of *Tie2-tTA;TRE-int3;ephrin-B2⁺/ltLacZ* mice (A) and draining veins (V) in the mutant (*D*) and not control (*C*). (Scale bar, 50 μm.)

Fig. 7. Repression of *int3* resolved ataxia and prevented death. (*A*) Repression of *int3* with Dox at P20 or P21 allowed the survival of mutant mice, as shown by the Kaplan–Meier curve. *Tie2-tTA;TRE-int3* Dox-off (*n* = 23) and *Tie2-tTA;TRE-int3* Dox-on (*n* = 15) at 20 days; *Tie2-tTA;TRE-int3* Dox-off (*n* = 0) and *Tie2-tTA;TRE-int3* Dox-on (*n* = 5) at 40 days. (*B*) Ataxia was resolved by *int3* repression. Still frames were taken from a movie of a severely ataxic mutant at P19, and upon its recovery at P22, after 3 days of Dox treatment.

repression of the causal genetic lesion could reverse disease progression in mutant mice. Vascular enlargement and shunting occurred in all mutant animals by P21, so this time-point was chosen for a regression study. Littermates were allowed to express the *int3* transgene from birth until P20 or P21, at which time sick mutants were fed doxycycline (Dox), a more stable derivative of tetracycline (Tet), to repress *int3* expression. No mutants survived to P32 without Dox treatment (*n* = 19), but 8 of 9 mutants fed Dox appeared outwardly healthy and active at P35, and were healthy until killed by P64 (Fig. 7*A*). The one exception was a severely affected mutant that died in the first day of treatment.

To investigate the reversal of brain abnormalities specifically, we examined the recovery of ataxic mice. Ataxia in all seven mice examined was resolved within just days of transgene repression (Fig. 7*B*). These findings suggest that repression of endothelial *int3* expression, the causal stimulus, recovers brain function in mutant mice.

Discussion

We demonstrate that increased Notch4 activity causes vascular abnormalities with the characteristics of BAVM, implying that increased Notch4 activation is a potential molecular cause of human BAVM. Our findings also suggest that regression of this devastating disease may be possible by targeting the causal molecular lesion. The activated Notch4 model provides a powerful platform for the study of the pathogenesis and regression of BAVM-like lesions. In addition, our studies of pathogenesis in this model provide experimental support for the hypothesis that BAVMs occur in the developing brain and that they can be induced by vessel enlargement.
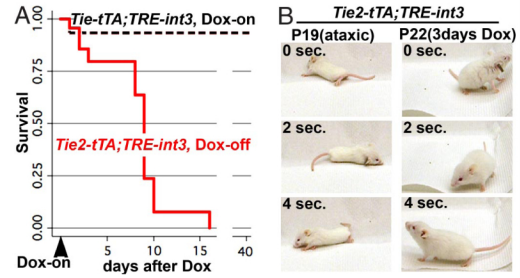
Notch4 Activation Is a Candidate in the Molecular Regulation of BAVM Pathogenesis. Molecular etiology of BAVM is unknown. Mutations in the TGF-β signaling pathway, primarily loss-of-function *ENG* (*endoglin*) and *ACVRL1* (*ALK-1*) alleles, have been associated with BAVMs (22). However, these mutations are implicated in only ≈2% of all BAVMs (23). We found that constitutively active Notch4 causes BAVM-like lesions promptly in neonates, identifying activation of the Notch4 pathway as a potent molecular candidate in the development of human BAVMs.

The primary characteristic of human BAVMs is the development of arteriovenous shunting (1). In patients, this is detected by arteriography, the gold standard in the diagnosis of this vascular lesion (24), and also by ultrasound measurement of increased carotid blood flow (25). We demonstrated the presence of arteriovenous shunting by similar methods in mice, including anatomical connections between arteries and veins, functional passage of beads too large for capillaries, and increased carotid blood velocity.

Enlarged and tangled vessels are another key characteristic of BAVMs (1). We detected massively enlarged and tangled vessels by perfusion labeling with a casting agent and fluorescently labeled lectins. In contrast to human BAVMs, which usually develop as a single nidus (23), the vascular abnormalities in mutants were multifocal and widespread. This difference is likely because of the expression of the *int3* transgene throughout the endothelium.

Hemorrhage, often resulting in neuronal damage and ataxia, is the most feared consequence of human BAVM (26). All of the sick mutants examined developed brain hemorrhage, often with adjacent neuronal cell death. Approximately 25% of the mice developed neurological deficits, including ataxia and seizure.

Repression of *int3* Expression Leads to Recovery of Sick Mice. It is commonly thought that natural regression of BAVMs does not occur (27); instead they increase in size and eventually rupture (26). Regression of BAVMs has been reported in only a handful of cases, which are thought to be caused by thrombotic occlusion, a naturally occurring event similar to the embolizing treatments used clinically (27). The recovery of brain function in our mutant mice that resulted from molecular intervention is provocative.

One potential caveat is that Dox, which is used to repress transgene expression, can also inhibit both vessel growth and hemorrhage (28–30), and may therefore contribute to recovery. Because the dose of Dox for transgene repression is similar to

that used for inhibition of vessel growth, we are currently unable to delineate these two effects. However, similar Tet-regulated mouse genetic approaches were used to show that tumors regress after repression of transgenic oncogene expression, inspiring the oncogene addiction theory (31–33). It is possible that Notch4-induced BAVM-like lesions require continuous Notch4 activation for their maintenance.

Regardless whether the Dox-mediated regression is because of repression of transgene expression or because of its direct effect on vessel growth and hemorrhage, the recovery of the ill mice is evocative. Although further studies are required to determine whether this is a result of regression of the BAVM-like lesions, our findings raise the hope that inhibition of the causal molecular lesion may lead to regression of the disease.

High Penetrance and Rapid Onset of BAVM-Like Lesions in the Activated Notch4 Mutants Provide a Robust Platform to Model Human BAVM Pathogenesis. Our transgenic mice provide a much needed mouse model for the study of BAVM pathogenesis. The study of the cellular and molecular etiology of BAVMs is limited by the lack of a good animal model for this disease (34). Mice with mutations in endoglin or ALK-1 have advanced the understanding of molecular contributions to AVMs. Autosomal dominant mutations in these genes are responsible for the human hereditary hemorrhagic telengectasia (HHT) (22), which involves AVMs primarily in the skin, liver and lung, along with a 4% incidence in the brain (35). Of 22 $endoglin^{+/-}$ mice that developed an HHT phenotype, 8 showed signs of brain hemorrhage by ≈40 weeks of age (36). Vascular brain casts showed small clusters of capillaries or aneurismal dilations in 3 of 10 $endoglin^{+/-}$ mice (37). Cerebrovascular abnormalities are also observed in ≈2% of $Alk-1^{+/-}$ mice (38). However, it is unknown whether either the $endoglin^{+/-}$ or $Alk-1^{+/-}$ mice develop arteriovenous shunting. Therefore, our activated Notch4 mice provide a model for molecular understanding of both the development and potentially the regression of BAVMs.

Notch4 Activity May Selectively Induce BAVM-Like Lesions in Growing Brains. BAVMs typically affect children and younger people. Based primarily on the belief that BAVMs retain embryonic vascular structures, it has been speculated that BAVMs occur during brain growth (26). Our data supports the theory that the growing brain is more vulnerable to BAVM formation. First, we found that hallmarks of BAVM are prominent when the transgene is expressed in the neonatal period, when the brain grows rapidly, but not when it is expressed in the postweaning mouse (11), when brain growth is reduced. Second, we found that vessel enlargement was greatest in the cerebellum and cortex and least in the brainstem, which correlates with the greater growth in the cortex and cerebellum than in the brainstem at this stage (39). Third, when AVMs occur in older mice, they appear to affect the liver, skin, and uterus, three actively remodeling tissues in adult mice (11). These data support the hypothesis that Notch functions in a temporal and spatial specific manner, and that the developing brain is particularly susceptible to Notch4-mediated formation of BAVM-like lesions.

Vessel Enlargement May be a Mechanism for the Onset of BAVMs. The cellular mechanism of BAVM formation is currently unknown. A few models, however, are proposed. The most favored model is that BAVMs represent a failed transition from embryonic brain vasculature to adult brain vasculature (3). Supporting evidence for this theory has rested heavily on the interpretation of the morphological structure of adult BAVMs. Another theory is that BAVMs are not necessarily congenital abnormalities, but can form *de novo* through vessel enlargement. This theory is based on the observation that enlargement of postcapillary

venules is the first observable phenotype in the development of AVMs in human skin (4).

Our data support the theory of *de novo* formation of BAVMs through vessel enlargement in the context of growing brain. We are able to measure carotid blood flow, a sensitive indicator of brain arteriovenous shunting, longitudinally in our mutant mice. By this measurement, we were able to show that in individual mutant mice, there was no shunting at P15, but that shunting increased dramatically over the subsequent 6-day period. In addition, the diameters of all vessels, including those at the capillary level, were enlarged. The enlargement of vessels before brain hemorrhage or neurological phenotypes suggests that it plays a causal role in the development of BAVM-like lesions. Thus, our data support the hypothesis that vessel enlargement promotes the development of BAVMs.

An alternative possibility is that Notch activation disrupts the arteriovenous interface by increasing arterial specification. We and others have shown that Notch activity promotes arterial specification in ECs *in vivo* in embryonic and adult mice, as determined by the expression of arterial markers, such as ephrin-B2 (9–11). In this study we found that in neonatal brain endothelium, Notch4 activity increased ephrin-B2 expression in capillaries and veins. Interestingly, expression was most markedly increased in direct arteriovenous connections, suggesting that induction of arterial specification in these ECs may disrupt the proper formation of the capillary bed connecting the artery and vein.

Notch Activity May Promote Vessel Enlargement by Inhibiting Sprouting. We previously reported that Notch activity promotes vessel enlargement (11), and others subsequently demonstrated a reduction in vessel density (18), but the relationship of these functions is unclear. We observed a correlation between vessel enlargement and vessel density, suggesting that Notch's role in decreasing vessel density might be intimately involved with vessel enlargement and BAVM development. Supporting our finding, it was recently reported that retroviral expression of the Notch ligand Dll4 increases lumen diameters and reduces vessel density in grafted tumors in mice (40). The observation that impaired endothelial sprouting can result in vessel enlargement was first made in mice exclusively expressing the $VEGF_{120}$ isoform (41). In both the VEGF mutant and our previous studies (11), proliferation was not significantly altered, suggesting that increased vessel size may simply reflect the retention of cells that would have otherwise contributed to sprouts. Therefore, Notch activation may promote vessel enlargement by inhibiting vessel sprouting.

In summary, we believe that this work opens an area of research to advance the molecular understanding of BAVM pathogenesis and provides hope for the treatment of this devastating disease.

Methods

Mice. Tet sucrose solution (0.5-mg/ml Tet, 50-mg/ml sucrose, Sigma) was administered to pregnant mothers from plugging, and withdrawn from pups at birth, and Dox (200-mg/kg diet, Bio-Serv) diet was administered to mutant mice at P20–21 as we described (11, 42). All animals were treated in accordance with the guidelines of the University of California San Francisco Institutional Animal Care and Use Committee.

Vascular Imaging. β-gal was detected by activity or with an anti-β-gal antibody as we described (11). Casting and FITC-lectin staining were performed as we described (11). Cy3-streptavidin (Jackson Immuno) was used to detect biotinylated lectin (Vector Labs); these reagents were coinjected into circulation (25 μg of each in 200-μl PBS). Immunostaining was performed with anti-CD31, anti-α-SMA, and anti-Notch4 (Upstate) according to our published protocols (43, 44).

19

Statistical Analysis. All values represent the mean $\pm$ SEM. Kaplan–Meier survival curves were generated with STATA-IC software. See *SI Methods* for density and diameter analysis.

Vascular Shunting. Fifteen-μm fluorescent microspheres (Molecular Probes) were injected into the left carotid artery of anesthetized mice, and tissues were examined with a fluorescence dissecting microscope. For ultrasound measurements of carotid velocity, mice were anesthetized with isoflurane and body temperature was maintained on a heat pad. Carotid blood flow and diameter were measured noninvasively by ultrasound biomicroscopy (Vevo 770; Visualsonic Inc.). Doppler incident angles were between 70° and 80°. A two-tailed student's *t* test, assuming equal variation, was performed to determine the significance of differences in carotid blood velocity.

1. Friedlander RM (2007) Clinical practice. Arteriovenous malformations of the brain. *N Engl J Med* 356:2704–2712.
2. Stapf C, *et al.* (2006) Invasive treatment of unruptured brain arteriovenous malformations is experimental therapy. *Curr Opin Neurol* 19:63–68.
3. Mullan S, Mojtahedi S, Johnson DL, Macdonald RL (1996) Embryological basis of some aspects of cerebral vascular fistulas and malformations. *J Neurosurg* 85:1–8.
4. Braverman IM, Keh A, Jacobson BS (1990) Ultrastructure and three-dimensional organization of the telangiectases of hereditary hemorrhagic telangiectasia. *J Invest Dermatol* 95:422–427.
5. Murray CD (1926) The physiological principle of minimum work: I. The vascular system and the cost of blood volume. *Proc Natl Acad Sci USA* 12:207–214.
6. Wang HU, Chen ZF, Anderson DJ (1998) Molecular distinction and angiogenic interaction between embryonic arteries and veins revealed by ephrin-B2 and its receptor Eph-B4. *Cell* 93:741–753.
7. Lai EC (2004) Notch signaling: Control of cell communication and cell fate. *Development* 131:965–973.
8. Villa N, *et al.* (2001) Vascular expression of Notch pathway receptors and ligands is restricted to arterial vessels. *Mech Dev* 108:161–164.
9. Lawson ND, Weinstein BM (2002) Arteries and veins: Making a difference with zebrafish. *Nat Rev Genet* 3:674–682.
10. Krebs LT, *et al.* (2004) Haploinsufficient lethality and formation of arteriovenous malformations in Notch pathway mutants. *Genes Dev* 18:2469–2473.
11. Carlson TR, *et al.* (2005) Endothelial expression of constitutively active Notch4 elicits reversible arteriovenous malformations in adult mice. *Proc Natl Acad Sci USA* 102:9884–9889.
12. Lawson ND, *et al.* (2001) Notch signaling is required for arterial-venous differentiation during embryonic vascular development. *Development* 128:3675–3683.
13. Uyttendaele H, Ho J, Rossant J, Kitajewski J (2001) Vascular patterning defects associated with expression of activated Notch4 in embryonic endothelium. *Proc Natl Acad Sci USA* 98:5643–5648.
14. Zhang J, *et al.* (2005) Mapping postnatal mouse brain development with diffusion tensor microimaging. *NeuroImage* 26:1042–1051.
15. Redfern CH, *et al.* (1999) Conditional expression and signaling of a specifically designed Gi-coupled receptor in transgenic mice. *Nat Biotechnol* 17:165–169.
16. Capron L (1988) in *Vascular Diseases*, ed Vinken PJ (Elsevier, New York), pp 35–62.
17. (2001) Reporting terminology for brain arteriovenous malformation clinical and radiographic features for use in clinical trials. *Stroke* 32:1430–1442.
18. Hellstrom M, *et al.* (2007) Dll4 signaling through Notch1 regulates formation of tip cells during angiogenesis. *Nature* 445:776–780.
19. Marks MP, Pelc NJ, Ross MR, Enzmann DR (1992) Determination of cerebral blood flow with a phase-contrast cine MR imaging technique: Evaluation of normal subjects and patients with arteriovenous malformations. *Radiology* 182:467–476.
20. Davy A, Soriano P (2007) Ephrin-B2 forward signaling regulates somite patterning and neural crest cell development. *Dev Biol* 304:182–193.
21. Scremin OU (1995) in *The Rat Nervous System*, ed Paxinos G (Academic, San Diego), pp 3–35.
22. Abdalla SA, Letarte M (2006) Hereditary haemorrhagic telangiectasia: Current views on genetics and mechanisms of disease. *J Med Genet* 43:97–110.
23. Matsubara S, *et al.* (2000) Angiographic and clinical characteristics of patients with cerebral arteriovenous malformations associated with hereditary hemorrhagic telangiectasia. *Am J Neuroradiol* 21:1016–1020.
24. Ogilvy CS, *et al.* (2001) Recommendations for the management of intracranial arteriovenous malformations: A statement for healthcare professionals from a special writing group of the Stroke Council, American Stroke Association. *Circulation* 103:2644–2657.
25. Anbarasu A, Gould DA (2002) Diagnosis of an intracranial arteriovenous malformation using extracranial carotid Doppler sonography. *J Clin Ultrasound* 30:249–252.
26. Fleetwood IG, Steinberg GK (2002) Arteriovenous malformations. *Lancet* 359:863–873.
27. Patel MC, Hodgson TJ, Kemeny AA, Forster DM (2001) Spontaneous obliteration of pial arteriovenous malformations: A review of 27 cases. *Am J Neuroradiol* 22:531–536.
28. Manning MW, Cassis LA, Daugherty A (2003) Differential effects of doxycycline, a broad-spectrum matrix metalloproteinase inhibitor, on angiotensin II-induced atherosclerosis and abdominal aortic aneurysms. *Arterioscler Thromb Vasc Biol* 23:483–488.
29. Lee CZ, *et al.* (2004) Doxycycline suppresses cerebral matrix metalloproteinase-9 and angiogenesis induced by focal hyperstimulation of vascular endothelial growth factor in a mouse model. *Stroke* 35:1715–1719.
30. Lee CZ, *et al.* (2007) Matrix metalloproteinase-9 inhibition attenuates vascular endothelial growth factor-induced intracerebral hemorrhage. *Stroke* 38:2563–2568.
31. Felsher DW, Bishop JM (1999) Reversible tumorigenesis by MYC in hematopoietic lineages. *Mol Cell* 4:199–207.
32. Wang R, *et al.* (2001) Activation of the Met receptor by cell attachment induces and sustains hepatocellular carcinomas in transgenic mice. *J Cell Biol* 153:1023–1034.
33. Weinstein IB (2002) Cancer. Addiction to oncogenes—the Achilles heal of cancer. *Science* 297:63–64.
34. Young WL, Yang GY (2004) Are there genetic influences on sporadic brain arteriovenous malformations? *Stroke* 35:2740–2745.
35. Maher CO, *et al.* (2001) Cerebrovascular manifestations in 321 cases of hereditary hemorrhagic telangiectasia. *Stroke* 32:877–882.
36. Bourdeau A, *et al.* (2001) Potential role of modifier genes influencing transforming growth factor-beta1 levels in the development of vascular defects in endoglin heterozygous mice with hereditary hemorrhagic telangiectasia. *Am J Pathol* 158:2011–2020.
37. Satomi J, *et al.* (2003) Cerebral vascular abnormalities in a murine model of hereditary hemorrhagic telangiectasia. *Stroke* 34:783–789.
38. Srinivasan S, *et al.* (2003) A mouse model for hereditary hemorrhagic telangiectasia (HHT) type 2. *Hum Mol Genet* 12:473–482.
39. Winick M (1976) in *Malnutrition and Brain Development*, ed Winick M (Oxford Univ Press, New York), pp 35–62.
40. Li JL, *et al.* (2007) Delta-like 4 Notch ligand regulates tumor angiogenesis, improves tumor vascular function, and promotes tumor growth in vivo. *Cancer Res* 67:11244–11253.
41. Ruhrberg C, *et al.* (2002) Spatially restricted patterning cues provided by heparin-binding VEGF-A control blood vessel branching morphogenesis. *Genes Dev* 16:2684–2698.
42. Carpenter B, *et al.* (2005) VEGF is crucial for the hepatic vascular development required for lipoprotein uptake. *Development* 132:3293–3303.
43. Braren R, *et al.* (2006) Endothelial FAK is essential for vascular network stability, cell survival, and lamellipodial formation. *J Cell Biol* 172:151–162.
44. Carlson TR, *et al.* (2008) Cell-autonomous requirement for {beta}1 integrin in endothelial cell adhesion, migration and survival during angiogenesis in mice. *Development* 135:2193–2202.

20

Endothelial Notch signaling is upregulated in human brain arteriovenous malformations and a mouse model of the disease

Patrick A Murphy[1], Gloria Lu[1], Steven Shiah[1], Andrew W Bollen[2] and Rong A Wang[1]

Brain arteriovenous malformations (BAVMs) can cause lethal hemorrhagic stroke and have no effective treatment. The cellular and molecular basis for this disease is largely unknown. We have previously shown that expression of constitutively-active Notch4 receptor in the endothelium elicits and maintains the hallmarks of BAVM in mice, thus establishing a mouse model of the disease. Our work suggested that Notch pathway could be a critical molecular mediator of BAVM pathogenesis. Here, we investigated the hypothesis that upregulated Notch activation contributes to the pathogenesis of human BAVM. We examined the expression of the canonical Notch downstream target Hes1 in the endothelium of human BAVMs by immunofluorescence, and showed increased levels relative to either autopsy or surgical biopsy controls. We then analyzed receptor activity using an antibody to the activated form of the Notch1 receptor, and found increased levels of activity. These findings suggest that Notch activation may promote the development and even maintenance of BAVM. We also detected increases in Hes1 and activated Notch1 expression in our mouse model of BAVM induced by constitutively active Notch4, demonstrating molecular similarity between the mouse model and the human disease. Our work suggests that activation of Notch signaling is an important molecular candidate in BAVM pathogenesis and further validates that our animal model provides a platform to study the progression as well as the regression of the disease.
Laboratory Investigation (2009) 89, 971–982; doi:10.1038/labinvest.2009.62; published online 22 June 2009

KEYWORDS: angiogenesis; arteriovenous malformation; brain; endothelial cell; Notch signaling; stroke

Brain arteriovenous malformations (BAVMs) are characterized by a nidus of coiled, tortuous, and enlarged vascular lesions that shunt blood directly from feeding arteries to veins.[1] They often rupture, resulting in hemorrhagic stroke in young people, most commonly between 20 and 40 years of age.[1] BAVMs contribute to half of the hemorrhagic strokes in children,[2] and 2% of all strokes.[1] Currently, surgical resection is the primary treatment, but not all BAVMs can be removed safely.[3] Most BAVMs are sporadic, making it difficult to identify the molecular cause by genetic association.[1] To date, the cellular and molecular basis for BAVM pathogenesis remains largely unknown. This limited knowledge of BAVM etiology has impeded the rational design of molecular interventions.

Fundamentally, AVMs are a disruption of normal arteriovenous (AV) hierarchy, which was historically thought to be governed by hemodynamic forces.[4] The discovery of genes with arterial or venous-specific expression in the developing mouse embryo has catalyzed advances in our understanding of the genetic control of AV specification and the establishment of AV hierarchy.[5] Notch, a transmembrane receptor first identified in fruit fly, and involved in cell fate determination and tissue patterning throughout metazoans, has emerged as a critical mediator of AV differentiation.[6] Studies in zebrafish and mouse development demonstrated that Notch signaling was necessary and sufficient for the expression of arterial-specific genes.[6,7] Furthermore, we have demonstrated that endothelial Notch signaling regulates the luminal size of developing mouse arteries by promoting of arterial specification, and increasing the arterial allocation of endothelial cells.[8] Abnormal Notch signaling induced

enlarged AV connections and shunting in both mouse and zebrafish embryo, suggesting a link between AV specification and arteriovenous malformations (AVMs).[6,7]

Among the four mammalian Notch receptors and five ligands, Notch receptors 1 and 4 and their ligands Dll1, Dll4, and Jag1 are preferentially expressed in the arterial and not venous endothelium.[9] Cell–cell mediated activation of the Notch receptor, by ligand binding to the extracellular domain, results in sequential cleavage events and release of an active intracellular domain (ICD).[10] Once cleaved, the ICD translocates to the nucleus, where it must form a complex with the sequence-specific DNA-binding protein Rbpj to promote the transcription of downstream genes.[10] Transcription factors of the Hairy/Enhancer of Split (Hes) and Hes-related families of proteins, such as Hes1, are canonical target genes, and mediate many of Notch's downstream functions.[10] Therefore, Notch-ICD is a constitutively active mutant. Likewise, the Notch4 mutant that lacks the extracellular domain is constitutively cleaved and activated (Notch4*).[11] Thus, nuclear localization of cleaved Notch-ICD and expression of Hes1 are features of active Notch signaling.

To investigate whether upregulation of endothelial Notch signaling can disrupt AV hierarchy and cause AVMs in adult mice, we used a tetracycline-regulated transgenic system to express Notch4* transgene specifically in the endothelium of adult mice (*Notch4*-Tet), and reported AVMs in liver, skin, and uterus.[12] Expression of the transgene in immature *Notch4*-Tet mice during post-natal brain growth resulted in hallmarks of BAVM in all mice, including enlarged and tortuous AV connections, shunting, and hemorrhagic stroke.[13] In both adult and immature *Notch4*-Tet mice, the disease progression was reversed when the *Notch4* transgene was turned off, demonstrating that Notch4* is critical to sustain the disease[12,13] The urgent question that arose out of this fundamental research is whether increased Notch signaling underlies the development and maintenance of human BAVM.

Notch loss-of-function mutations in *JAG1*, *NOTCH3*, and *NOTCH1* are known to cause Alagille syndrome,[14] cerebral autosomal dominant arteriopathy with subcortical infarcts and leukoencephalopathy,[14] and aortic valve anomalies,[15] respectively, but it is not clear whether Notch signaling is involved in human BAVM pathogenesis. In this study, we test the hypothesis that Notch signaling is upregulated in human BAVMs by examining Notch-signaling activity in the endothelium of human BAVM relative to autopsy and surgical biopsy controls. We demonstrate increased levels of the activated-Notch1 receptor and canonical Notch target Hes1 in BAVM tissue. We reveal similar increases in our *Notch4*-Tet mouse model of BAVM-like abnormalities. Our work puts forward the hypothesis that Notch activation causes and maintains human BAVMs, and provides molecular validation of our *Notch4*-Tet model of BAVM as a valuable system to dissect the molecular and cellular basis of BAVM pathogenesis.

MATERIALS AND METHODS
Clinical Samples
The UCSF Committee on Human Research approved the use of human tissue samples for this study. BAVM samples and surgical biopsy controls were obtained by surgical resection and prepared by the UCSF hospital pathology lab. Samples were fixed in 10% neutral-buffered formalin, paraffin embedded, and cut at 5 μm. Control sections were either cerebral cortex or cerebellum. The cerebral cortex control sections were histologically normal temporal lobe from seizure resection cases or cerebral cortex from autopsy brains, which were histologically normal in patients without evidence of neoplastic disease. Cerebellar control sections were also from autopsy brains in patients with no evidence of neoplastic disease. In addition to two autopsy controls from UCSF, five autopsy controls were received as formalin-fixed sections from the Harvard Brain Tissue Resource Center, which is supported in part by PHS Grant number R24-MH 068855. These autopsy samples were also paraffin embedded and cut at 5 μm. Human small intestine biopsy was formalin-fixed, paraffin-imbedded, and sectioned at 5 μm by the UCSF hospital pathology lab. Snap frozen human small intestine tissue samples were provided by the Cooperative Human Tissue Network, which is funded by the National Cancer Institute, and sectioned at 10 μm.

Mice
Brain tissue was harvested from *Notch4*-Tet (Tie2-tTA;TRE-Notch4*) mutants and littermate genetic controls (Tie2-tTA) at post-natal day 20.[13] To suppress the gene expression, Tet sucrose solution (0.5 mg/ml Tet, 50 mg/ml sucrose, Sigma) was administered to pregnant mothers from plugging, and withdrawn from pups at birth as we described.[13] All animals were treated in accordance with the guidelines of the UCSF Institutional Animal Care and Use Committee.

Preparation of Mouse Tissue
Endovascular labeling of perfused vessels was performed with FITC-lectin (Vector Labs, Burlingame, CA, USA) as described.[13] Following perfusion with 1% paraformaldehyde (PFA) at 100 mm Hg, brain tissue was fixed overnight in 4% PFA, and then dehydrated in 70% ethanol in water, and 100% ethanol before xylene treatment and paraffin embedding. Small and large intestine was fixed overnight in 4% PFA, and paraffin-embedded according to the methods used for brain tissue.

Immunofluorescent Staining
For the purposes of comparison, BAVM sections were always stained with control sections. Tissue sections were deparaffinized in xylene and rehydrated. Following antigen retrieval by sodium citrate, the samples were blocked with Avidin/Biotin Blocking Kit (Vector Labs) and then 10% goat-serum and 0.2% Triton X-100 in PBS. Hes1-stained samples were also treated with 500 U/ml DNAse I for 10 min at 37°C

22

(Promega, Madison, WI, USA) before blocking. Primary treatment was performed overnight at 4°C in block. Secondary treatment was performed with biotinylated anti-rabbit or anti-mouse antibodies (Vector Labs) in block. Tertiary treatment was performed with streptavidin-Cy3 in PBS (JacksonImmuno, West Grove, PA, USA). Slides were stored in VectaShield plus DAPI (Vector Labs).

Antibodies

Hes1 antibody was kindly provided by Dr Nadean Brown (at the Children's Hospital Medical Center, Cincinnati, OH, USA). We also used activated-Notch1 antibody (Val1744, Cell Signaling, Beverly, MA, USA) and human CD31 antibody (JC70/A, DAKO, Carpinteria, CA, USA).

Data Analysis

Stained tissue sections were imaged using a $\times 40$ objective on a Zeiss Axiovert fluorescent microscope (Thornwood, NY, USA) with Intelligent Imaging software (Denver, CO, USA). In BAVM sections, the three or four vessels with the strongest endothelial cell staining were imaged. Large vessels with a thick media, characteristic of arteries, were imaged. In autopsy control and surgical biopsy control samples, three or four vessels of similar caliber to the BAVM vessels were imaged. CD31 or non-specific IgG was imaged in the same vessel in adjacent sections. The same exposure time was used for all slides stained with a given antibody and the non-specific IgG control. Individual fluorescent channel intensities were exported as 16-bit TIFF files and analyzed by a blinded examiner using ImageJ. The examiner picked the three cells, lining each vessel lumen, which showed the most intense Hes1 or activated-Notch1 staining by eye. They then circumscribed the DAPI-labeled nuclei of these cells, and measured the mean intensity of Hes1 or activated-Notch1 signal in the enclosed area. Paraffin sections of brain from *Notch4*-Tet (Tie2-tTA:TRE-Notch4*)* mutants and genetic controls *(Tie2-tTA)* were processed in the same way. Hes1 and activated-Notch1 staining in the nuclei of endothelial cells of mouse tissue was normalized to non-specific IgG staining. Staining in human tissue is shown as unadjusted mean intensity values.

Statistical Analysis

Each individual case or control, consisting of at least three intensity measurements from each of three separate vessels, was processed to provide a mean value and s.e.m. A two-tailed Wilcoxon's rank sum non-parametric test was performed with STATA-IC (College Station, TX, USA) to determine the significance of the difference between these mean values from the BAVM cases relative to those of the autopsy controls. The same analysis was performed to determine the significance of the difference in mean values between BAVM cases and surgical biopsy controls.

Confocal Imaging of Crypt Cells

For nuclear localization of Hes1 staining in the crypt cells of human small intestine, sections were imaged using a $\times 63$ oil-immersion objective on a Zeiss LSM510 microscope. The same exposure settings were used for Hes1-stained samples and IgG control.

RESULTS

Notch Signaling Pathway Activity is Increased in the Endothelium of Human BAVMs

To examine Notch activity in BAVMs we analyzed the expression of the canonical Notch downstream target Hes1 in endothelium of human BAVMs by immunofluorescence. We chose Hes1 because it is a direct transcriptional target of activated Notch both *in vitro*[16,17] and *in vivo*[18,19] and because Hes1 antibodies have been well-characterized in immunostaining of Notch gain- and loss-of-function tissue.[20–24] To verify the specificity of the Hes1 antibody in our brain samples, we examined Hes1 staining in a control. In the mouse intestine, Hes1 expression has been well characterized in the nuclei of the crypt cells at the base of the villi.[22,24–26] We found that the Hes1 antibody staining faithfully replicated the established pattern in both paraffin-fixed (Figure 1a, b) and fresh frozen (data not shown) mouse large and small intestine. To confirm the specificity of the Hes1 antibody in human tissue, we also stained paraffin-fixed (Figure 1e) and fresh frozen (data not shown) human small intestine, and found that the Hes1 antibody stained the nuclei of crypt cells in the human tissue as well (Figure 1e–3). As a negative control, we performed staining of adjacent sections of small intestine with the same concentration of non-specific IgG, and did not observe similar patterns (Figure 1c, d, f).

We then stained paraffin sections of human BAVMs by immunofluorescence (Supplementary Table 1). We detected Hes1 protein in areas of the endothelium of human BAVMs (Figure 2b), where it was found in the nuclei of endothelial cells (ECs), consistent with the nuclear localization of the transcription factor (Figure 2b–1).

To determine whether Notch activity was increased in the endothelium of human BAVMs, we compared staining intensity with control human brain sections from autopsy (Supplementary Table 1). We detected little or no Hes1 in autopsy controls, although strong CD31 staining confirmed the endothelium was intact in these samples (data not shown). We quantified this difference by measuring the fluorescent intensity of nuclear Hes1 in the most strongly stained EC nuclei in BAVM samples, and comparing this to controls. We found that the average Hes1 intensity in the strongly stained areas of BAVMs is significantly higher than autopsy controls (Figure 2f; $N = 12$ BAVM samples, $N = 7$ controls; $P = 0.001$). Among individual samples, 9 of 12 BAVM samples had higher mean Hes1 intensity than the most intense autopsy control. As
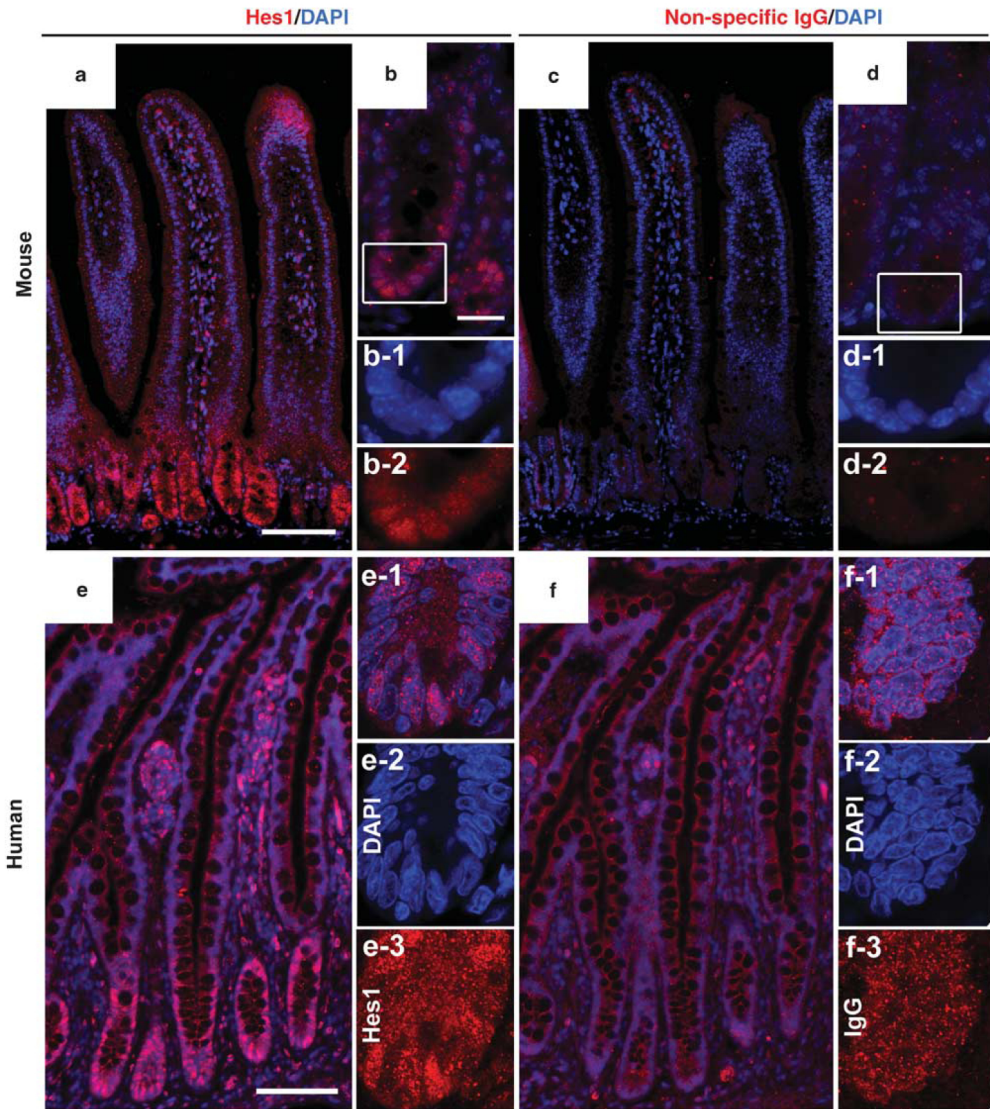
23

Figure 1 Hes1 staining of crypt cell nuclei of the gut confirms antibody specificity. (**a**, **b**) Positive control stained with Hes1 antibody. Typical staining pattern shown by immunofluorescence in the crypt cells of mouse large (**a**) and small intestine (**b**), demonstrates specificity of the Hes1 antibody. High magnification of the crypt (boxed area in **b**) shows co-localization of Hes1 and DAPI nuclear label (**b-1** to **b-2**). (**c–d**) Negative control for Hes1 staining, non-specific IgG in adjacent sections. (**e**) Typical staining pattern shown by immunofluorescence in the crypt cells of human small intestine, demonstrates the specificity of the Hes1 antibody. High magnification confocal imaging of the crypt shows co-localization of Hes1 and DAPI nuclear label (**e-1** to **e-3**). (**f**) Negative control with non-specific IgG in an adjacent section to (**e**) does not show the same staining pattern. Scale bars (**a** & **c**) 100 μm, (**b** & **d**) 50 μm, (**e** & **f**) 100 μm.

a negative control, we used a non-specific IgG primary antibody on adjacent tissue sections, and did not see a similar staining pattern (Figure 2c).

Autopsy samples are excellent controls for human BAVM because they are screened for the absence of any detectable brain pathologies, however they are not subject to the same
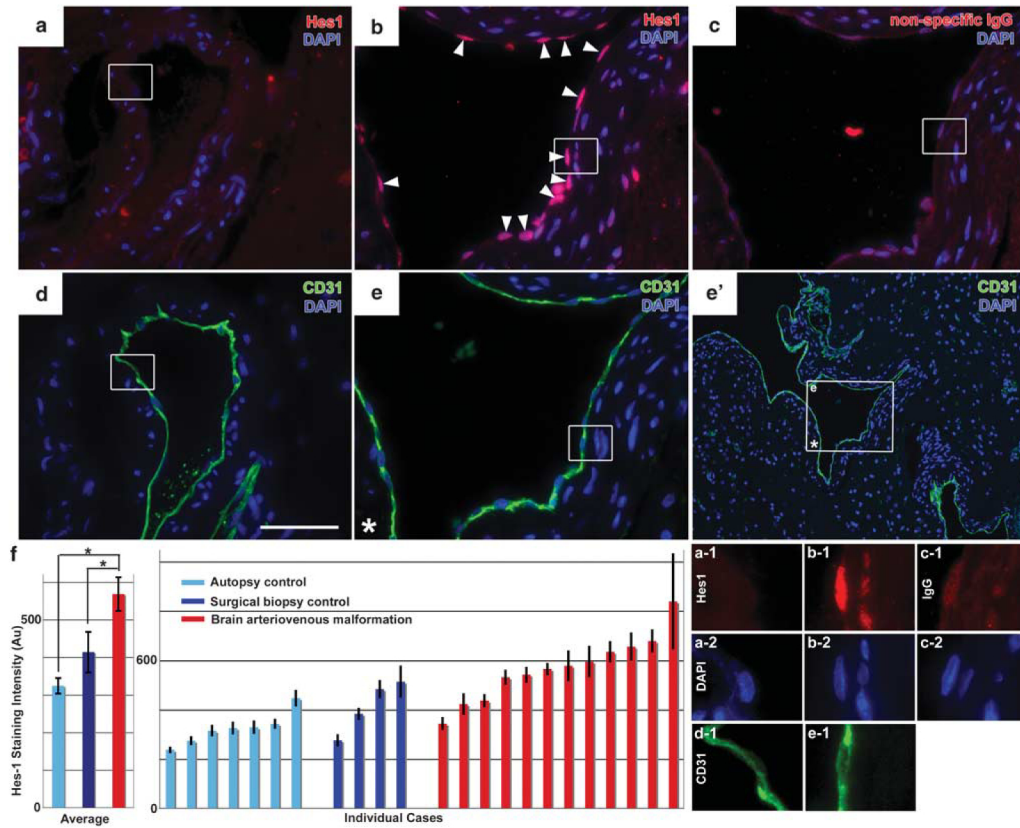
24

Figure 2 Increased Hes1 staining in the endothelium of human brain arteriovenous malformations (BAVMs). (**a**, **b**) Immunofluorescent staining for Hes1 in paraffin sections from surgical biopsy controls (**a**) and human BAVMs (**b**). Increased Hes1 staining is evident in the endothelium of human BAVMs (arrowheads, **b**). (**c**) Negative control for Hes1 staining, non-specific IgG in an adjacent section to (**b**). (**d** & **e**) CD31-stained sections adjacent to (**a** & **b**), respectively. Low-magnification (**e′**) shows the location of (**e**) within a large vascular structure (box with asterisk). High magnification of the boxed areas in (**a**–**e**) shows co-localization of Hes1 staining with the DAPI nuclear label (**a-1** to **c-1** and **a-2** to **c-2**) in cells lining CD31-labeled vessels (**d-1** & **e-1**). (**f**) Quantification of Hes1 staining in BAVM cases and autopsy or surgical biopsy controls. Scale bars (**a**–**e**) 200 μm. In graph ($N = 12$ BAVM samples, $N = 7$ autopsy controls, $N = 4$ biopsy controls; BAVM *vs* autopsy controls $P = 0.0003$; BAVM *vs* biopsy controls $P = 0.05$). Average represents mean ± s.e.m. of cases. Individual cases represent mean ± s.e.m. of individual endothelial cells in each case.

surgical manipulation as BAVM biopsies, and not fixed as quickly. This difference in tissue handling is particularly important because Hes1 can be degraded within hours in some non-endothelial cell types.[27] Therefore, we also examined levels of Hes1 staining in ECs of surgical brain biopsies from patients without BAVM (Supplementary Table 1), controls which are subject to the same manipulation and fixation as BAVM samples. Since brain biopsies are not taken from patients with normal brain function, we have selected biopsy samples from the least affected patients, to minimize the potential effects of brain pathology. The combination of these controls provides the most vigorous baseline expression. We found that, as in the autopsy controls,

levels of Hes1 staining in the nuclei of ECs was low or absent (Figure 2a, a-1). We quantified staining intensity in these samples, as we did in the autopsy controls. We found that average Hes1 intensity in BAVMs is significantly higher than in biopsy controls (Figure 2f; $N = 12$ BAVM samples, $N = 4$ controls; $P = 0.039$). Among individual samples, 9 of 12 BAVM samples had higher mean Hes1 intensity than the most intense surgical biopsy control. As a negative control, we used a non-specific IgG primary antibody on adjacent tissue sections, and did not see a similar staining pattern (Figure 2c). CD31 staining confirmed the integrity of the endothelium in tissue sections from BAVMs (Figure 2e) and surgical biopsy controls (Figure 2d).
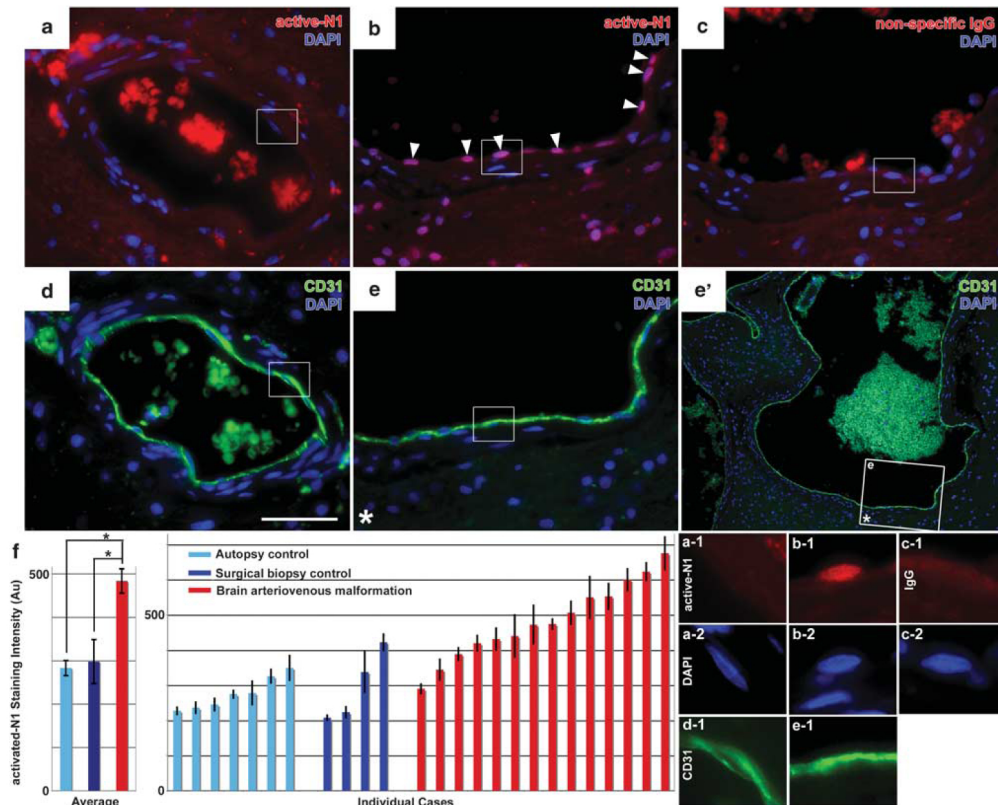
25

Figure 3 Increased activated-Notch1 staining in the endothelium in human brain arteriovenous malformations (BAVMs). (**a**, **b**) Immunofluorescent staining for activated-Notch1 in paraffin sections from surgical biopsy controls (**a**) and human BAVMs (**b**). Increased activated-Notch1 staining is evident in the endothelium of human BAVMs (arrowheads, **b**). (**c**) Negative control for activated-Notch1 antibody staining, non-specific IgG in an adjacent section to (**b**). (**d** & **e**) CD31 stained adjacent sections to (**a** & **b**) respectively. Low-magnification (**e′**) shows the location of the stained area within a large vascular structure (box with asterisk). (**f**) High magnification of the boxed areas shows co-localization of activated-Notch1 staining with the DAPI nuclear label (**a-1** to **c-1** and **a-2** to **c-2**) in cells lining the CD31-labeled vessels (**d-1** & **e-1**). (**f**) Quantification of activated-Notch1 staining in BAVM cases and autopsy or surgical biopsy controls ($N = 14$ BAVM samples, $N = 7$ autopsy controls, $N = 4$ biopsy controls; BAVM vs autopsy controls $P = 0.0001$; BAVM vs biopsy controls $P = 0.008$). Scale bar is 200 μm. Average represents mean $\pm$ s.e.m. of cases. Individual cases represent mean $\pm$ s.e.m. of individual endothelial cells in each case.

To examine Notch receptor activation directly, we measured the levels of activated-Notch1 by immunofluorescence in our sample set. We chose to use the activated-Notch1 antibody because it has previously been validated in mouse tissue[28,29] and also detects human forms of activated-Notch1,[30] since it was raised against a human antigen. As with Hes1, we found that ECs in some of the vessels of BAVM biopsy were strongly positive (Figure 3b). In these ECs, we detected activated-Notch1 in the nucleus, consistent with the nuclear translocation of the activated receptor (Figure 3b–1). As a negative control, we stained adjacent sections of brain with the same concentration of non-specific IgG, and did not observe the same pattern (Figure 3c, c-1). Nuclear staining in

autopsy or surgical biopsy controls was not as intense as in BAVM samples (Figure 3a, a-1). We quantified differences in activated-Notch1 staining between BAVM samples and autopsy or surgical biopsy controls, and found that average activated-Notch1 intensity in BAVM is significantly higher than autopsy controls (Figure 3f; $N = 14$ BAVM samples, $N = 7$ autopsy controls; $P = 0.0006$), and surgical biopsy controls (Figure 3f; $N = 4$ biopsy controls; $P = 0.015$). Among individual samples, 12 of 14 BAVM samples had higher mean activated-Notch1 intensity than the most intense autopsy control, and 10 of 14 had higher mean activated-Notch1 intensity than the most intense surgical biopsy control.

26

Notch-signaling Pathway Activity is Increased in Murine BAVM-like Abnormalities Caused by Endothelial-specific Expression of Notch4*

We previously reported that endothelial expression of Notch4*, encoding the truncated intracellular domain of Notch4, results in Notch4* activity, indicated by nuclear localization of the intracellular domain of the Notch4 receptor.[13] However, because Notch4 antibody staining cannot differentiate between the Notch4* transgene and endogenous Notch4, we were unable to determine whether Notch4* expression increased endogenous Notch signaling. We also demonstrated the increased expression of Notch downstream genes in whole tissue homogenate from Notch4*-Tet mice,[12] but the lack of spatial resolution prevented the identification of the cells in which Notch signaling was activated. Here, we tested whether endogenous Notch1 activity and expression of Notch downstream target Hes1 is upregulated in the endothelium of Notch4*-Tet mice.

To determine whether expression of Notch4* increased Notch-signaling activity in the endothelium during BAVM formation in Notch4*-Tet mice, we examined the expression of the canonical Notch downstream gene Hes1 in paraffin-fixed brain sections from Notch4*-Tet mice with BAVM-like abnormalities. We detected Hes1 in the nuclei of ECs, consistent with the nuclear localization of the transcription factor (Figure 4a, a-1). To control for non-specific staining, we stained an adjacent section with non-specific IgG of the host species used to generate the Hes1 antibody, at the same concentration as the specific primary (Figure 4c, c-1). Nuclear staining in genetic controls was not as intense as in Notch4*-Tet mice (Figure 4b, b-1). Antibody staining intensity was calculated from the ratio of Hes1 staining to non-specific IgG staining. We found an increase in Hes1 signal intensity in the Notch4*-expressing mice, relative to controls (Figure 4d; $N=5$ controls, $N=3$ Notch4*-Tet mutants; $P=0.0253$).

To determine whether expression of Notch4* increased levels of endogenous Notch signaling, we examined the levels of activated-Notch1 in the endothelium in paraffin-fixed brain sections from Notch4*-Tet mice using an antibody to the activated form of Notch1. We detected activated-Notch1 in the nuclei of ECs, consistent with the nuclear translocation of the activated-Notch1 receptor (Figure 5a, a-1). We controlled for non-specific staining and quantified staining intensity as we had for Hes1 (Figure 5c). Nuclear staining in genetic controls was not as intense as in Notch4*-Tet mice (Figure 5b, b-1). We found increased levels of activated-Notch1 signal intensity in Notch4*-Tet mice, relative to controls (Figure 5d; $N=5$ controls, $N=3$ Notch4*-Tet mutants; $P=0.0253$).

In summary, we show that Notch signaling is increased in human BAVM, using the same tissue preparation, antibodies, and quantification that we use to show increased Notch-signaling in our Notch4*-Tet transgenic mouse model of the disease.

DISCUSSION

Our study demonstrates that Notch activity is increased in human BAVMs, supporting the hypothesis that Notch activation causes and maintains human BAVM.

We found increased levels of the canonical Notch downstream gene Hes1 in the endothelium of human BAVMs relative to levels in autopsy or surgical biopsy controls, as well as increased levels of activated-Notch1 receptor. Furthermore, we demonstrate molecular similarity between the BAVM-like abnormalities of our Notch4*-Tet mouse model and human BAVM, providing molecular validation for this model of the human disease.

Notch Signaling is Increased in the Endothelium of Human BAVM

Hes1 is a canonical Notch downstream gene, and increased endothelial Hes1 expression indicates increased endothelial Notch pathway activity. Hes1 is a direct transcriptional target of Notch activity.[16] In the vascular endothelium, Hes1 expression is regulated by Notch activity. Transfection of human umbilical vein endothelial cells with Notch4* resulted in an approximately sixfold increase in Hes1 expression by quantitative PCR.[17] Hes1 expression is also increased by the induction of endogenous endothelial Notch signaling in vitro[31] and general Notch signaling in vivo.[32] Conversely, interference with endogenous endothelial Notch signaling decreases Hes1 expression in vitro.[31] and in vivo[18,19] Therefore, increased Hes1 expression in the endothelium of human BAVMs indicates increased Notch-signaling activity.

The specificity of Hes1 staining in BAVM is supported by extensive evaluation in mouse and human tissue. We systematically tested five Hes1 antibodies on frozen and paraffin-fixed tissue, and found that only one gave the expected staining pattern in the positive controls, intestinal crypt cells in mouse and human tissue. We chose this positive control because the distinctive crypt-specific Hes1 expression pattern has been repeatedly demonstrated at both the protein and RNA level by several investigators.[22,24–26] Demonstrating its dependence on Notch signaling, Hes1 protein expression in the crypt cells is lost when Notch receptors are deleted in the crypt cells, or the γ-secretase activity required for Notch receptor activation is pharmacologically blocked.[22,24] The specificity of staining with this particular Hes1 antibody has been reported in both frozen and paraffin-fixed mouse tissue.[20,21,33] Although the mouse-derived antigen used to generate the antibody is 90% similar to human Hes1,[20] confirmation of Hes1 staining in human crypt cells was a critical step to verify the antibody-detected Hes1 in human as well as mouse tissue. Our finding of increased Hes1 expression in the endothelium of human BAVMs is strongly supported by the validation of antibody specificity in positive controls.

Notch1 is a critically important receptor in the endothelium, and the upregulation of Notch1 activity that we
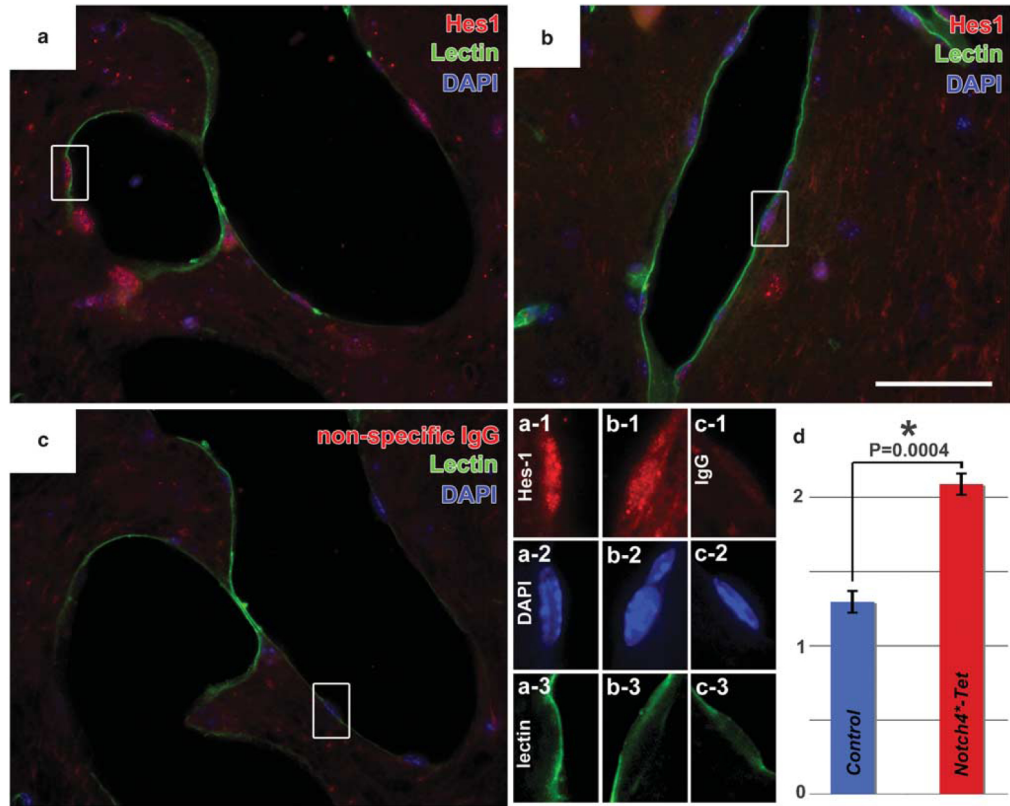
27

Figure 4 Increased Hes1 staining in the endothelium of the *Notch4*-Tet* mouse model of brain arteriovenous malformation (BAVM)-like lesions.
(**a**–**b**) Immunofluorescent staining for Hes1 in paraffin sections from *Notch4*-Tet* mice (**a**) and genetic controls (**b**). Increased Hes1 staining is evident in the endothelium of FITC-lectin perfused vessels in *Notch4*-Tet* mice. (**c**) Negative control for Hes1 staining, non-specific IgG in an adjacent section to (**a**). High magnification of the boxed areas shows co-localization of Hes1 staining with the DAPI nuclear label (a-1 to c-1 and a-2 to c-2) in cells lining the lectin-perfused vessel lumen (a-3 to c-3). (**d**) Quantification of Hes1 staining relative to non-specific IgG staining in Notch4*-expressing mutant mice and controls ($N = 5$ genetic controls, $N = 3$ *Notch4*-Tet* mutants, values represent mean ± s.e.m., $P = 0.0004$). Scale bars (a–c) 200 μm.

have demonstrated in human BAVM may be involved in the development and progression of the disease. Notch1 is necessary for vascular development, and subtle changes in Notch1 levels in humans and mice can cause severe vascular defects.[6] In humans, inheritance of a single mutated loss-of-function allele of Notch1 can cause aortic valve disease and increase the risk of thoracic aorta anuerysm.[15,34] Studies in mice demonstrated the importance of endothelial Notch1 signaling, because endothelial-specific deletion of just one Notch1 allele significantly impaired blood flow recovery in the hindlimb after the femoral artery was occluded,[31] and deletion of both alleles is embryonic lethal.[8,31] At a cellular level, Notch1 deletion in endothelial cells increases their contribution to angiogenic sprouts rather than retention in existing vessels.[36] Expression of the constitutively active in-

tracellular domain of the Notch1 receptor (Notch1-ICD) specifically in the endothelium is also embryonic lethal[37] (our own unpublished data). We found that even at an adult stage, expression of Notch1* in the endothelium was sufficient to cause vascular malformations,[12] demonstrating a requirement for Notch-signaling homeostasis in adult mice. Therefore, the requirement for tightly regulated Notch1 signaling in the endothelium suggests that the increased activity we observed may disrupt vascular organization.

The cause for upregulated Notch activity in the endothelial cells of BAVM is not yet apparent. Elevated activity may be a secondary effect of BAVM formation. For example, the endothelial cells of BAVMs are exposed to a massive increase in blood flow, which has been shown to increase the expression of Notch ligand *Jag1*, *Notch4* receptor, and down-
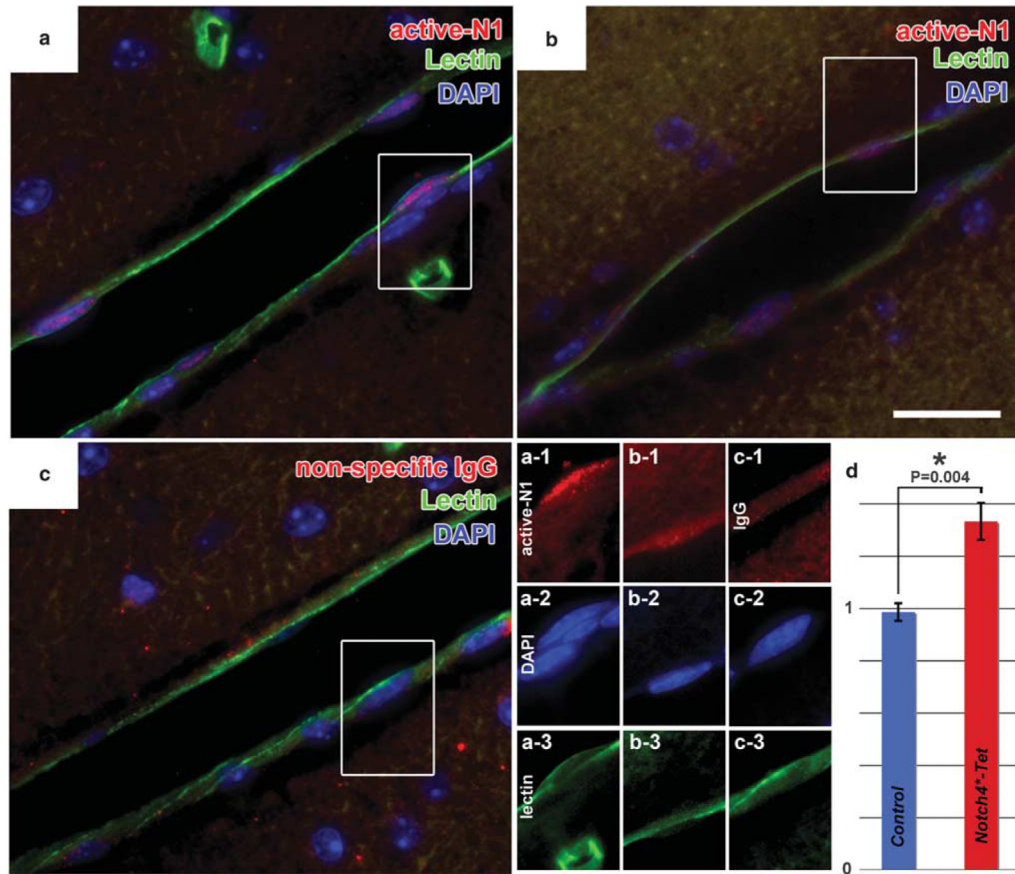
Figure 5 Increased activated-Notch1 staining in the endothelium of the *Notch4*-*Tet* mouse model of brain arteriovenous malformation (BAVM)-like lesions. (**a**, **b**) Immunofluorescent staining for activated-Notch1 in paraffin sections from *Notch4*-*Tet* mice (**a**) and genetic controls (**b**). Increased activated-Notch1 staining is evident in the endothelium of FITC-lectin perfused vessels in *Notch4*-*Tet* mice (**a**). (**c**) Negative control for activated-Notch1 staining, non-specific IgG in an adjacent section to (**a**). High magnification of the boxed areas shows co-localization of activated-Notch1 staining with the DAPI nuclear label (a-1 to c-1 and a-2 to c-2) in cells lining the lectin-perfused vessel lumen (a-3 to c-3). (**d**) Quantification of activated-Notch1 staining relative to non-specific IgG staining in Notch4*-expressing mutant mice and controls. ($N = 5$ genetic controls, $N = 3$ *Notch4*-*Tet* mutants, values represent mean $\pm$ s.e.m., $P = 0.004$). Scale bar is 100 μm.

stream genes *Hey1* and *ephrin-B2* in endothelial cells *in vitro*.[38,39] However, our animal data have demonstrated that increased Notch4 signaling can initiate BAVM-like pathology in mice,[13] suggesting that the elevated Notch activity may be a causal molecular lesion. Therefore, increased Notch activity seen in human BAVM may not only be a secondary effect of increased blood flow, but may also be an initial molecular pathology.

The increase in Notch activity in the endothelium of human BAVM appears subtle, but this small change is likely sufficient to cause biological effects. Haploinsufficiencies of Notch1[15,34] or its ligands Dll1,[35] Dll4,[18,40,41] and Jag1[42]

impair vascular function in mice and humans. Of the ligands, Dll4 may be the most critical, because haploinsufficiency of this gene is embryonic lethal.[18,40,41] Such sensitivity in the endothelium to receptor or ligand dosage is rare; vascular endothelial growth factor A (Vegfa) is the only other protein known to exert such profound vascular effects as a result of haploinsufficiency.[43,44] Other biological systems have shown a similar threshold requirement for Notch activity. For example, in left–right differentiation in the chick, a transient increase in extracellular calcium slightly increases Notch receptor activation on the left side of the developing embryo,[45] resulting in the subsequent establishment of asymmetry.

29

Similarly, in neuronal development in the fly, small changes in Notch activity between daughter cells are necessary to establish asymmetric fates, and mutations that cause either a general increase or decrease in Notch signaling results in loss of asymmetry.[46] Therefore, even small changes in the level of Notch activity have the potential to cause severe vascular effects.

Notch Activation may be a Key Regulator of BAVM Development

Our study demonstrates increased Notch-pathway activation in the endothelium of human BAVM. Until now, the involvement of Notch signaling in the development of human BAVM has not been reported. Genetic understanding of human BAVM has been limited by the sporadic nature of the disease. An exception is the development of BAVM in 10–20% of patients suffering from the autosomal-dominant disease Hereditary Hemorrhagic Telangectasia (HHT).[47] HHT causes widespread AVMs through many tissues, including the brain, and has been linked to mutations in the TGF-β receptors *Alk1 (ACVRL1)* and *endoglin (ENG)*.[48] Although HHT is implicated in only 2% of all BAVM,[49] it has been the most studied pathway in human BAVM due to this genetic association. In mouse models, homozygous mutations in these receptors are embryonic lethal, and heterozygous mutations result in vessel enlargement and hemorrhage, although high-flow arteriovenous shunting characteristic of BAVMs has not been reported.[50–55] The low penetrance and focal development of BAVMs in HHT suggest that other causes, potentially other signaling pathways, cooperate with the TGF-β mutations to cause this pattern of BAVM development.

Other endothelial-signaling pathways appear to be upregulated in human BAVM samples, although animal studies have not demonstrated that these changes induce BAVM. *VEGFA* expression in the BAVM nidus has been observed at both the RNA and protein level and is increased at the RNA level in whole-tissue homogenate of the BAVM nidus relative to control brain biopsies.[56] However, while forced expression of VEGFA in the mouse brain results in increased angiogenesis, development of AV shunting has not been reported.[57–61] Similarly, increased expression of *angiopoietin-2 (ANGPT2)* has been reported at the RNA and protein level in the BAVM nidus[56,62] but expression of *ANGPT2* in the adult mouse brain has not been reported to result in AV shunting.[59] Gain- and loss-of-function mutations in *ANGPT2*'s endothelial receptor, *TIE2 (TEK)*, have been associated with venous malformations, but not AVMs.[63] *Integrin alpha V (ITGAV)* was also upregulated in the endothelium and smooth muscle cells of BAVMs.[56] However, no gain-of-function animal studies have been reported. Complete endothelial deletion of *Itgav* causes no detectable cerebrovascular defects,[64] although deletion of *Itgav* in neuronal cells results in dilation of blood vessels and hemorrhage,[64] suggesting a role in vascular stability through paracrine

effects, but not cell autonomous vascular effects. Therefore, the molecular basis of BAVM pathogenesis remains largely unknown.

Increased endothelial Notch signaling is sufficient to induce vascular abnormalities with the hallmarks of BAVM in *Notch4*-Tet* mice, and an increase in both Hes1 and activated-Notch1 protein in *Notch4*-Tet* mice demonstrates similarity at the molecular level to the human disease. We have reported that expression of constitutively active Notch4 receptor in the endothelium of our *Notch4*-Tet* mice results in enlarged and tortuous BAVM-like vascular abnormalities, shunting of blood, and hemorrhagic stroke.[13] Here, we demonstrate that Notch activity is increased in the endothelium of human BAVM, as it is in *Notch4*-Tet* mice. We found similar increases in Hes1 and activated-Notch1 in human BAVM and BAVM-like abnormalities in *Notch4*-Tet* mice. One key difference between human BAVM and the mouse model is that human BAVMs are focal,[1] whereas the BAVM-like abnormalities in *Notch4*-Tet* mice are pervasive.[13] This is likely a consequence of the transgenic expression of constitutively active Notch4 throughout the endothelium in the mouse model. Therefore, increased expression of Hes1 and activated-Notch1 demonstrates molecular similarity between BAVM-like abnormalities in *Notch4*-Tet* mouse model, caused by increased endothelial Notch activity, and human BAVMs.

It is commonly thought that, once they develop, BAVMs do not regress, but remain as a constant threat of hemorrhagic stroke.[65] Our animal studies have suggested the tantalizing possibility that, in animals at least, BAVM-like lesions are reversible.[13] The dependence of BAVMs on the activity of molecular-signaling pathways is a novel concept, but we have also shown that AVMs that form in the livers of *Notch4*-Tet* mice regress completely after the Notch4* transgene is suppressed, demonstrating that endogenous machinery exists for the reversal of AVMs once the causative molecular lesion is removed.[12] Our human data does not demonstrate that increased Notch activity promotes the development and growth of BAVM in humans. Nonetheless, we found that Notch activity is upregulated in a large portion of human BAVMs, after their initiation, suggesting that increased Notch activation may be a potential molecular lesion in human BAVM pathogenesis.

In conclusion, this study demonstrates increased activation of endothelial Notch signaling, which we have shown causes BAVM-like abnormalities in mice, in human BAVMs. It suggests that activation of Notch signaling is an important molecular candidate in BAVM pathogenesis, and further validates that our animal model provides a platform to study BAVM progression and regression. These findings open a new area of research to advance the knowledge and treatment of this devastating disease.

1. Friedlander RM. Clinical practice. Arteriovenous malformations of the brain. N Engl J Med 2007;356:2704–2712.
2. Meyer-Heim AD, Boltshauser E. Spontaneous intracranial haemorrhage in children: aetiology, presentation and outcome. Brain Dev 2003;25:416–421.
3. Stapf C, Mohr JP, Choi JH, et al. Invasive treatment of unruptured brain arteriovenous malformations is experimental therapy. Curr Opin Neurol 2006;19:63–68.
4. Thoma R. Untersuchungen über die Histogenese und Histomechanik des Gefässsytems. Ferdinand Enke: Stuttgart, 1893.
5. Wang HU, Chen ZF, Anderson DJ. Molecular distinction and angiogenic interaction between embryonic arteries and veins revealed by ephrin-B2 and its receptor Eph-B4. Cell 1998;93:741–753.
6. Gridley T. Notch signaling in vascular development and physiology. Development 2007;134:2709–2718.
7. Lawson ND, Scheer N, Pham VN, et al. Notch signaling is required for arterial-venous differentiation during embryonic vascular development. Development 2001;128:3675–3683.
8. Kim YH, Hu H, Guevara-Gallardo S, et al. Artery and vein size is balanced by Notch and ephrin B2/EphB4 during angiogenesis. Development 2008;135:3755–3764.
9. Hofmann JJ, Iruela-Arispe ML. Notch signaling in blood vessels: who is talking to whom about what? Circ Res 2007;100:1556–1568.
10. Bray SJ. Notch signalling: a simple pathway becomes complex. Nat Rev Mol Cell Biol 2006;7:678–689.
11. Kopan R, Schroeter EH, Weintraub H, et al. Signal transduction by activated mNotch: importance of proteolytic processing and its regulation by the extracellular domain. Proc Natl Acad Sci USA 1996;93:1683–1688.
12. Carlson TR, Yan Y, Wu X, et al. Endothelial expression of constitutively active Notch4 elicits reversible arteriovenous malformations in adult mice. Proc Natl Acad Sci USA 2005;102:9884–9889.
13. Murphy PA, Lam MT, Wu X, et al. Endothelial Notch4 signaling induces hallmarks of brain arteriovenous malformations in mice. Proc Natl Acad Sci USA 2008;105:10901–10906.
14. Roca C, Adams RH. Regulation of vascular morphogenesis by Notch signaling. Genes Dev 2007;21:2511–2524.
15. Garg V, Muth AN, Ransom JF, et al. Mutations in NOTCH1 cause aortic valve disease. Nature 2005;437:270–274.
16. Jarriault S, Brou C, Logeat F, et al. Signalling downstream of activated mammalian Notch. Nature 1995;377:355–358.
17. Shawber CJ, Das I, Francisco E, et al. Notch signaling in primary endothelial cells. Ann N Y Acad Sci 2003;995:162–170.
18. Gale NW, Dominguez MG, Noguera I, et al. Haploinsufficiency of delta-like 4 ligand results in embryonic lethality due to major defects in arterial and vascular development. Proc Natl Acad Sci USA 2004;101:15949–15954.
19. Dou GR, Wang YC, Hu XB, et al. RBP-J, the transcription factor downstream of Notch receptors, is essential for the maintenance of vascular homeostasis in adult mice. FASEB J 2008;22:1606–1617.
20. Lee HY, Wroblewski E, Philips GT, et al. Multiple requirements for Hes 1 during early eye formation. Dev Biol 2005;284:464–478.
21. Blanpain C, Lowry WE, Pasolli HA, et al. Canonical notch signaling functions as a commitment switch in the epidermal lineage. Genes Dev 2006;20:3022–3035.
22. Ridgway J, Zhang G, Wu Y, et al. Inhibition of Dll4 signalling inhibits tumour growth by deregulating angiogenesis. Nature 2006;444:1083–1087.
23. Fre S, Huyghe M, Mourikis P, et al. Notch signals control the fate of immature progenitor cells in the intestine. Nature 2005;435:964–968.
24. Riccio O, van Gijn ME, Bezdek AC, et al. Loss of intestinal crypt progenitor cells owing to inactivation of both Notch1 and Notch2 is accompanied by derepression of CDK inhibitors p27Kip1 and p57Kip2. EMBO Rep 2008;9:377–383.
25. Jensen J, Pedersen EE, Galante P, et al. Control of endodermal endocrine development by Hes-1. Nat Genet 2000;24:36–44.
26. van Es JH, van Gijn ME, Riccio O, et al. Notch/gamma-secretase inhibition turns proliferative cells in intestinal crypts and adenomas into goblet cells. Nature 2005;435:959–963.
27. Hirata H, Yoshiura S, Ohtsuka T, et al. Oscillatory expression of the bHLH factor Hes1 regulated by a negative feedback loop. Science 2002;298:840–843.
28. Geffers I, Serth K, Chapman G, et al. Divergent functions and distinct localization of the Notch ligands DLL1 and DLL3 in vivo. J Cell Biol 2007;178:465–476.
29. Lin MH, Kopan R. Long-range, nonautonomous effects of activated Notch1 on tissue homeostasis in the nail. Dev Biol 2003;263:343–359.
30. Niranjan T, Bielesz B, Gruenwald A, et al. The Notch pathway in podocytes plays a role in the development of glomerular disease. Nat Med 2008;14:290–298.
31. Takeshita K, Satoh M, Li M, et al. Critical role of endothelial Notch1 signaling in postnatal angiogenesis. Circ Res 2007;100:70–78.
32. Tetzlaff MT, Yu W, Li M, et al. Defective cardiovascular development and elevated cyclin E and Notch proteins in mice lacking the Fbw7 F-box protein. Proc Natl Acad Sci USA 2004;101:3338–3345.
33. Yaron O, Farhy C, Marquardt T, et al. Notch1 functions to suppress cone-photoreceptor fate specification in the developing mouse retina. Development 2006;133:1367–1378.
34. McKellar SH, Tester DJ, Yagubyan M, Majumdar R, Ackerman MJ, Sundt 3rd TM. Novel NOTCH1 mutations in patients with bicuspid aortic valve disease and thoracic aortic aneurysms. J Thorac Cardiovasc Surg 2007;134:290–296.
35. Limbourg A, Ploom M, Elligsen D, et al. Notch ligand Delta-like 1 is essential for postnatal arteriogenesis. Circ Res 2007;100:363–371.
36. Hellstrom M, Phng LK, Hofmann JJ, et al. Dll4 signalling through Notch1 regulates formation of tip cells during angiogenesis. Nature 2007;445:776–780.
37. Venkatesh DA, Park KS, Harrington A, et al. Cardiovascular and hematopoietic defects associated with Notch1 activation in embryonic Tie2-expressing populations. Circ Res 2008;103:423–431.
38. Chen BP, Li YS, Zhao Y, et al. DNA microarray analysis of gene expression in endothelial cells in response to 24-h shear stress. Physiol Genomics 2001;7:55–63.
39. Dai G, Kaazempur-Mofrad MR, Natarajan S, et al. Distinct endothelial phenotypes evoked by arterial waveforms derived from atherosclerosis-susceptible and -resistant regions of human vasculature. Proc Natl Acad Sci USA 2004;101:14871–14876.
40. Krebs LT, Shutter JR, Tanigaki K, et al. Haploinsufficient lethality and formation of arteriovenous malformations in Notch pathway mutants. Genes Dev 2004;18:2469–2473.
41. Duarte A, Hirashima M, Benedito R, et al. Dosage-sensitive requirement for mouse Dll4 in artery development. Genes Dev 2004;18:2474–2478.
42. Oda T, Elkahloun AG, Pike BL, et al. Mutations in the human Jagged1 gene are responsible for Alagille syndrome. Nat Genet 1997;16:235–242.
43. Ferrara N, Carver-Moore K, Chen H, et al. Heterozygous embryonic lethality induced by targeted inactivation of the VEGF gene. Nature 1996;380:439–442.
44. Carmeliet P, Ferreira V, Breier G, et al. Abnormal blood vessel development and lethality in embryos lacking a single VEGF allele. Nature 1996;380:435–439.
45. Raya A, Kawakami Y, Rodriguez-Esteban C, et al. Notch activity acts as a sensor for extracellular calcium during vertebrate left-right determination. Nature 2004;427:121–128.
46. Guo M, Jan LY, Jan YN. Control of daughter cell fates during asymmetric division: interaction of Numb and Notch. Neuron 1996;17:27–41.
47. Begbie ME, Wallace GM, Shovlin CL. Hereditary haemorrhagic telangiectasia (Osler-Weber-Rendu syndrome): a view from the 21st century. Postgrad Med J 2003;79:18–24.
48. Abdalla SA, Letarte M. Hereditary haemorrhagic telangiectasia: current views on genetics and mechanisms of disease. J Med Genet 2006;43:97–110.
49. Matsubara S, Mandzia JL, ter Brugge K, et al. Angiographic and clinical characteristics of patients with cerebral arteriovenous malformations

31

associated with hereditary hemorrhagic telangiectasia. AJNR Am J Neuroradiol 2000;21:1016–1020.

50. Bourdeau A, Faughnan ME, McDonald ML, *et al*. Potential role of modifier genes influencing transforming growth factor-beta1 levels in the development of vascular defects in endoglin heterozygous mice with hereditary hemorrhagic telangiectasia. Am J Pathol 2001;158:2011–2020.

51. Arthur HM, Ure J, Smith AJ, *et al*. Endoglin, an ancillary TGFbeta receptor, is required for extraembryonic angiogenesis and plays a key role in heart development. Dev Biol 2000;217: 42–53.

52. Torsney E, Charlton R, Diamond AG, *et al*. Mouse model for hereditary hemorrhagic telangiectasia has a generalized vascular abnormality. Circulation 2003;107:1653–1657.

53. Li DY, Sorensen LK, Brooke BS, *et al*. Defective angiogenesis in mice lacking endoglin. Science 1999;284:1534–1537.

54. Bourdeau A, Faughnan ME, Letarte M. Endoglin-deficient mice, a unique model to study hereditary hemorrhagic telangiectasia. Trends Cardiovasc Med 2000;10:279–285.

55. Srinivasan S, Hanes MA, Dickens T, *et al*. A mouse model for hereditary hemorrhagic telangiectasia (HHT) type 2. Hum Mol Genet 2003;12:473–482.

56. Hashimoto T, Lawton MT, Wen G, *et al*. Gene microarray analysis of human brain arteriovenous malformations. Neurosurgery 2004;54: 410–423; discussion 423–425.

57. Yang GY, Xu B, Hashimoto T, *et al*. Induction of focal angiogenesis through adenoviral vector mediated vascular endothelial cell growth factor gene transfer in the mature mouse brain. Angiogenesis 2003;6:151–158.

58. Xu B, Wu YQ, Huey M, *et al*. Vascular endothelial growth factor induces abnormal microvasculature in the endoglin heterozygous mouse brain. J Cereb Blood Flow Metab 2004;24:237–244.

59. Zhu Y, Lee C, Shen F, *et al*. Angiopoietin-2 facilitates vascular endothelial growth factor-induced angiogenesis in the mature mouse brain. Stroke 2005;36:1533–1537.

60. Zhu Y, Shwe Y, Du R, *et al*. Effects of angiopoietin-1 on vascular endothelial growth factor-induced angiogenesis in the mouse brain. Acta Neurochir Suppl 2006;96:438–443.

61. Hao Q, Su H, Marchuk DA, *et al*. Increased tissue perfusion promotes capillary dysplasia in the ALK1-deficient mouse brain following VEGF stimulation. Am J Physiol Heart Circ Physiol 2008;295:H2250–H2256.

62. Hashimoto T, Lam T, Boudreau NJ, *et al*. Abnormal balance in the angiopoietin-tie2 system in human brain arteriovenous malformations. Circ Res 2001;89:111–113.

63. Limaye N, Wouters V, Uebelhoer M, *et al*. Somatic mutations in angiopoietin receptor gene TEK cause solitary and multiple sporadic venous malformations. Nat Genet 2009;41:118–124.

64. McCarty JH, Lacy-Hulbert A, Charest A, *et al*. Selective ablation of alphav integrins in the central nervous system leads to cerebral hemorrhage, seizures, axonal degeneration and premature death. Development 2005;132:165–176.

65. ApSimon HT, Reef H, Phadke RV, *et al*. A population-based study of brain arteriovenous malformation: long-term treatment outcomes. Stroke 2002;33:2794–2800.

32

Notch reversibly converts veins to arteries and regulates arteriovenous hierarchy in mice

Patrick A. Murphy[1], Tyson N. Kim[1], Andrew W. Bollen[2], Chris B. Schaffer[3], Rong A. Wang[1]

Affiliations:

Laboratory for Accelerated Vascular Research, Division of Vascular Surgery,

Department of Surgery, University of California, San Francisco

Department of Pathology, University of California, San Francisco

Department of Biomedical Imaging, Cornell University

Key words: Angiogenesis, Notch, Arterial Specification, Arteriovenous malformation, Endothelial Cell, Cerebrovascular

<u>**Summary**</u>

Although genetic programs are implicated in arterial venous (AV) differentiation in embryos, whether AV specification structurally determines AV hierarchy is unknown. Here, using two-photon excited fluorescent (2PEF) 4D imaging with cellular resolution in living mice, we demonstrate that endothelial expression of a constitutively-active, pro-arterial gene, Notch4 (Notch4*), caused high-flow AV shunts by arterializing the venous portion of the AV connections. Turning off Notch4* restored the venous identity and normal AV hierarchy by causing specific regression of AV shunts. The normalization of

the high-flow AV shunts required EphB4 signaling and involved the prompt loss-less

reorganization of endothelial cells in narrowing vessels, leading to blood flow reductions.

Finally, the regression of AV malformations returned shunted blood to perfusing vessels,

reversing tissue hypoxia and neuronal dysfunction. Our data provide direct, *in vivo*

evidence that Notch4-mediated AV specification can exert dominant effects over

hemodynamics in regulating the AV hierarchy structurally and functionally. Our findings

imply that Notch4 inhibition may lead to degeneration of AV malformations.

Introduction

The vasculature plays a principal role in health and disease. Its arteries carry blood from the heart to the capillaries, successively reducing vessel caliber and blood flow. Capillaries, where exchange of nutrients and wastes occurs, are the smallest diameter vessels with lowest blood flow. Post-capillary venules join sequentially wider veins to return blood back to the heart. This arterial venous (AV) hierarchy is critical for proper tissue perfusion. All blood vessels are lined by endothelial cells (ECs). Arteries have stronger, veins have weaker, and capillaries have no smooth muscle cell (SMC) layers. Hemodynamics are known to regulate vessel diameter, EC shape, and SMC content (*1*) and are required for the establishment of the AV hierarchy in embryos (*2, 3*). However, the biological signals which maintain the AV hierarchy remain unknown.

Notch signaling has emerged as a critical mediator of the genetic programming of arteries and veins (*4*). Notch receptors and ligands are transmembrane proteins that promote arterial at the expense of venous fate by enhancing expression of the arterial molecular marker ephrin-B2 and suppressing the expression of the venous marker EphB4. The transmembrane signaling molecule ephrin-B2 was the first gene found to be expressed in the ECs of arteries and not veins, serving as the most recognized arterial endothelial marker. Its cognate tyrosine kinase receptor, EphB4, is a venous endothelial marker. Upstream of Notch, COUP-TFII, a member of the orphan nuclear receptor superfamily, expressed in venous and not arterial ECs, actively promotes venous differentiation likely by repressing the expression of Notch (*5*). These AV specific genes are crucial in the

morphogenesis of the embryonic vasculature, and their expression patterns are maintained in adult vascular endothelium (*6*), suggesting that these genes function in maintaining the established AV hierarchy.

We have reported that Notch activity is increased in the endothelium of patients with brain AV Malformation (AVM) disease (*7*). AVMs are vascular lesions characterized by a structural disruption of AV hierarchy, in which the direct connection of arteries to veins displaces the intervening capillaries and creates high-flow AV shunts that cannot perfuse tissues (*8*). AVMs generally do not regress in patients (ref). We have generated a mouse model of AVM by expressing constitutively-active Notch4 (*Notch4**) specifically in ECs, using a temporally-regulatable tetracycline (Tet)-repressible system (*Tie2-tTA; TRE-Notch4**) (*9, 10*). Strikingly, repression of Notch4* expression in severely affected mice resulted in a reversal of ataxic neurologic symptoms and recovery from illness. These results suggest a previously unappreciated possibility that established high-flow AV shunts may regress, thereby allowing tissue perfusion.

Here, using imaging by advanced two-photon excited fluorescent (2PEF) in the brains of live Notch4* mice, we obtained 4D vascular topology and blood velocity data necessary to prove this concept. We demonstrate that Notch4* can arterialize venous segments, leading to high-flow AVM, which are remarkably converted to capillaries when Notch4* is repressed. This Notch control of reversible AV conversion is mediated by an ephrin-B2/EphB4-dependent mechanism.

Results

Repression of Notch4* causes the specific normalization of AV shunts

To test whether repression of endothelial Notch4* causes the regression of existing brain AV shunts, we combined two-photon microscopy with a cranial window technique to visualize brain vasculature over time (Supplementary Figure 2). By postnatal day 12 (P12) most *Tie2-tTA;TRE-Notch4** mutants had developed AV shunts. The minimum diameter of AV shunts at P11-13 averaged 22.2μm ± s.d. 7.3, ranging from 8.1 to 51.3μm (*n*=46 AV shunts examined in 13 mice), approximately 2 to 10 times the diameter of the capillaries in age-matched controls, which averaged 4μm ± s.d. 0.5, ranging from 2.7 to 5.0μm (*n*=9 capillaries examined in 3 mice, Supplementary Figure 3). Centerline blood velocity through AV shunts was much higher than in control capillaries, averaging 37.7mm/S ± s.d. 14.4 (*n*=11 AV shunts in 11 mice), compared to 2.1mm/S ± s.d. 1.0 in control capillaries (*n*=9 capillaries in 3 mice, Supplementary Figure 3), and as previously reported[8].

To determine the timing of Notch4* repression, levels of Notch4* protein in the brains were assayed by quantitative immunofluorescence, using an antibody to the intracellular domain of Notch4. Although the antibody detects endogenous and transgenic Notch4, the signal in *Tie2-tTA;TRE-Notch4** mutants over that in controls reflects transgenic Notch4* expression. Notch4* expression was reduced within 12 hrs of Dox treatment (data not shown), and decreased to nearly baseline levels within 24 hrs (Supplementary Figure 4).

Since Notch4* is rapidly repressed by Dox, for clarity we refer to the period of Notch4* repression, rather than Dox treatment time.

Because ataxia in the mutants is alleviated within 72 hrs of Notch4* repression (9), we measured changes in the minimal diameter of AV connection at varying timepoints within the first 48 hrs of Notch4* repression. Strikingly, all abnormally enlarged AV shunts were reduced (Figure 1, *n*=22 AV shunts in 10 mice). In untreated mutants, approximately half of the AV shunts increased and half decreased (Figure 1 and Supplementary Figure 5, *n*=35 AV shunts in 11 mice), an underlying variability likely caused by vascular "steal" effects, a diversion of flow through proximal AV shunts which "steals" blood flow from distal vessels, ultimately causing their regression (Supplementary Movie 1). When individual shunts were followed for several timepoints, 10 of 10 AV shunts (in 8 mice) enlarged prior to but regressed after Notch4* repression (Supplementary Figure 6), but 5 of 5 AV shunts (in 2 mice) continued to enlarge without Notch4* repression. When imaging for >1 week was possible, we observed the complete regression of the AV shunt to capillary diameter (Supplementary Figure 7), a finding confirmed by *ex vivo* analysis (Supplementary Figure 7).

Since reduction of blood flow is an important aspect of AV shunt regression, we measured blood velocity, and found that velocity was reduced in all AV shunts after Notch4* repression (*n*=7) (Figure 1). The onset of diameter and velocity reductions coincided within 12-24hrs of Notch4* repression (Supplementary Figure 8).

Interestingly, the regression of enlarged AV shunts did not coincide with a general

reduction in the diameters of non-AV shunt vessels. Dramatic regression of the AV shunt

vessel was observed adjacent to arterial or venous vessels with very little change in

diameter (Figure 1). Taken together, these data suggest Notch4* repression leads to

specific normalization of established AV shunts.

Coup-TFII expressing endothelial cells within AV shunts upregulate EphB4
following repression of Notch4*

The specific regression of AV shunts suggested that loss of venous specification in the

presence of Notch4* and recovery of venous specification following Notch4* repression

may underlie the regression. Coup-TFII is a venous marker upstream of Notch. Its

expression should not be affected by Notch4*, and thus it can demarcate the AV

boundary in the AV shunt, making it possible to trace the original venous segment and to

assess the re-establishment of venous specification upon Notch4* repression (*5*). To

determine Coup-TFII expression, we used a nuclear *lacZ* reporter of Coup-TFII promoter

activity, *Coup-TFII*$^{+/fl\text{-}stop\text{-}nLacZ}$;*Tie2-Cre* (*11*). The *lacZ* expression is controlled by a

floxed-STOP sequence. Tie2-Cre-mediated excision ensures that the *lacZ* reports the

expression of *Coup-TFII* in Tie2+ endothelial and hematopoetic cell lineages.

In the control, the *Coup-TFII* expression was localized to the endothelial nuclei of the

venous branches, including capillaries, but absent in the arterial branches in the brain

(Figure 2a, a'). In Notch4* mutants, either with mild (Figure 2b, b') or severe (Figure 2c,

c') phenotype, regardless whether Notch4* was ON (Figure 2b, b', c, c') or OFF (Figure 2d, d'), *Coup-TFII* expression was maintained throughout the venous branches, as in controls. Thus *Coup-TFII* expression clearly marked the venous boundary of AV shunt and suggests part of the AV shunt originated from the vein.

EphB4, in contrast to *Coup-TFII,* is a Notch downstream venous marker (*12, 13*), making it possible to trace the effect of Notch4* on venous repression. We used a *lacZ* reporter of *EphB4* promoter activity (*12*) to examine the *EphB4* expression before and after Notch4* repression. In controls, *EphB4$^{tau-lacZ}$* was expressed throughout the veins, venules, and into the capillaries of the brains (Figure 2e,e'). *Notch4* expression decreased the expression of *EphB4$^{tau-lacZ}$*, resulting in patchy expression in the vein and very little expression in AV shunts (Figure 2f,f'). We have previously shown that the entire AV shunt in the Notch4* mutants is ephrinB2 positive. These data combined with the *Coup-TFII* expression pattern suggest that Notch4* induced arterial identity and repressed venous identity of venous segment. Repression of *Notch4* resulted in an increase in *EphB4* expression in the regressing AV shunts (Figure 2g,g').

Loss-less reorganization of endothelial cells in the normalization of AV shunts

The reduction of endothelial diameter suggested that either the total number of ECs was decreased or that the spacing of the individual ECs was reduced. To examine changes in EC number and position during AV shunt regression, we used the *ephrin-B2-H2B-eGFP* mouse line to provide nuclear labeling of ECs within the AV shunt (*14*). In the presence

of Notch4*, all ECs in the AV shunt, regardless of arterial or venous origin, expressed *ephrin-B2-H2B-eGFP*. The H2B-eGFP fusion protein is extremely stable and can persist for months (*15, 16*). Thus, within the AV shunt, in the short time-course of regression, *ephrin-B2-H2B-eGFP* acts as a general EC marker without arterial specificity.

Chronic observation of eGFP+ nuclei in the AV shunts of *Tie2-tTA;TRE-Notch4*;ephrin-B2-H2B-eGFP* mutants revealed that Notch4* repression did not affect total cell number but their relative spacing, in the regressing AV shunts (Figure 3 and Supplementary Figure 9, *n=23* AV shunts in 7 mice). *Ex vivo* staining of VE-cadherin showing cell-cell junctions in mutants before and after repression of Notch4* suggests that the footprint of individual ECs is reduced in the regression (Supplementary Figure 11).

Inhibition of EphB4 signaling impairs regression of AV shunts

To determine whether EphB4 signaling is necessary for the regression of AV shunts, we used a soluble form of the EphB4 receptor to competitively inhibit EphB4 receptor signaling (*17*) following repression of Notch4* (Figure 3). The mean change in the diameter of AV shunts was -17.8% ± s.d. 24.1 (*n=26* AV shunts in 5 mice), significantly less than that without sEphB4 (-47% ± s.d. 19.3, *n=22* AV shunts in 10 mice; P<0.0004). As a control for the recombinant protein, we examined regression in mice injected with recombinant human fibronectin. The mean change in AV shunt diameter in these mice

was -35.1% ± s.d. 26.2 (*n*=13 AV shunts in 2 mice), close to that without sEphB4

(P<0.05). Thus sEphB4 significantly impaired the regression of AV shunts.

Regression of brain AV shunts reverses vascular "steal" effects and alleviates hypoxia

Brain AVMs are reported not to repress spontaneously (*18*). Provocatively, we observed

that neurologic dysfunction was promptly reversed by Notch4* repression in mice with

AVM-like lesions, suggesting a physiologic recovery (*9*). Imaging of brain vasculature in

mutants revealed that high blood velocity through enlarged AV shunts coincided with

slowed and even stopped flow in distal branches of the arterial tree (Supplementary

Movie 1), reflecting the vascular "steal" effect. These findings suggest that focal brain

hypoxia caused by ischemia leads to neurologic dysfunction in Notch4* mutants.

Reduced blood flow is known to reversibly impair neuronal function in the stroke

penumbra (*19*). Thus we hypothesize that rapid reversal of this hypoxia might underlie

the recovery of neuronal defects.

To test this hypothesis, we first examined blood velocity in arterial branches distal to the

AV shunt and found blood velocity increased with Notch4* repression but decreased with

Notch4* expression (Supplementary Figure 12). Strikingly, velocity decreased with

Notch4* in four AV shunts examined but increased after Notch4* repression and

proximal AV shunts regressed (Supplementary Figure 6, *n*=4). Furthermore, increased

lectin perfusion of capillary vessels (Supplementary Figure 13) suggests a global increase in tissue perfusion following AV shunt regression.

We then examined hypoxia in Notch4* mutants with neurologic defects before and after Notch4* repression, using hypoxyprobe staining. The hypoxyprobe detects tissue exposed to a partial oxygen pressure of <10mmHg, close to the hypoxic threshold expected to cause dysfunction of neuronal cells (*20*). We detected an increase in cerebellum and cerebral cortex of sick Notch4*-expressing mice, relative to their littermate controls. Staining intensity correlated with the severity of AV shunting phenotype, as assessed by staining of surface vasculature (data not shown). When Notch4* was repressed for 72 hrs in sick Notch4* mutants, hypoxyprobe staining intensity was significantly reduced, and approached control levels (Figure 4).

Finally, we determined the histopathological changes in the brain parenchyma without and with Notch4* repression. Histological analysis of Notch4* mutants without Notch4* repression revealed foci of pyknotic nuclei, often surrounding a core of decreased nuclear density, consistent with ischemia-induced necrosis (4 of 6 mice, Figure 4). Such regions occasionally also contained evidence of hemorrhage. Notch4* repression for several weeks eliminated these pyknotic and acellular regions (9 of 9 mice), although structural damage could still be detected, presumably representing the evolution of the earlier ischemic damage (1 of 9 mice). In support of this, hemosiderin depositions suggested the resolution of earlier hemorrhages. These findings suggest structural healing of earlier lesions after Notch4* repression.

Discussion

We show that arterial specification in the postnatal vasculature is genetically reprogrammable. Endothelial Notch4* expression arterializes venous vessels, and Notch4* repression restores venous programming in the abnormally arterialized, high-flow vessels. Using *in vivo* time-lapse imaging with single-cell resolution, we show that venous reprogramming leads to reorganization of ECs, leading to the normalization of AVMs. At a physiologic level, this normalization reverses vascular perfusion defects and neurological deficiencies (Supplementary Figure 1). Thus, postnatal AV hierarchy remains plastic, amenable to re- programming by Notch.

Postnatal vessels can be reversibly programmed to arteries by Notch signaling

We previously observed expanded expression of the arterial marker ephrin-B2 in the adult vasculature following Notch4* expression, but could not determine whether venous ECs had been arterialized, or if arterial ECs had expanded into venous territory. Using venous markers upstream (Coup-TFII) and downstream (EphB4) of Notch, we now show that Notch is sufficient to cause the arterialization of differentiated venous endothelium in the postnatal mouse. In normal brain endothelium, Coup-TFII is expressed specifically in venous cells. As Coup-TFII is upstream of Notch, its expression should not be affected by Notch4* expression, identifying ECs of venous origin. Expression of Notch4* led to the mis-expression of ephrin-B2, the quintessential arterial marker, in Coup-TFII positive cells, confirming that Notch4* expression converts venous ECs into arterial ECs.

Expression of Notch4* also led to the suppression of the venous marker EphB4 in the Coup-TFII positive cells, demonstrating a simultaneous loss of venous expression in ECs of venous lineage.

We further demonstrate that conversion of venous vessels to arteries by a single genetic manipulation is reversible. Notch4*-converted vessels exhibit the major hallmarks of arteries, including expression of arterial molecular markers, structural changes, and arterial flow velocities. Notch4* repression led to re-expression of EphB4 in Coup-TFII positive vessels, as well as structural and hemodynamic normalization. Thus, our results suggest that venous vessels arterialized by Notch4* are converted back to veins upon repression of Notch4*. The reversible arterial specification in post-natal vasculature suggests that AV lineage specification is genetically pliable, and a single genetic manipulation is sufficient to switch AV specification postnatally.

Reprogramming of AV specification restores AV hierarchy

Provocatively, we show the restoration of AV hierarchy by a single genetic manipulation, despite the presence of pathological blood flow patterns. Notch4* repression caused the eventual narrowing of large AV shunts to capillaries. The narrowed AV shunts exhibited the features capillaries. Importantly, this normalization was specific to the AV shunts, as adjacent arteries and veins generally were unchanged. Thus, Notch4* repression causes prompt normalization of AV specification and a restoration of AV hierarchy.

AV reprogramming elicits reorganization of endothelial cells and structural alteration of high-flow vessels

The mechanism underlying the restoration of AV hierarchy following Notch4* repression involves ephrin-B2 and EphB4-mediated EC re-organization, rather than a reduction of EC number. While the role of Eph/ephrin signaling in the endothelium is not yet clear, our finding is consistent with the established functions of ephrin-B2/EphB4 in regulating cell migration through repulsive cues (*22, 23*). We think that once re-expressed in Coup-TFII+ ECs, EphB4 mediates ephrin-B2 signaling, likely eliciting the EC repulsion. Supporting a critical role for ephrin-B2/EphB4 signaling in this normalization process, the specific regression of vessels occurs at the AV interface, while the adjacent arteries and veins often do not regress. Furthermore, the normalization of AV hierarchy following Notch4* repression can be blocked by sEphB4.

Our data also suggests that EphB4 re-expression elicits EC organization and initiates the cascade of AV structural normalization. Cellular reorganization is a cause and not a consequence of reduction in shunting blood flow. It is well known that blood vessels can regress due to decreased flow, thus it critical to delineate whether the normalization of AV shunts is a primary effect of genetic manipulation or a consequence of reduced flow. High-resolution blood flow measurements following Notch4* repression demonstrate that regression of AV shunts is the primary effect, causing a specific reduction in flow in the AV shunt, and not adjacent vessels..Thus, structural reorganization actively opposes hemodynamic forces by increasing resistance to flow in the AV shunt through narrowing of the lumen.

The cell reorganization mechanism of AV normalization following Notch4* repression is distinct from the apoptotic mechanism of vessel regression following VEGF withdrawal. Microvessels in tumors and normal trachea regress following VEGF inhibition (24). Regression in these vessels is attributed to apoptosis of ECs (24). *Ex vivo* analysis suggests that it is similar to the programmed regression of the hyaloid microvasculature after birth, which has been linked to reduced VEGF signaling (25). *In vivo* imaging of hyaloid vessel regression shows that the apoptosis of ECs obstructs the lumen and capillary blood flow, triggering the apoptosis of remaining ECs in the capillary segment (26). Thus, apoptosis and a subsequent reduction in blood flow serves as a precipitating event for the regression in these settings. Our findings suggest that the cellular mechanism underlying the regression of the high-flow vessels following Notch4* repression does not involve EC apoptosis, but rather EC reorganization.

Targeting Notch to induce normalization of AVMs offers a new therapeutic strategy to treat this disease.

AVMs "steal" blood flow from adjacent capillaries, causing ischemic hypoxia. It is generally believed that AVMs are perpetuated by the abnormal hemodynamics they develop (27) and do not spontaneously regress. In the few cases in which spontaneous regression has occurred, it has been attributed to thrombotic occlusion and reduction in flow (28). Our direct *in vivo* imaging demonstrates the regression of AVMs to capillaries without occlusion or hemorrhage. Strikingly, the structural reorganization which reverses tissue hypoxia and neurological dysfunction can be induced by a single genetic

manipulation. Our demonstration of complete and safe normalization of dangerous high-flow AVMs in animals may inspire new therapeutic strategies to induce the regression of even well established AVMs to treat this devastating disease.

Methods:

Mice

Tie2-cre, Tie2-tTA and *TRE-Notch4** mice were previously published (*7, 9, 10, 30*), as were *Ephrin-B2*$^{+/H2B-eGFP}$ (*14*), *EphB4*$^{+/tau-lacZ}$ (*12*), *ephrin-B2*$^{+/tau-lacZ}$ (*13*), and mT/mG mice (*31*). *Coup-TFII*$^{+/fl-stop-nLacZ}$ mice, in which gene deletion results in expression of nuclear localized lacZ, were also previously published (*11*), and kindly provided by the Tsai lab. Tetracycline sucrose solution (0.5 mg/ml Tet, 50 mg/ml sucrose, Sigma) was administered to pregnant mothers from plugging, and withdrawn from pups at birth as we described (*9*). Doxycycline treatment was initiated with intraperitoneal injection of 500uL of 1 mg/mL solution in phosphate buffered saline (PBS), followed by doxycyline diet (200-mg/kg diet, Bio-Serv) as we described (*9, 10*). All animals were treated in accordance with the guidelines of the University of California San Francisco Institutional Animal Care and Use Committee.

Soluble EphB4 treatment

Treatment was modified from published protocols (*17*). Before doxycycline treatment, 200mL of 200μg/mL recombinant human EphB4 extracellular domain (R&D systems)

was injected by tail vein, achieving a final concentration of ~4μg/gm, followed by a

second injection of 100mL of 200μg/mL 24hrs later. Recombinant human fibronectin

(R&D systems), also His-tagged and produced in NSO cells, was used as a negative

control at the same concentration.

In vivo imaging

Chronic *in vivo* imaging of the brains of immature mice was performed as described (*32*),

with modifications for chronic imaging in immature mice (*33, 34*). Briefly, a craniotomy

was performed over the right cortex. The window, a 5mm glass coverslip (World

Precision Instruments), was placed over artificial cerebrospinal fluid above the

craniotomy, and fixed into place. To stabilize the head for imaging, a custom milled

metal bar with adaptor bolt-holes was attached adjacent to the window, allowing it to be

secured by a custom built adaptor arm on a stereotaxic base (Cunningham). At imaging

timepoints, mice were anesthetized with isoflurane (1.25-1.5%) in pure oxygen, and

warmed with a homeothermic heat blanket (Harvard Apparatus). Fluorescent contrast in

blood plasma was provided by tail vein injection of 2000 kDa FITC-dextran (Sigma), 155

kDa TRITC-dextran (Sigma), or 2000 kDa Texas Red-dextran (prepared according to

published protocols (*35*) and filtered by dialysis). Two-photon microscopy was

performed with a locally constructed microscope, to be described in detail in a future

publication.

Immunostaining

To prepare tissue for whole mount staining, 1% paraformaldehye (PFA) fixation by the right ventricle and biotinylated or FITC-conjugate *lycopersicon esculentum*-lectin (Vector Labs) injection was performed as we described (*9, 10*). Following perfusion, the cortex surface was removed by scalpel for staining. Tissue was blocked (2% bovine serum albumin, 0.1% TritonX-100 in PBS) for 1hr at room temperature, and treated with primary antibody in block overnight at 4C. Tissue was then washed 3x 1.5hrs at 4C with 0.1% TritonX-100 in PBS and treated with secondary antibody in block overnight at 4C. Tissue was then again washed 3x 1.5hrs at 4C with 0.1% TritonX-100 in PBS and post-fixed in 1% PFA. Flat mount imaging was performed by placing cortex between a glass coverslip and slide, as previously described (*36*). Antibodies used were anti-VE-Cadherin (BD Pharminogen 555289, 1:200 dilution) and anti-α-SMA (Sigma F377, Clone 1A4, 1:200 dilution) according to our published protocols (*10, 37*).

Notch4 staining of brain in section was performed according to published protocols (*9*). Briefly, brains were perfusion-fixed with or without prior *lycopersicon esculentum*-lectin (Vector Labs) injection. After 24hrs of fixation in 1% PFA at 4C, brains were sagittally bisected and dehydrated in 30% sucrose in PBS overnight at 4C and imbedded in OCT. 10mm sections were cut, washed in PBS, blocked (3% donkey serum, 2% BSA, 0.2% TritonX-100 in PBS) for 1hr at room temperature, and then treated with primary antibody overnight at 4C in block. After 3x PBS-T (0.1% TritonX-100 in PBS) washes, sections were incubated with secondary antibody for 1hr at room temperature, washed 2x 10min in PBS-T and 2x 10min in PBS, and then stored in VectaShield +DAPI (Vector Labs).

Antibody used was anti-Notch4 ICD (Millipore 07-189, formerly Upstate, 1:500 dilution).

X-gal/DAB co-staining

Beta-galactosidase staining by X-gal was performed with 3,3'-diaminobenzidine (DAB) co-staining, according to a published protocol (*38*) with modifications. Under ketamine/xylazine and isoflurane anesthesia, 25mg biotinylated *lycopersicon esculentum-*lectin (Vector Labs) in PBS was injected via inferior vena cava and allowed to circulate for 2 minutes. Perfusion was performed through the right ventricle with PBS, followed by fixation (0.25% gluteraldehyde, 50mM EGTA and 100mM MgCl2 in PBS). After 10 minutes of fixation on ice, the cortex was X-gal stained at room temperature according to published protocols (*39*). The cortex was then fixed with 1% PFA, and blocked (10% bovine serum albumin and 0.1% TritonX-100 in PBS) for 1hr at room temperature, incubated with 1:1000 streptavidin conjugated horse-radish peroxidase (Jackson Immuno) in block for 2hrs at room temperature before washing and staining with DAB kit (Vector Labs). Stained samples were imaged as flatmounts.

Acknowledgements

References :
1.　R. Thoma, *Untersuchungen über die Histogenese und Histomechanik des Gefässsytems.* (Ferdinand Enke, Stuttgart, 1893).
2.　W. B. Chapman, *The American Journal of Anatomy* **23**, 175 (1918).
3.　J. L. Lucitti *et al.*, *Development* **134**, 3317 (Sep, 2007).
4.　M. R. Swift, B. M. Weinstein, *Circ Res* **104**, 576 (Mar 13, 2009).
5.　L. R. You *et al.*, *Nature* **435**, 98 (May 5, 2005).
6.　D. Shin *et al.*, *Dev Biol* **230**, 139 (Feb 15, 2001).
7.　P. A. Murphy, G. Lu, S. Shiah, A. W. Bollen, R. A. Wang, *Lab Invest* **89**, 971 (Sep, 2009).
8.　R. M. Friedlander, *N Engl J Med* **356**, 2704 (Jun 28, 2007).
9.　P. A. Murphy *et al.*, *Proc Natl Acad Sci U S A* **105**, 10901 (Aug 5, 2008).
10.　T. R. Carlson *et al.*, *Proc Natl Acad Sci U S A* **102**, 9884 (Jul 12, 2005).
11.　N. Takamoto *et al.*, *Development* **132**, 2179 (May, 2005).
12.　S. S. Gerety, H. U. Wang, Z. F. Chen, D. J. Anderson, *Mol Cell* **4**, 403 (Sep, 1999).
13.　H. U. Wang, Z. F. Chen, D. J. Anderson, *Cell* **93**, 741 (May 29, 1998).
14.　A. Davy, J. O. Bush, P. Soriano, *PLoS Biol* **4**, e315 (Oct, 2006).
15.　K. Brennand, D. Huangfu, D. Melton, *PLoS Biol* **5**, e163 (Jul, 2007).
16.　E. Fuchs, *Cell* **137**, 811 (May 29, 2009).
17.　N. Kertesz *et al.*, *Blood* **107**, 2330 (Mar 15, 2006).
18.　D. R. Buis *et al.*, *J Neurol* **251**, 1375 (Nov, 2004).
19.　E. H. Lo, *Nat Med* **14**, 497 (May, 2008).
20.　E. L. Rolett *et al.*, *Am J Physiol Regul Integr Comp Physiol* **279**, R9 (Jul, 2000).
21.　F. le Noble *et al.*, *Development* **131**, 361 (Jan, 2004).
22.　E. B. Pasquale, *Cell* **133**, 38 (Apr 4, 2008).
23.　S. Kuijper, C. J. Turner, R. H. Adams, *Trends Cardiovasc Med* **17**, 145 (Jul, 2007).
24.　F. Baffert *et al.*, *Am J Physiol Heart Circ Physiol* **290**, H547 (Feb, 2006).
25.　A. P. Meeson, M. Argilla, K. Ko, L. Witte, R. A. Lang, *Development* **126**, 1407 (Apr, 1999).

26. A. Meeson, M. Palmer, M. Calfon, R. Lang, *Development* **122**, 3929 (Dec, 1996).
27. M. Morgan, M. Winder, *J Clin Neurosci* **8**, 216 (May, 2001).
28. M. C. Patel, T. J. Hodgson, A. A. Kemeny, D. M. Forster, *AJNR Am J Neuroradiol* **22**, 531 (Mar, 2001).
29. Q. ZhuGe *et al.*, *Brain* **132**, 3231 (Dec, 2009).
30. Y. H. Kim *et al.*, *Development* **135**, 3755 (Nov, 2008).
31. M. D. Muzumdar, B. Tasic, K. Miyamichi, L. Li, L. Luo, *Genesis* **45**, 593 (Sep, 2007).
32. C. B. Schaffer *et al.*, *PLoS Biol* **4**, e22 (Feb, 2006).
33. C. Portera-Cailliau, R. M. Weimer, V. De Paola, P. Caroni, K. Svoboda, *PLoS Biol* **3**, e272 (Aug, 2005).
34. A. Holtmaat *et al.*, *Nat Protoc* **4**, 1128 (2009).
35. S. Hornig *et al.*, *Soft Matter* **4**, 1169 (2008).
36. A. Y. Shih *et al.*, *J Cereb Blood Flow Metab* **29**, 738 (Apr, 2009).
37. R. Braren *et al.*, *J Cell Biol* **172**, 151 (Jan 2, 2006).
38. T. Makinen *et al.*, *Nat Med* **7**, 199 (Feb, 2001).
39. B. Carpenter *et al.*, *Development* **132**, 3293 (Jul, 2005).
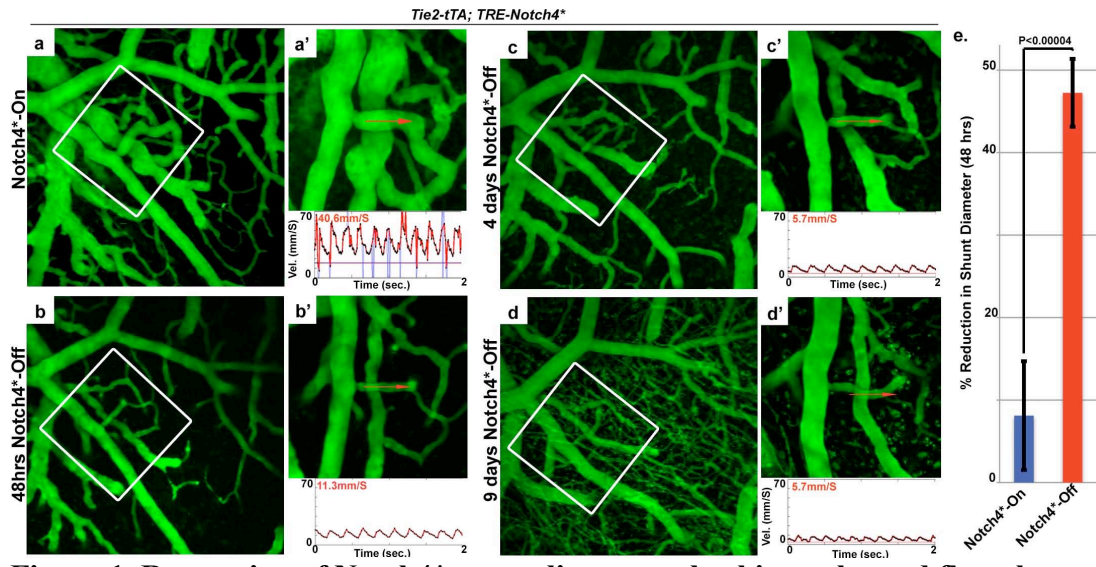
Figure 1. Repression of Notch4* normalizes vascular hierarchy and flow through regression of arteriovenous shunts

Two-photon timelapse imaging of cortical brain vessels through cranial window in Notch4* mutant mice. Plasma labeled by intravenous FITC-dextran. Arteriovenous shunt (a) is reduced in diameter following the repression of Notch4* (b-d). Centerline velocity in the regressing AV shunt was obtained by direct measurement of the velocity of individual red blood cells (panels, a-d). Repression of Notch4* decreased blood flow velocity in shunt by 48hrs (panels, a&b). (e) Quantification of the changes in shunt diameter without repression of Notch4* (Notch4*-On) or with repression of Notch4* (Notch4*-Off) for 48 hrs. Diameter was measured at the narrowest point between artery and vein in Notch4*-On mice before and after treatment (n=22 AV shunts in 10 mice with Notch repression, and n =35 AV shunts in 11 mice without Notch repression). Error bars represent s.e.m. between individual AV shunts.
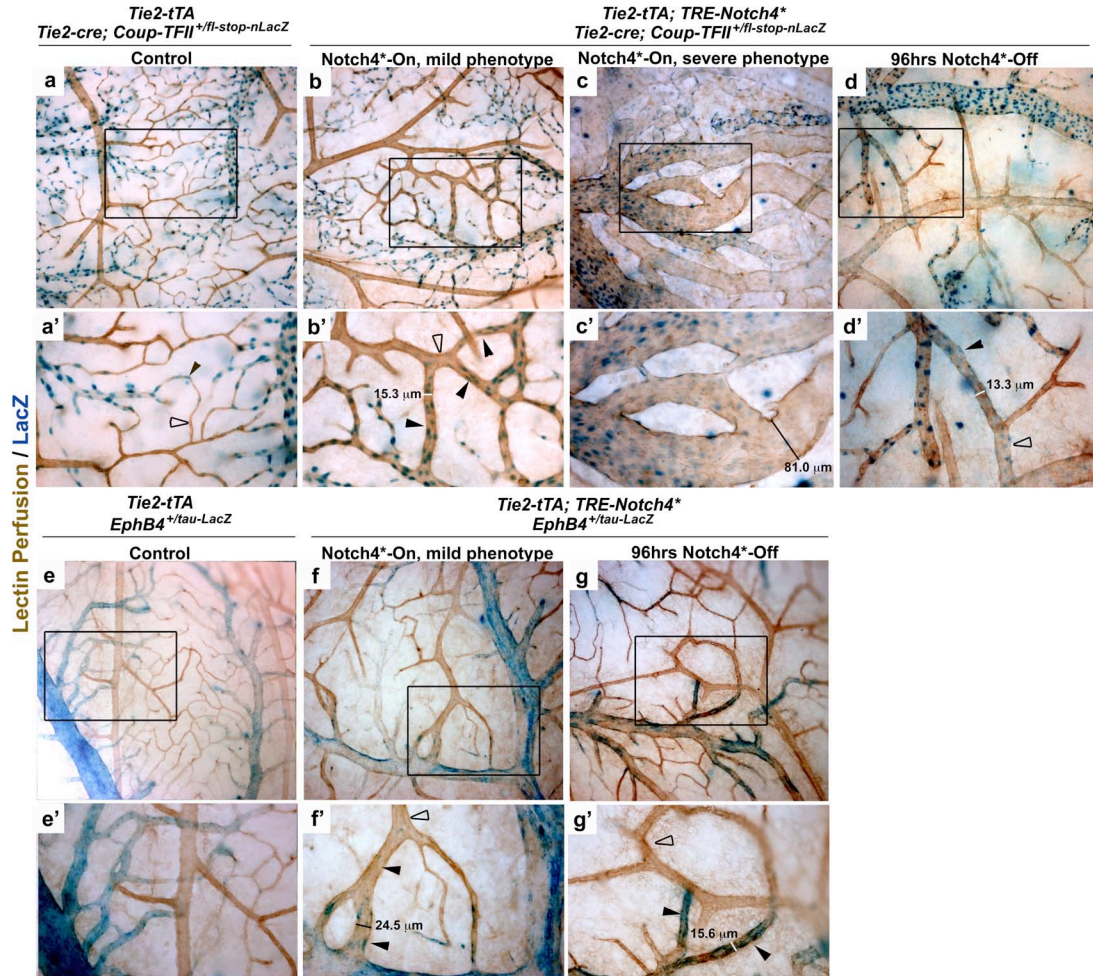
Figure 2. Venous marker EphB4 is reversibly repressed in arteriovenous shunts by Notch4*

Whole mount LacZ staining of the surface vasculature of the cerebral cortex to reveal expression of Notch upstream venous specification gene Coup-TFII, and Notch downstream venous marker EphB4. Perfused vessels are counterstained by colorimetric 3,3'-diaminobenzidine (DAB) reaction with horseradish peroxidase (HRP) bound tomato-lectin. (a-d) LacZ staining of *Tie2-cre* activated Coup-TFII reporter. (a) In control mice, Coup-TFII is expressed in the veins, venules and capillaries up to the arterioles. (b&c) In Notch4* expressing mutants, Coup-TFII is expressed in the vein, and venous portion of the AV shunt. (d) After repression of Notch4*, the narrowest point in arteriovenous shunts is found between Coup-TFII positive and Coup-TFII negative endothelium. (e-g) LacZ staining of EphB4 reporter. (e) In control mice, EphB4 is expressed in the veins and venules up to the capillaries. (f) In Notch4* expressing mutants, EphB4 expression is reduced through arteriovenous shunts, venules and veins. (g) Following the repression of Notch4*, EphB4 expression is increased in the regressing arteriovenous shunt. Closed arrowheads indicate venules; open arrowheads indicated arterioles. *n*=3 for each condition.
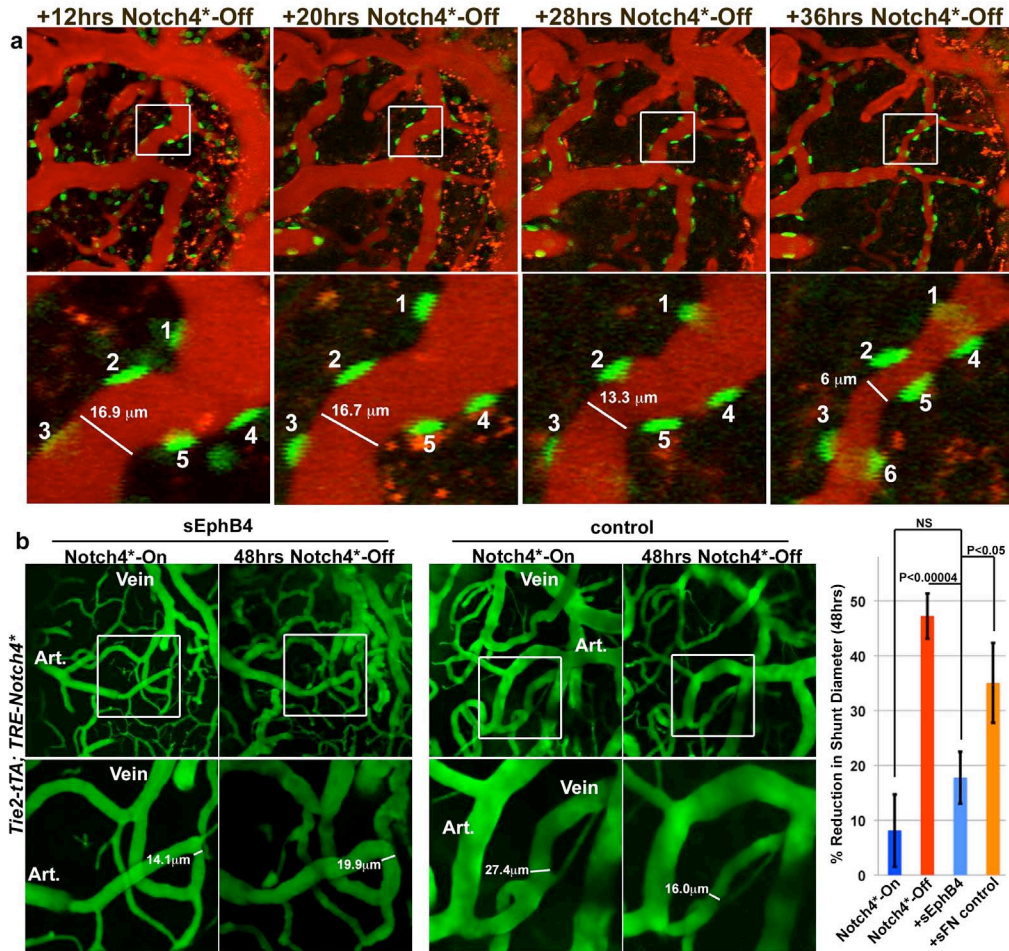
Figure 3. Regression involves the loss-less reorganization of endothelial cells and is inhibited by sEphB4

(a) Two-photon timelapse imaging through cranial window of nuclei marked by *ephrinB2*$^{+/H2B-eGFP}$ in Notch4* mutant mouse. Plasma labeled by intravenous Texas Red-dextran. During arteriovenous shunt regression between 20 and 36hrs after repression of Notch4*, there is no loss of GFP+ nuclei. However, the nuclei are closer to each other. Because these images are Z-stacks through the vessel, cell 6 seems to appear at 36hrs, despite being present earlier, but out of the imaging plane. *n*=23 AV shunts in 7 mice.

(b) Two-photon timelapse imaging of cortical brain vessels through cranial window in Notch4* mutant mice. Plasma labeled by intravenous FITC-dextran. (a) Treating Notch4* mutant mice with soluble EphB4 (sEphB4) inhibits the regression of the measured AV shunt over 48hrs of Notch4* repression. In a littermate Notch4* mutant treated with control soluble human fibronectin (sFN), the AV shunt is reduced in diameter following 48hrs of Notch4* repression. Quantification of changes in minimal AV shunt diameter over 48hrs in mice without repression of Notch4* (Notch4*-On, *n*=35 AV shunts in 11 mice), with repression of Notch4* (Notch4*-Off, *n*=22 AV shunts in 10 mice), with repression of Notch4* and sEphB4 intravenous treatment (+sEphB4, *n*=26 AV shunts in 5 mice), and with repression of Notch4* and sFN control intravenous treatment (+sFN control, *n*=13 AV shunts in 2 mice). Error bars represent s.e.m. between individual AV shunts.
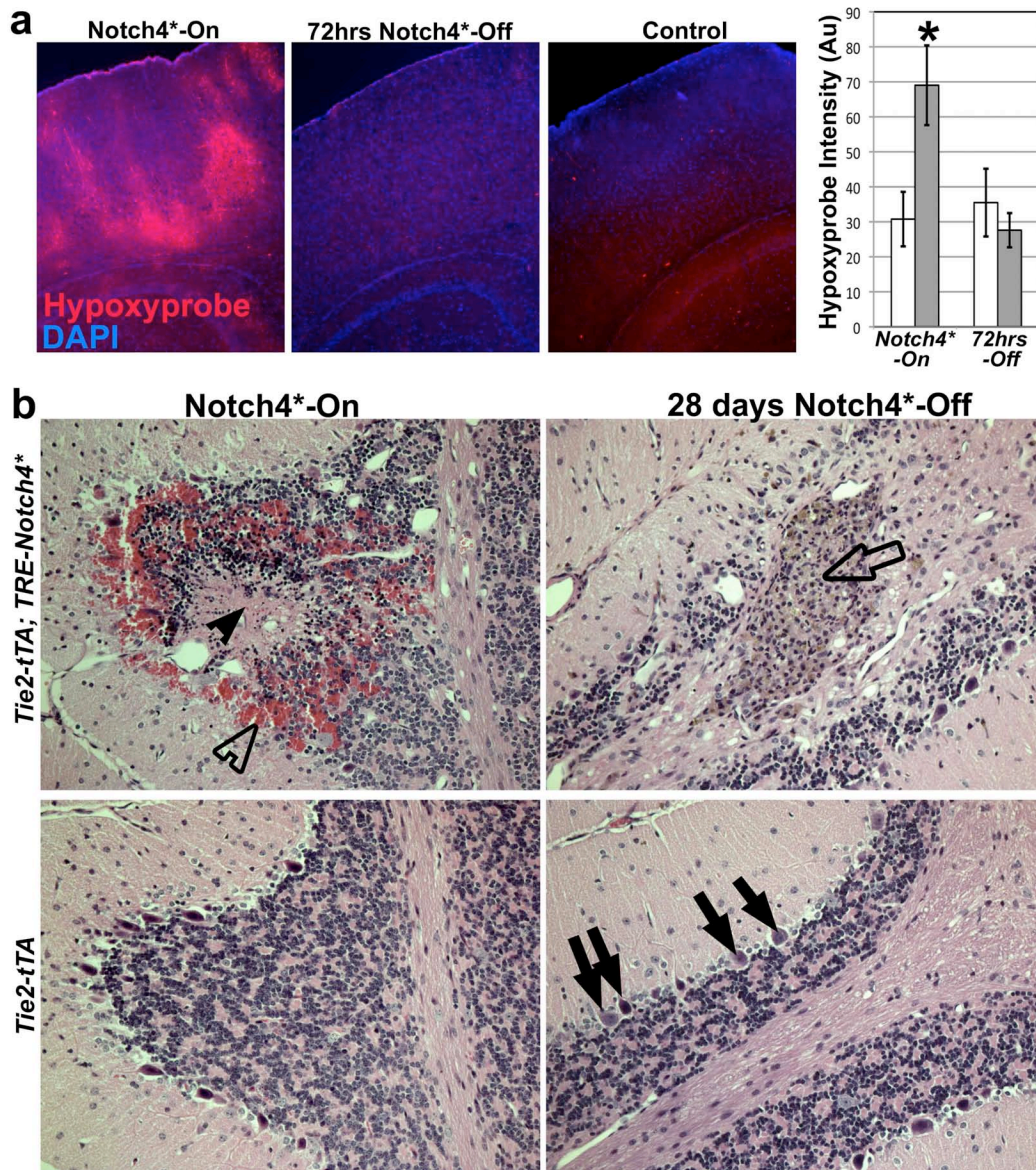
Figure 4. Hypoxia and parenchymal damage is reduced with normalization of AV hierarchy

(a) Immunofluorescent (red) staining for hypoxyprobe (pimonidazole) adduct in coronal section of mouse cortex. Patches of staining are visible in mutant Notch4*-On mice with neurologic defects. Staining is reduced after 72hrs of Dox treatment. Control tissue shows an absence of staining. Quantification of staining intensity in cortical brain relative to non-specific IgG controls (*P<0.05 vs. all other groups). (b) Hematoxylin and eosin staining of sagittal paraffin sections of cerebellum. In Notch4*-On mutant, areas of hemorrhage (open arrowhead) and necrotic tissue (closed arrowhead) are visible. After 28 days of Notch4*-Off, areas of scarring are visible (open arrowhead), but hemorrhage and necrotic tissue has been resolved. Decreased numbers of purkinje cells (arrowheads), and granular cells are found in the scarred area. Note that large vessels are visible within the brain parenchyma both before and after repression of Notch4*.
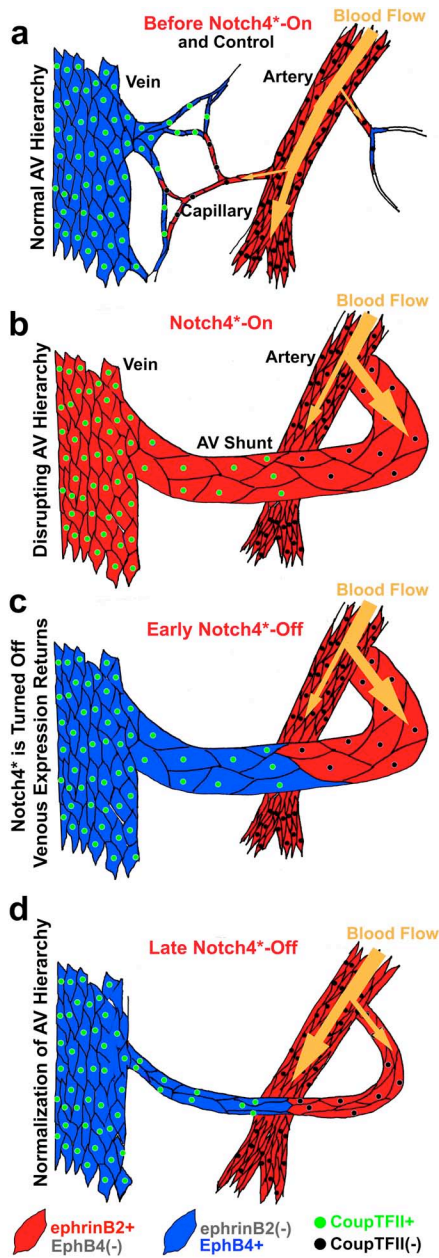
Supplementary Figure 1. Model for normalization of arteriovenous hierarchy elicited by repression of Notch4*

(a) In control mice, Notch and ephrinB2 are expressed in arteries and into capillaries. Coup-TFII is expressed in veins, and into capillaries. EphB4 is also expressed in veins, overlapping with Coup-TFII. (b) In mutant mice, Notch4* is forcibly expressed throughout the endothelium, causing the repression of EphB4, and the expression of ephrinB2 through AV shunts. As expected, the venous marker Coup-TFII is retained, since it is upstream of Notch, and unlikely to be affected by Notch expression. (c) Repression of Notch4* allows EphB4 to be re-expressed in Coup-TFII+ cells. EphB4 is then hypothesized to be activated by ephrinB2 in the AV connection, resulting in reorganization of endothelial cells. (d) As endothelium reorganize in a ephrinB2-EphB dependent manner, the AV shunt narrows.
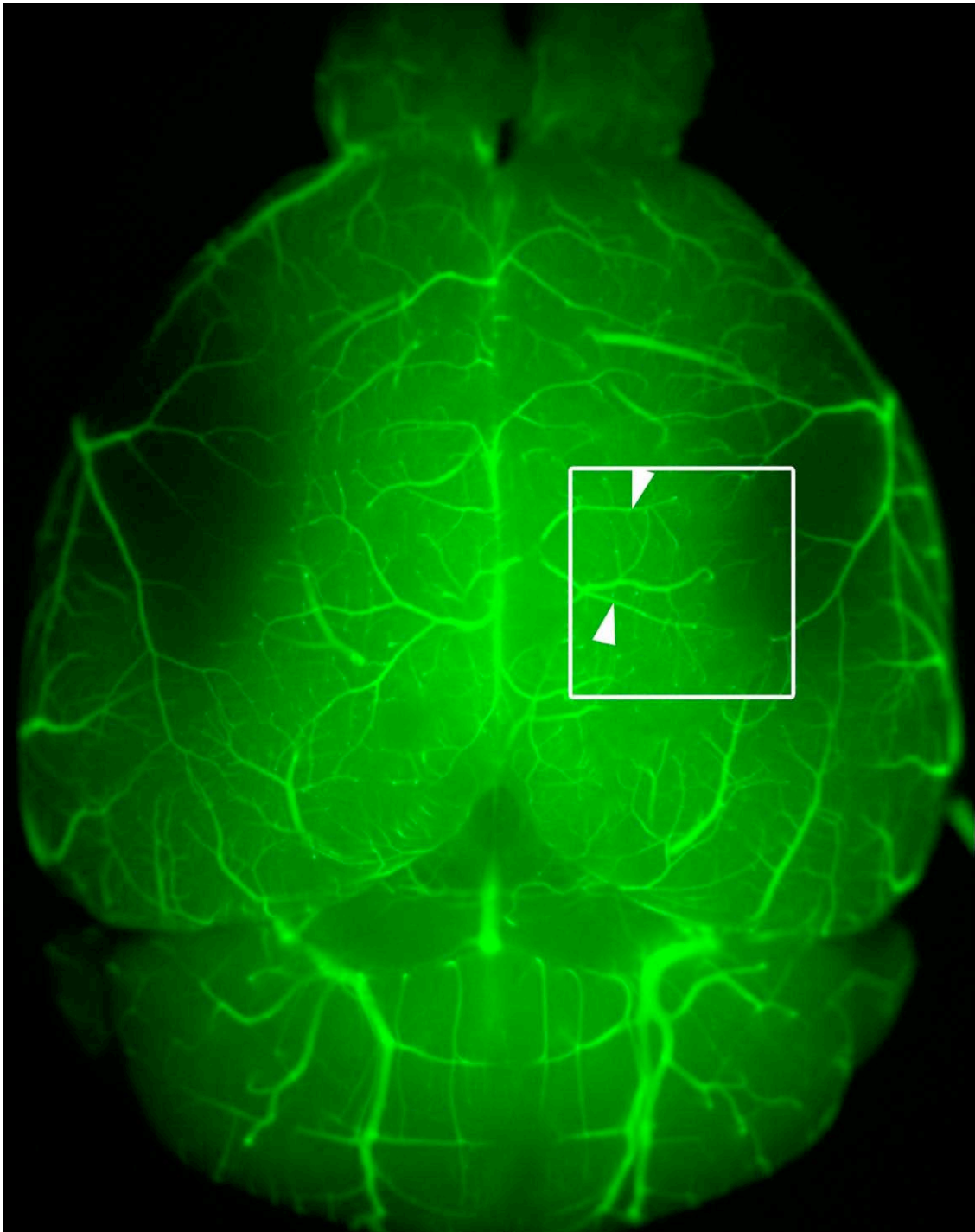
Supplementary Figure 2. Placement of the chronic imaging window
Two-photon timelapse imaging of cortical brain vessels in wild-type mouse. Perfusion of the whole brain with fluorescein-labeled agarose shows pial arteries (arrowheads) and the typical placement of the window (boxed area).
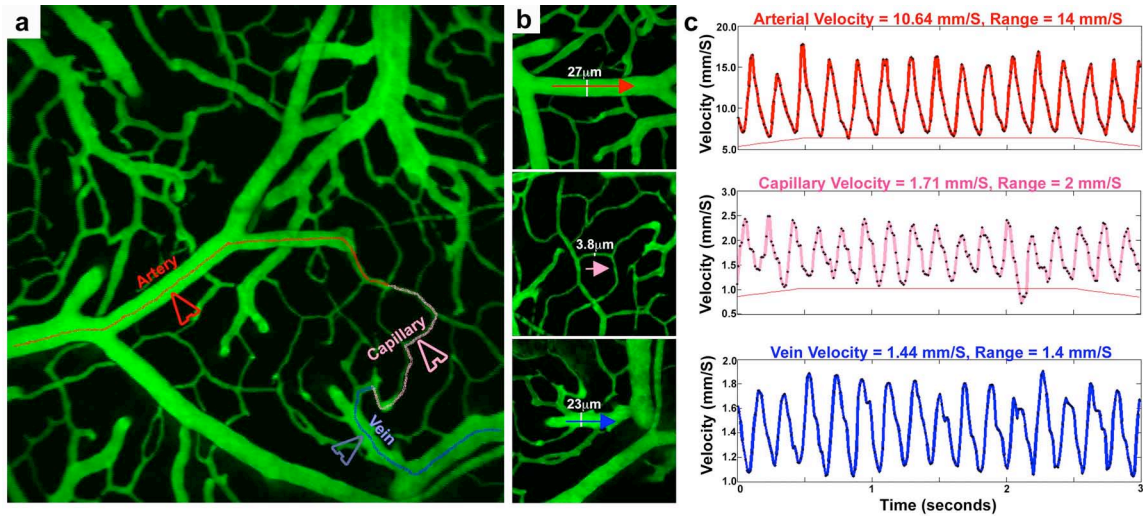
Supplementary Figure 3. Normal blood velocities in artery, capillary and vein in wild-type mice

Two-photon timelapse imaging of cortical brain vessels through cranial window in wild-type mouse. Plasma labeling is provided by intravenous FITC-dextran. (a) Line depicts the path of blood from artery through arteriole, capillary, venule and vein. (b) Images of the artery, capillary and vein in which blood velocity was measured by line scan along the axis depicted. Diameter of the vessel is measured tranaxially. (c) Velocity tracing, as calculated from line scans. Note that both velocity and the pulse (the range in velocity) are reduced from artery to capillary to vein.
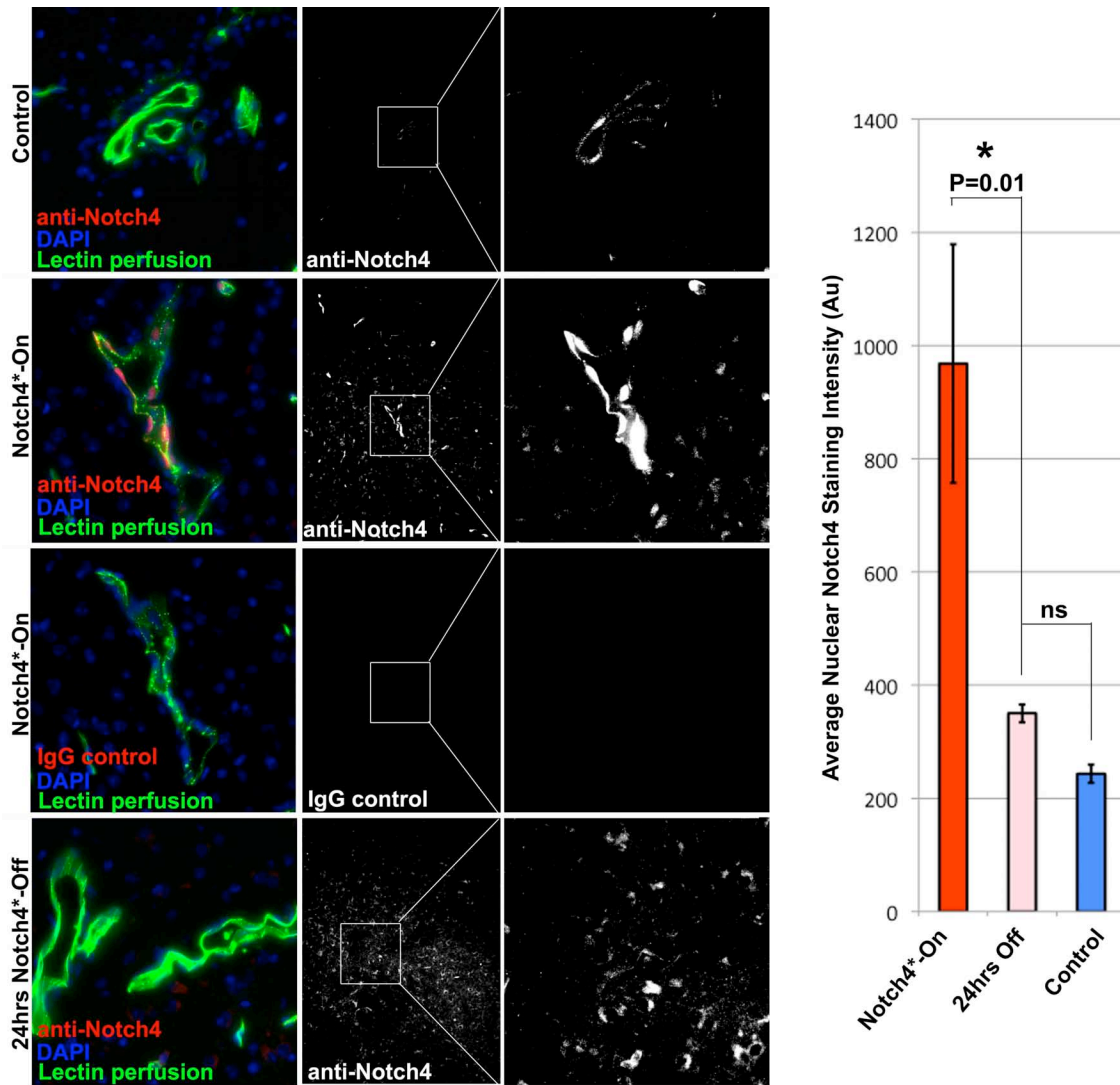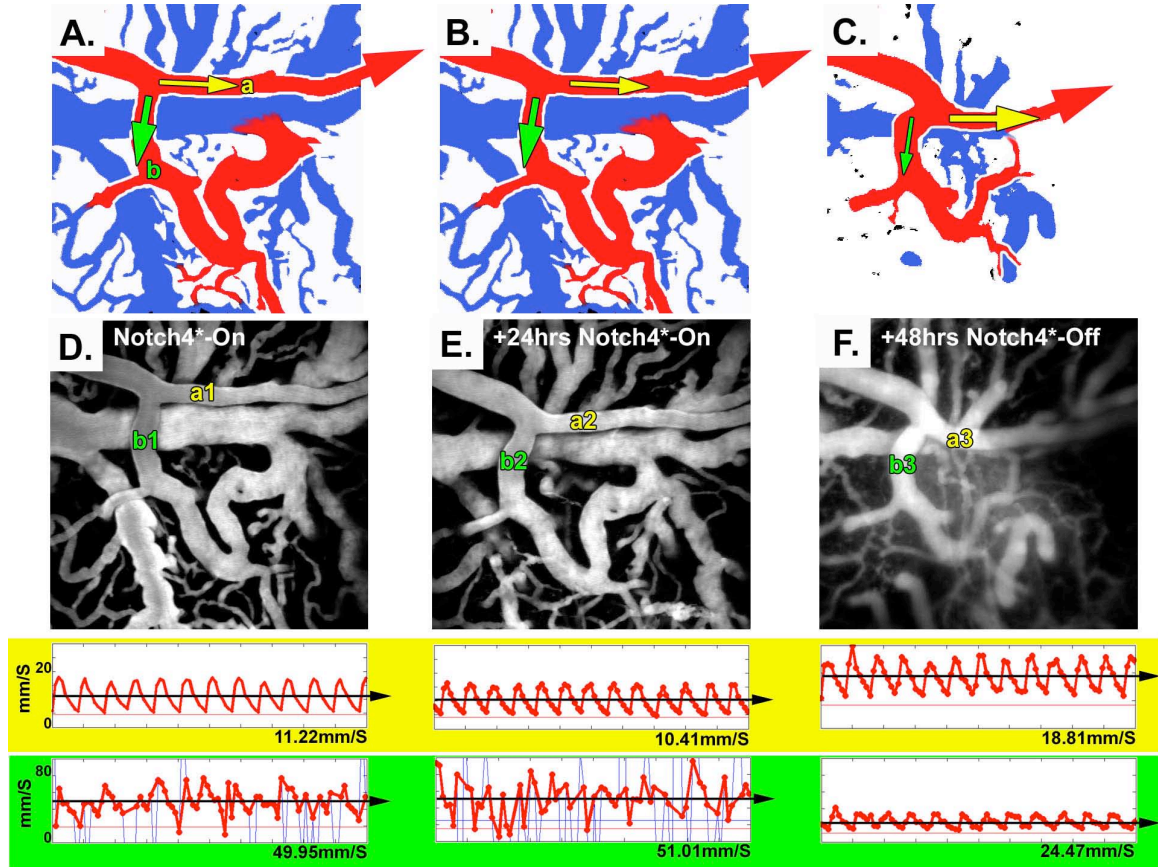
Supplementary Figure 4. Notch4* gene suppression occurs within 24hrs of doxycycline

Frozen sagittal brain sections with fluorescent immunostaining for Notch4 intracellular domain, with labeling of perfused vessels with tomato lectin staining, and nuclear labeling by DAPI. Images show overlap of Notch4 stain with DAPI in cells lining lectin-perfused vessels. Isolation and amplification of the Notch4 staining shows light Notch4 signal in the control vessel nuclei, strong expression in the Notch4*-On vessels, and light expression after 24hrs doxycycline treatment (24hrs Notch4*-Off). Graph shows quantification of fluorescent intensity in endothelial cell nuclei of brain vasculature in Notch4* mutants before and after Dox treatment, and their littermate controls. Error bars represent s.d. between individual animals (*n*=4 Notch4*-On, *n*=5 at 24hrs Notch4*-Off, and *n*=5 controls). In each animal, three nuclei in each of three vessels were quantified to yield an average intensity. *P<0.01.
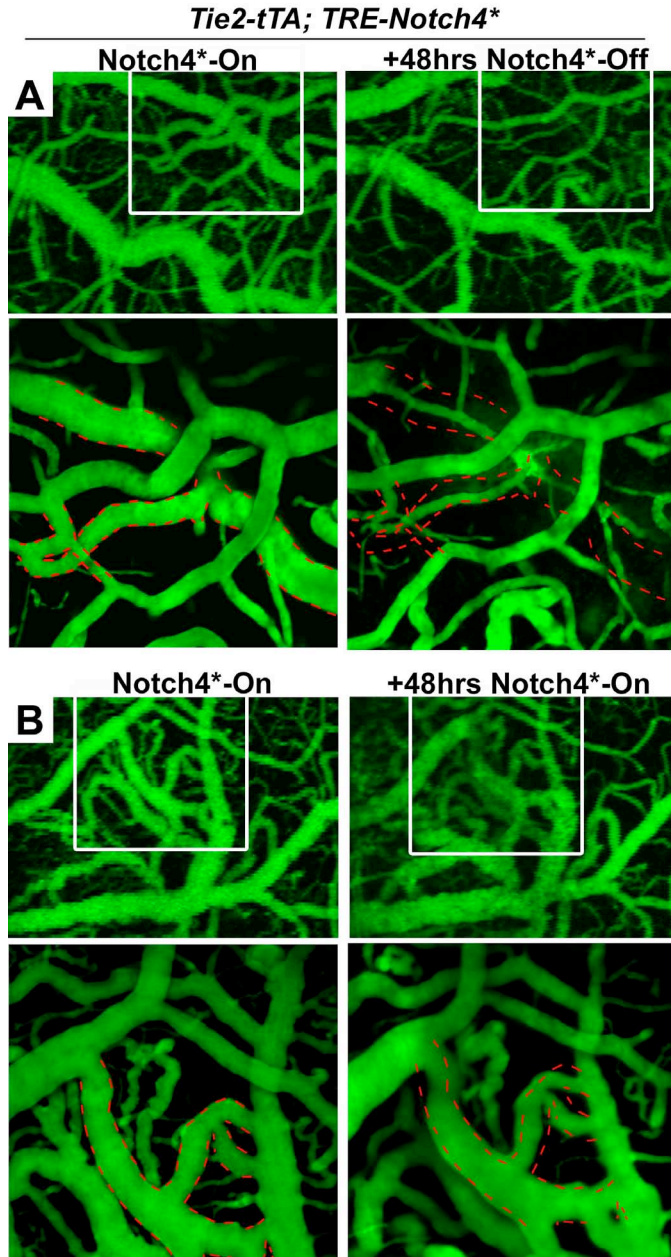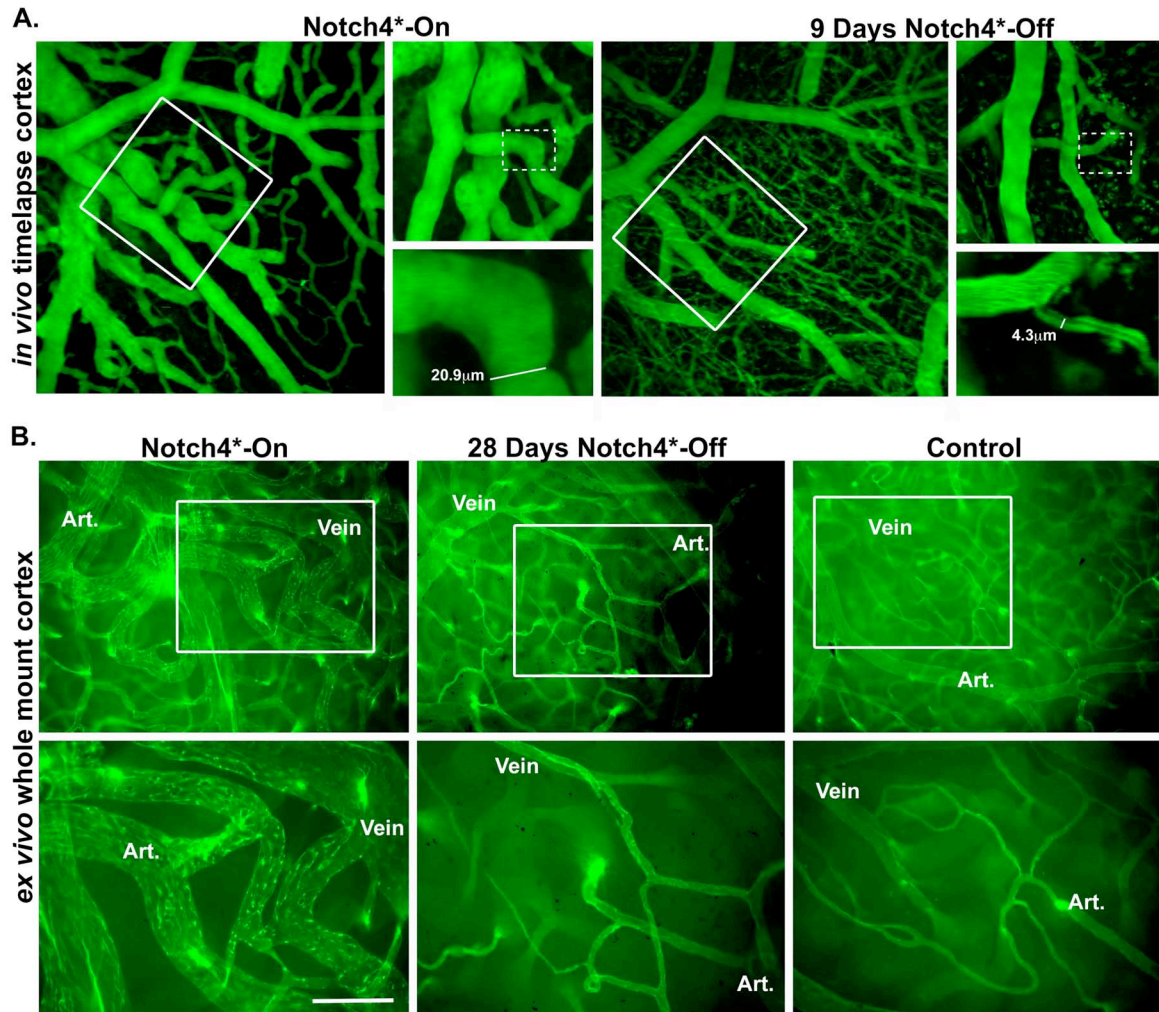
Supplementary Figure 5. Specific regression of arteriovenous shunts after repression of Notch4*

Two-photon timelapse imaging of cortical brain vessels through cranial window in Notch4* mutant mice. Plasma labeling is provided by intravenous FITC-dextran. (A) Regression of existing arteriovenous shunts following 48hrs of Notch4* repression (B) Regression does not occur without Notch4* repression. Note the reduction in the size of the distal vessels to the enlarging AV shunt in B.

Supplementary Figure 6. Arteriovenous shunts are stable until repression of Notch4*.

(A-C) Color-coded depiction of the arteriovenous shunt imaged by two-photon timelapse imaging in (D-F), arteries are in red and veins are in blue. AV shunt remains without repression of Notch4* (B&E), but regresses with 48hrs of Notch4* repression (C&F). Bottom panels show velocity traces obtained by line scan in the vessels indicated by yellow or green arrows (A-C). Velocity in AV shunt feeding artery (green) decreases, resulting in an increase in velocity in the non-AV shunt artery (yellow), during regression of the AV shunt.

Supplementary Figure 7. Regression of arteriovenous shunts to capillary diameter vessels in mice with and without cranial window treatment

(A) Two-photon timelapse imaging of cortical brain vessels through cranial window in Notch4* mutant mouse. Plasma labeling is provided by intravenous FITC-dextran. Large AV shunt regresses to capillary diameter within 9 days of Notch4* repression. (B) *Ex vivo* imaging of whole mount cortex from mice perfused with FITC-lectin. Prior to Notch4* repression, large AV shunts can be observed between artery and vein. In a similarly affected littermate mutant, following 28 days of Notch4* repression, AV connections are reduced to the diameter of capillaries in littermate control mice. Scale bar = 100μm
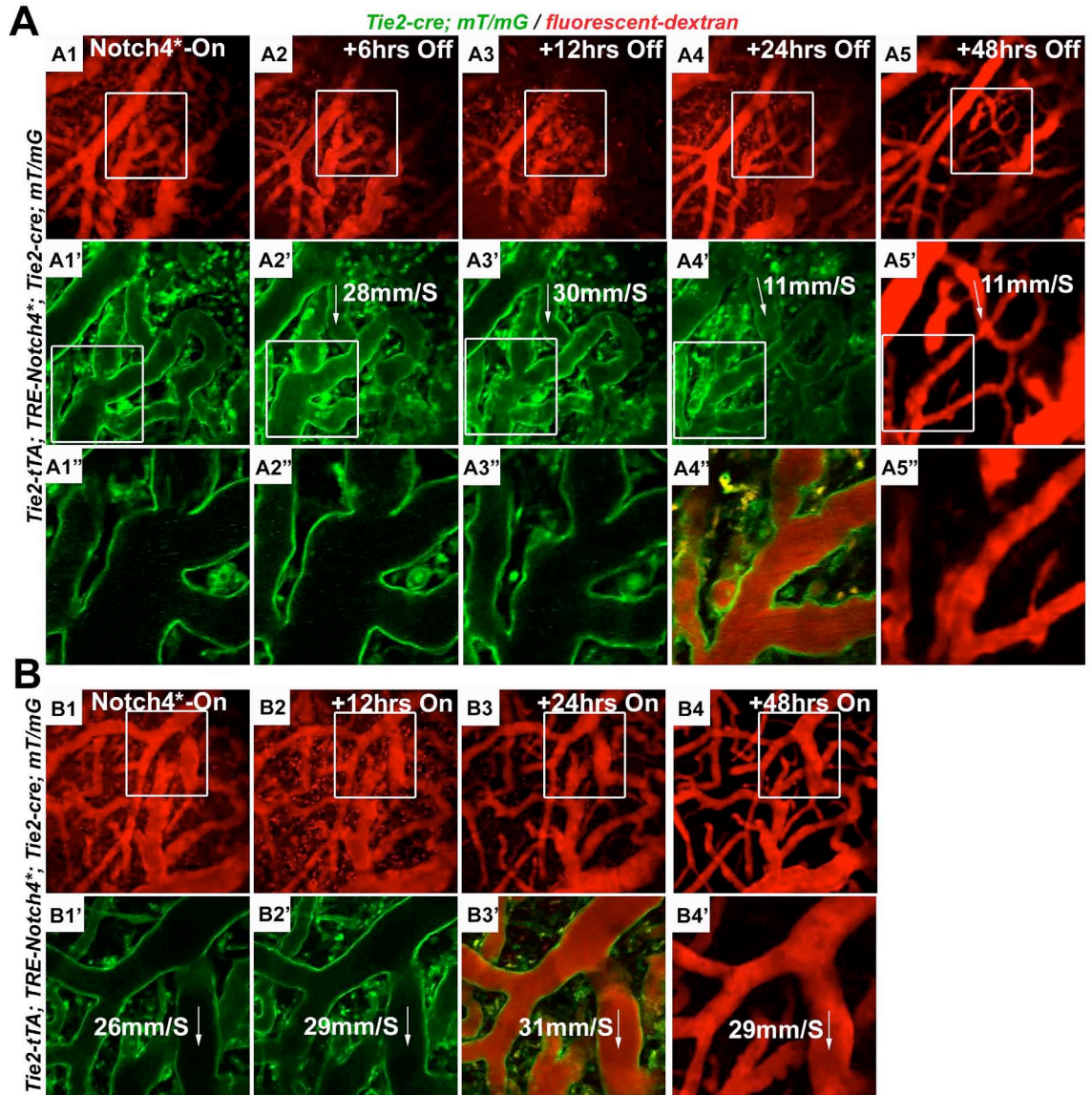
Supplementary Figure 8. Velocity changes coincide with narrowing of AV shunts and distal vein beginning by 12-24hrs after Notch4* repression

In vivo timelapse imaging of *Tie2-tTA; TRE-Notch4*; Tie2-cre; mT/mG* mice (green endothelial fluorescence), with TRITC-dextran labeling of plasma (red). (A) With repression of Notch4*, AV shunt regression begins between 12 and 24hrs, coinciding with a reduction in blood velocity through the AV shunt. (B) Without repression of Notch4*, AV shunt diameter and velocity are maintained. Note the reduction of distal vessel size. Blood flow was measured in this distal vessel, and was reduced over time.
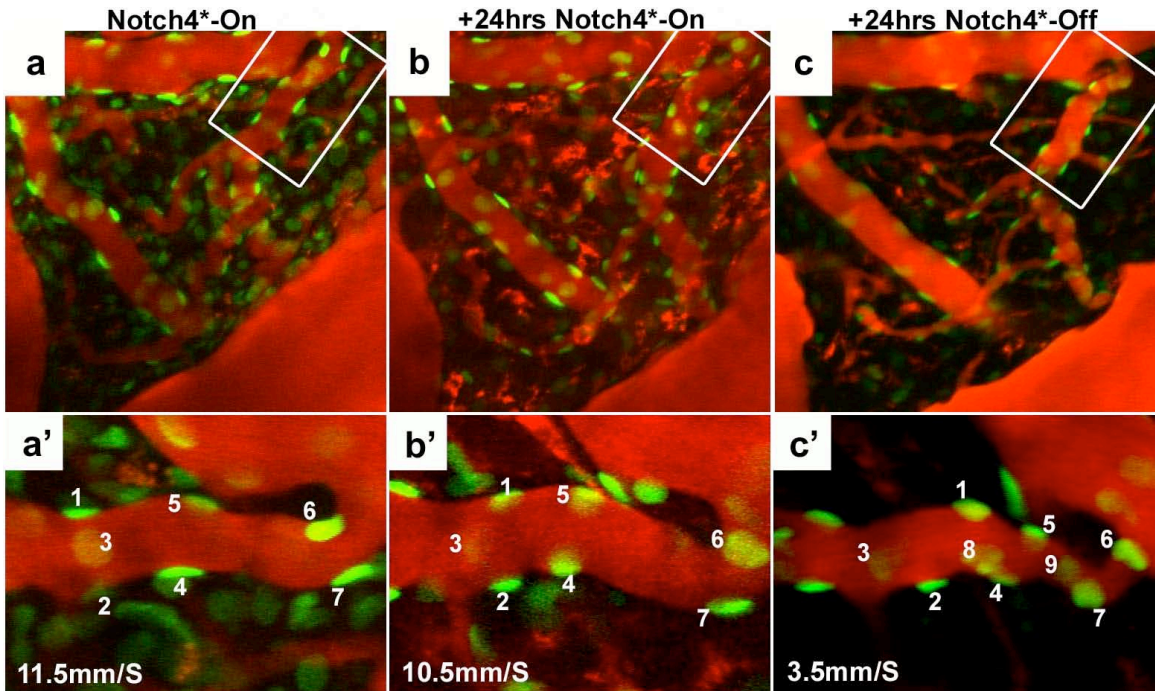
Supplementary Figure 9. Narrowing of ephrinB2-GFP+ AV shunt occurs specifically after Notch4* repression

Two-photon time-lapse imaging through a cranial window following repression of Notch4* in *ephrinB2*$^{+/H2B-eGFP}$ mutant with labeling of plasma by Texas-Red dextran. An AV shunt shows little change in diameter or centerline velocity (bottom left corner) after 24hrs without repression of Notch4* (b). Within 24hrs of Notch4* repression (c), the AV shunt was greatly reduced in diameter, with a reduction in blood velocity. Note that the same number of cells are present, but grouped closer.
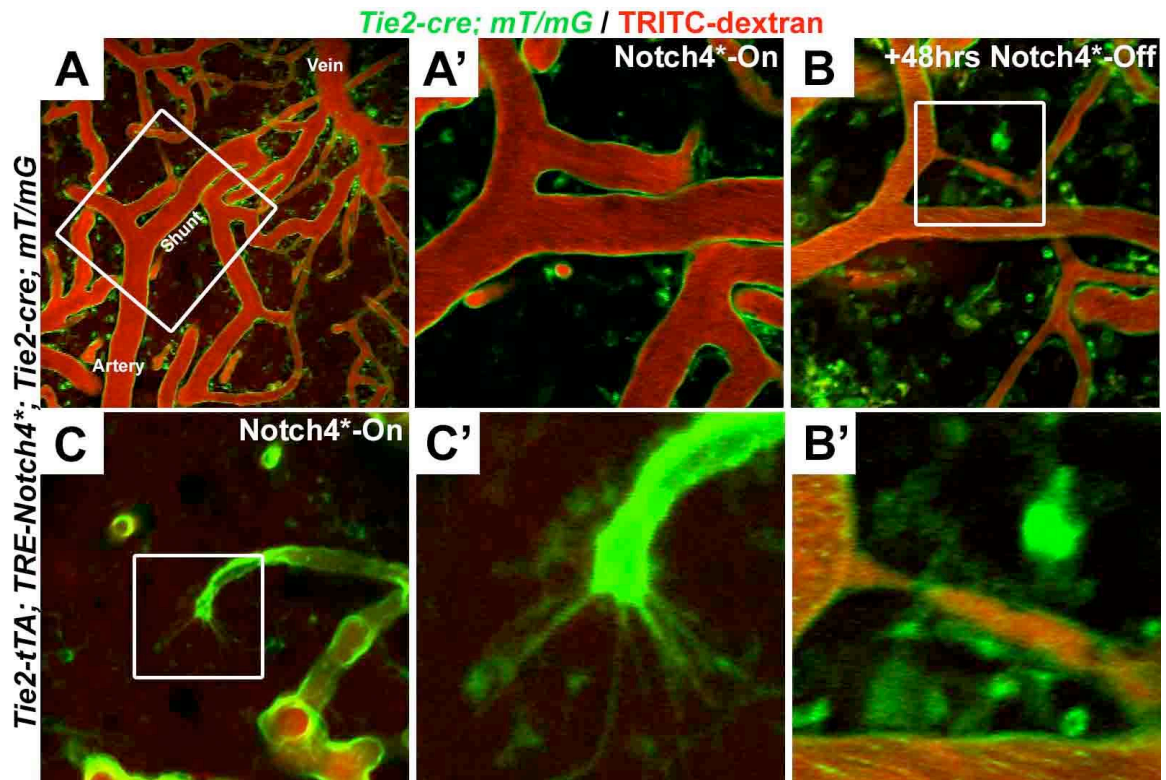
Supplementary Figure 10. Absence of obvious sprouting angiogenesis in regression *In vivo* imaging of tip cell in Tie2-cre; mT/mG mouse with TRITC-dextran plasma label. Large AV shunt before Dox treatment (A, A') regresses with 48hrs Notch4* repression (B, B'). No filopodia can be observed in the regressing vessel, although imaging resolution is sufficient to observe filopodia (C, C'). Note the filopodia extending from the cell body, which are illuminated by membrane bound GFP, and resolved by two-photon imaging.
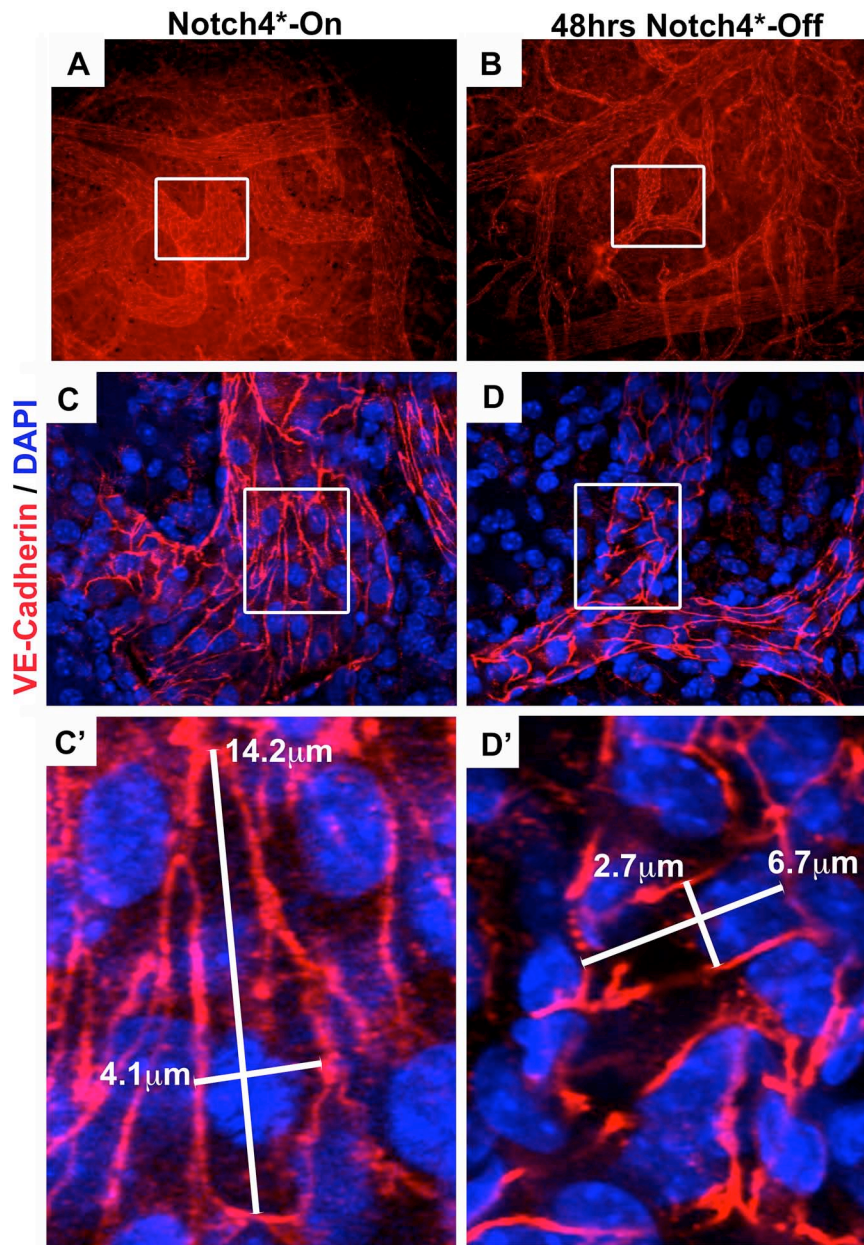
Supplementary Figure 11. Endothelial cells are narrowed in regressing arteriovenous shunts

(A-D) Fluorescent immunostaining of VE-cadherin in Notch4* mutant mice, imaged in whole mount. Areas shown in A&B were imaged by confocal microscopy at high magnification. Reduction in cell size occurred both axially and transaxially along the vessel. Note that the dimensions of endothelial cells are reduced both axially and paraxially along the AV shunt. EC area was reduced (n=4 shunts in 1 Notch4*-On mouse : 546μm^2 ± s.d. 193μm) vs. (n=4 shunts in each of 2 Notch4*-Off mice : 239μm^2 ± s.d. 68μm^2 and 211.4μm^2 ±s.d. 60μm^2)
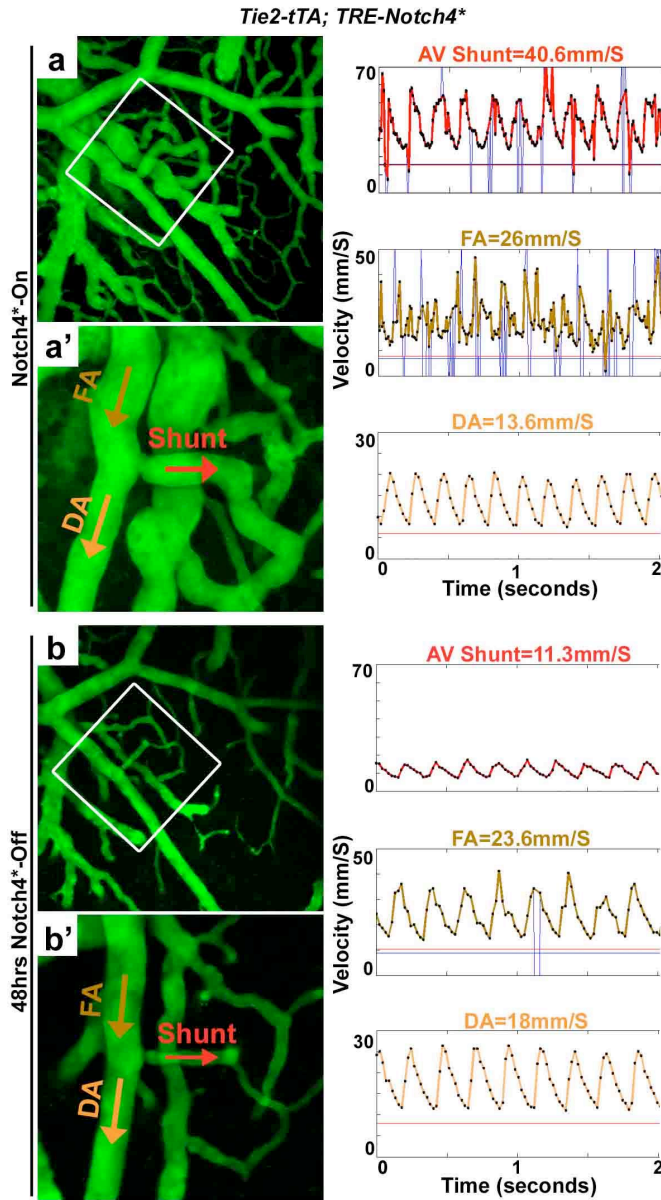
Supplementary Figure 12. Velocity in distal artery increases as shunt regresses
Two-photon timelapse imaging of cortical brain vessels through cranial window in
Notch4* mutant mouse. Plasma labeling is provided by intravenous FITC-dextran.
Arteriovenous shunt (a) is reduced in diameter following the repression of Notch4* (b).
Centerline velocity in the regressing AV shunt, feeding artery (FA) and distal artery (DA)
was obtained by direct measurement of the velocity of individual red blood cells (panels,
a-d). Repression of Notch4* decreases blood flow velocity in shunt by 48hrs (panels,
a&b) and FA, but increases velocity in DA. Table shows quantification of the changes in
velocity without repression of Notch4* (Notch4*-On) or with repression of Notch4*
(Notch4*-Off) for 48-72hrs.
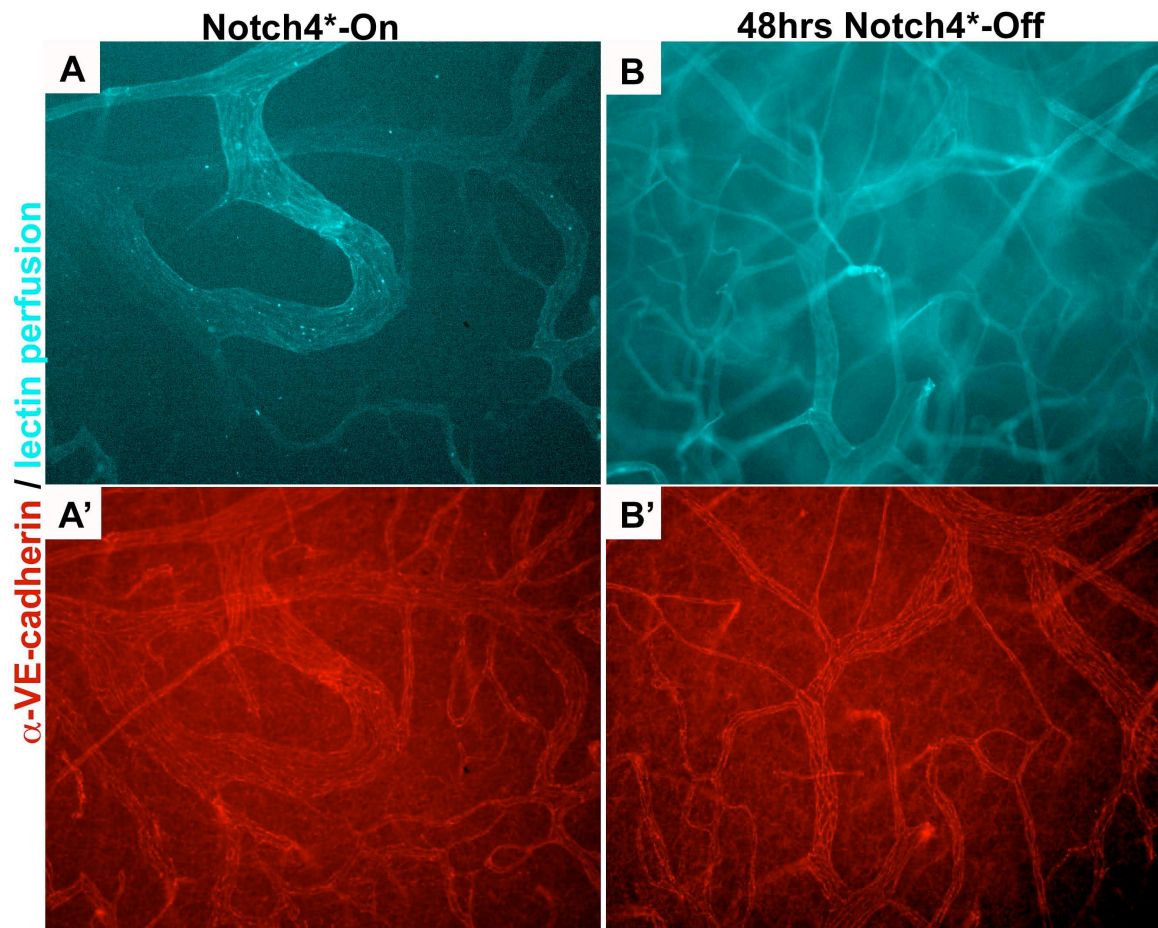
Supplementary Figure 13. Increased perfusion of capillary vessels following repression of Notch4*

Whole mount immunofluorescent imaging of surface of the cerebral cortex. (A&B) Perfused vessels highlighted by tomato-lectin in the same region shown by VE-cadherin immunostaining (A'&B'). Note that many of the VE-cadherin+ capillaries in the Notch4* mutant are not perfused. Following repression of Notch4*, capillary perfusion is increased.

Discussion

BAVMs are a devastating human disease, but the molecular events that lead to BAVM formation in most cases remain unknown. Although forward genetic approaches identified causal mutations in Alk1, endoglin, Smad4, RASA1, and PTEN, together these molecular lesions account for a small percentage of the human disease. In this thesis work, a novel reverse genetic approach implicates increased Notch signaling in their formation, and more generally suggests the involvement of other genes in the developmentally defined AV specification program. I find that disruption of AV specification, by endothelial-specific expression of constitutively-active Notch4, causes BAVM-like abnormalities in a mouse model, and that Notch signaling is upregulated in human BAVM tissue samples. Strikingly, restoration of AV specification upon the repression of constitutively-active Notch4 is sufficient to induce the regression of enlarged AV shunts to capillaries, reversing BAVMs in our animal model. This regression is mediated by Eph/ephrin signaling, key downstream genes in the AV specification program, and could be blocked by a soluble form of EphB4.

Although the work described has implicated Notch signaling as a candidate lesion in human brain AVMs, confirmation requires genetic association in the human disease. Alk1, endoglin, Smad4, RASA1, and PTEN have been linked to human AVMs by studies of familial inheritance. However, the majority of human AVMs are sporadic, which has limited such genetic linkage. Interestingly, *de novo* mutations in Smad4, RASA1 and PTEN have all been identified in AVMs.(8, 17)   Strikingly the

majority of AVM associated RASA1 mutations (9/17 AVM affected families) were *de novo*, suggesting that these mutations are detrimental to fitness, and therefore short-lived in the gene pool. In venous malformations, *de novo* germline mutations in the Tie2 receptor involved have been identified.(59, 60) Somatic mutation have also been identified in venous malformation foci, suggesting that this somatic genetic lesion is involved in the focal development of the disease.(61) It is possible that somatic genetic mutations may also be involved in the development of these sporadic AVMs.(62) This could be one explanation for the focal development of AVMs. In contrast to mutations in HHT, CM-AVM and PTEN related diseases, gain-of-function and some of the loss-of-function mutations in Notch signaling are embryonic lethal in the mouse, indicating that these types of mutations could not be transmitted through the germline. A precedent for somatic activating mutations in Notch signaling can be found in the proliferative blood disorder T-ALL, 50% of which is caused by these mutations.(63) It will be interesting to determine whether subtle mutations which increase Notch signaling predispose to AVM formation, and whether somatic activating mutations in Notch receptors have occurred in the vasculature of patients with AVMs.

Ideally, a better understanding of the role of Notch signaling in human AVMs, and the mechanism through which Notch activation induces AVMs in animal models will lead to molecular therapies. One of the significant hurdles is determining what types of Notch activating mutations are involved in AVM development, if any. For example, in leukemia, activating mutations can be gain-of-function mutations, such

as those in the extracellular domain of the Notch receptor that increase its ligand-independent activity(63), or loss-of-function mutations in Notch repressors, such as Fbxw7 ubiquitin ligase(64), which normally increases the degradation of the activated receptor. The level of the mutation will determine whether inhibition of the ligand binding(65-67), receptor cleavage(68, 69), or downstream transcriptional activity(70) are likely to be effective. Another significant hurdle is addressing a potential requirement for spatially restricted Notch activity in regression. In the regulated mouse model, endogenous Notch activity is retained once the Notch4* transgene is repressed. The difference in levels of endogenous Notch signaling between arterial cells and venous cells may be important in the separation of arterial and venous endothelium in the AVM. This would limit the effectiveness of broad inhibition of endothelial Notch signaling, and would require either specific inhibition of the Notch activating mutation (without effect on endogenous Notch activity), or venous cell-specific inhibition of Notch.

It may also be useful to re-examine the genes that have been identified in human AVMs by forward genetics from the perspective of AV specification. The specific cellular mechanisms through which these genes cause AVM remain unknown. It is interesting to speculate that they are involved in a common pathway mediating AV specification or effecting the refinement of the vascular plexus downstream of AV specification.

Hereditary Hemorhagic Telangectasia (HHT)

Although the relationship between the Alk1 and endoglin receptors and AV specification is still unclear, some work in that direction is notable. Alk1 is expressed primarily in arteries, not veins, and in Alk1 deficient embryos, ephrin-B2 expression is strongly reduced in arteries.(14, 71) Interestingly, no obvious changes in the expression of other Notch pathway genes have been detected.(14) Conditional deletion of Alk1 in adult mice results in spontaneous AVM formation in growing mice, but the AV specification in these AVMs has not yet been characterized.(12)

In contrast to the pro-arterial expression pattern and activity of Alk1, endoglin is expressed in both arteries and veins of the developing embryo, and does not appear to affect AV specification.(14, 72) In AVMs of embryos deficient in endoglin, ephrin-B2 expression is strikingly maintained specifically on the arterial side, suggesting that arterial specification is not altered.(14) Conditional deletion of endoglin also results in AVMs in growing tissues, and as in embryonic studies, the AVMs form between arteries and veins with proper specification.(13) Despite the complete absence of endoglin in the vasculature of these conditional knockouts, Jag1 and ephrin-B2 are properly expressed in the arteries and EphB4 is expressed in the veins.(13) So, while Alk1 may promote arterial specification, endoglin appears to cause AVMs without disrupting AV specification.

RASA1

RASA1 is critical for EphB/ephrinB mediated cell sorting.(56) By increasing the intrinsic GTPase activity of Ras family proteins (which includes the Rho of

GTPases important for directed cell migration), RASA1 locally reduces GTP-bound

active Ras. This localized activity has been implicated in regulation of cell

polarization and directed migration.(73) In mouse embryonic fibroblasts, derived

from a RASA1 null mouse, cell migration was dramatically impaired in a scratch

wound assay. The defect in the RASA1 null cells did not appear to be entirely

attributable to Ras regulation through GAP activity, since migration defects could be

partially rescued by expression of a catalytically inactive form of RASA1. Further

experiments suggested that RASA1 may regulate the activity of p190 GAP, which in

turn regulates Rho GTPase activity and is therefore linked to actin stress-fiber and

focal adhesion turnover. In endothothelial cells, RASA1 is recruited to EphB4

following ephrin-B2 ligand activation and phosphorylation of the receptor,

suggesting that the pathway might be active in ephrin-B2/EphB4 mediated cell-

migration within the endothelium.(74) In support of such a function, one of the

most obvious defects in embryos deficient in RASA1 is arrested vascular

development.(75, 76) Although endothelial cells are present in these embryos, the

initial vascular plexus fails to reorganize. Strikingly, in chimeric embryos generated

from a mixture of wild-type and RASA1 null ES cells, the presence of RASA1 null

cells results in the development of focal vascular abnormalities. Although

interactions of RASA1 with any of the diverse Ras signaling pathways could underlie

these defects in cellular migration, disruption of EphB signaling is a very likely

possibility. Given this connection between RASA1, directed cell migration and

ephrin-B2/EphB4 mediated repulsion, the involvement of RASA1 mutations in a

subset of hereditary human AVMs is provocative.(9, 17)

PTEN

PTEN is best known as a suppressor of Pi3k activity, which, among many other functions, has been implicated in AV specification. As discussed earlier, Pi3k signaling promotes venous specification and inhibits arterial specification in zebrafish.(41) While there are no direct connections between PTEN and AV specification in endothelial cells, it is intriguing that re-introduction of PTEN to deficient prostate cancer cells suppresses EphB4 expression.(77) It is possible that PTEN deficiency alters the balance of AV specification, by increasing the proportion of venous specification.

Our results have several more general implications in the genetic regulation of blood vessel structure. First, arterialization of venous vessels may enhance the durability and longevity of vein grafts. Technical reasons dictate the use of vein grafts in bypass surgeries, but their long-term patency is worse than arteries. Veins downregulate venous markers, but fail to upregulate arterial markers, when grafted to arterial positions, suggesting that the fundamental problem may be a failure to switch AV specification.(78) Second, Notch may be required to stabilize nascent large vessels, suggesting an unexpected target in the treatment of cancers with Notch inhibitors. Recent work has shown that upon treatment with Notch inhibitors, tumor vasculature becomes dense, but narrow and poorly perfused.(66) Although subsequent work suggested that this is caused by a suppression of sprouting by Notch signaling, our work suggests a complimentary interpretation.

Finally, the EphB-ephrin-B2 mediated refinement of AV connections we have observed may provide insight into role of these molecules in establishing AV hierarchy in normal vascular development. We and others have observed "bridges" between the dorsal aorta and cardinal vein, which fail to narrow in mutants with increased Notch4* signaling, or reduced expression of ephrin-B2 and EphB4.(21) Thus, the cellular behavior during the regression of AV shunts in the post-natal brain may reflect the process of artery and vein separation during normal vascular development.

References

1.   Reporting terminology for brain arteriovenous malformation clinical and radiographic features for use in clinical trials. Stroke2001 Jun;32(6):1430-42.

2.   Friedlander RM. Clinical practice. Arteriovenous malformations of the brain. N Engl J Med2007 Jun 28;356(26):2704-12.

3.   Fleetwood IG, Steinberg GK. Arteriovenous malformations. Lancet2002 Mar 9;359(9309):863-73.

4.   Stapf C, Mohr JP, Choi JH, Hartmann A, Mast H. Invasive treatment of unruptured brain arteriovenous malformations is experimental therapy. Curr Opin Neurol2006 Feb;19(1):63-8.

5.   Braverman IM, Keh A, Jacobson BS. Ultrastructure and three-dimensional organization of the telangiectases of hereditary hemorrhagic telangiectasia. J Invest Dermatol1990 Oct;95(4):422-7.

6.   Mullan S, Mojtahedi S, Johnson DL, Macdonald RL. Embryological basis of some aspects of cerebral vascular fistulas and malformations. J Neurosurg1996 Jul;85(1):1-8.

7.   Abdalla SA, Letarte M. Hereditary haemorrhagic telangiectasia: current views on genetics and mechanisms of disease. J Med Genet2006 Feb;43(2):97-110.

8.   Gallione CJ, Repetto GM, Legius E, Rustgi AK, Schelley SL, Tejpar S, Mitchell G, Drouin E, Westermann CJ, Marchuk DA. A combined syndrome of juvenile polyposis and hereditary haemorrhagic telangiectasia associated with mutations in MADH4 (SMAD4). Lancet2004 Mar 13;363(9412):852-9.

9.   Eerola I, Boon LM, Mulliken JB, Burrows PE, Dompmartin A, Watanabe S, Vanwijck R, Vikkula M. Capillary malformation-arteriovenous malformation, a new clinical and genetic disorder caused by RASA1 mutations. Am J Hum Genet2003 Dec;73(6):1240-9.

10.   Tan WH, Baris HN, Burrows PE, Robson CD, Alomari AI, Mulliken JB, Fishman SJ, Irons MB. The spectrum of vascular anomalies in patients with PTEN mutations: implications for diagnosis and management. J Med Genet2007 Sep;44(9):594-602.

11.   Zhou XP, Marsh DJ, Hampel H, Mulliken JB, Gimm O, Eng C. Germline and germline mosaic PTEN mutations associated with a Proteus-like syndrome of hemihypertrophy, lower limb asymmetry, arteriovenous malformations and lipomatosis. Hum Mol Genet2000 Mar 22;9(5):765-8.

12.   Park SO, Wankhede M, Lee YJ, Choi EJ, Fliess N, Choe SW, Oh SH, Walter G, Raizada MK, Sorg BS, Oh SP. Real-time imaging of de novo arteriovenous malformation in a mouse model of hereditary hemorrhagic telangiectasia. J Clin Invest2009 Nov;119(11):3487-96.

13.   Mahmoud M, Allinson KR, Zhai Z, Oakenfull R, Ghandi P, Adams RH, Fruttiger M, Arthur HM. Pathogenesis of arteriovenous malformations in the absence of endoglin. Circ Res Apr 30;106(8):1425-33.

14.   Sorensen LK, Brooke BS, Li DY, Urness LD. Loss of distinct arterial and venous boundaries in mice lacking endoglin, a vascular-specific TGFbeta coreceptor. Dev Biol2003 Sep 1;261(1):235-50.

15.   Gallione CJ, Richards JA, Letteboer TG, Rushlow D, Prigoda NL, Leedom TP, Ganguly A, Castells A, Ploos van Amstel JK, Westermann CJ, Pyeritz RE, Marchuk DA.

SMAD4 mutations found in unselected HHT patients. J Med Genet2006 Oct;43(10):793-7.

16.   Lan Y, Liu B, Yao H, Li F, Weng T, Yang G, Li W, Cheng X, Mao N, Yang X. Essential role of endothelial Smad4 in vascular remodeling and integrity. Mol Cell Biol2007 Nov;27(21):7683-92.

17.   Revencu N, Boon LM, Mulliken JB, Enjolras O, Cordisco MR, Burrows PE, Clapuyt P, Hammer F, Dubois J, Baselga E, Brancati F, Carder R, Quintal JM, Dallapiccola B, Fischer G, Frieden IJ, Garzon M, Harper J, Johnson-Patel J, Labreze C, Martorell L, Paltiel HJ, Pohl A, Prendiville J, Quere I, Siegel DH, Valente EM, Van Hagen A, Van Hest L, Vaux KK, Vicente A, Weibel L, Chitayat D, Vikkula M. Parkes Weber syndrome, vein of Galen aneurysmal malformation, and other fast-flow vascular anomalies are caused by RASA1 mutations. Hum Mutat2008 Jul;29(7):959-65.

18.   Hamada K, Sasaki T, Koni PA, Natsui M, Kishimoto H, Sasaki J, Yajima N, Horie Y, Hasegawa G, Naito M, Miyazaki J, Suda T, Itoh H, Nakao K, Mak TW, Nakano T, Suzuki A. The PTEN/PI3K pathway governs normal vascular development and tumor angiogenesis. Genes Dev2005 Sep 1;19(17):2054-65.

19.   Matsubara S, Mandzia JL, ter Brugge K, Willinsky RA, Faughnan ME. Angiographic and clinical characteristics of patients with cerebral arteriovenous malformations associated with hereditary hemorrhagic telangiectasia. AJNR Am J Neuroradiol2000 Jun-Jul;21(6):1016-20.

20.   Krebs LT, Starling C, Chervonsky AV, Gridley T. Notch1 activation in mice causes arteriovenous malformations phenocopied by ephrinB2 and EphB4 mutants. Genesis Mar;48(3):146-50.

21.   Kim YH, Hu H, Guevara-Gallardo S, Lam MT, Fong SY, Wang RA. Artery and vein size is balanced by Notch and ephrin B2/EphB4 during angiogenesis. Development2008 Nov;135(22):3755-64.

22.   Krebs LT, Shutter JR, Tanigaki K, Honjo T, Stark KL, Gridley T. Haploinsufficient lethality and formation of arteriovenous malformations in Notch pathway mutants. Genes Dev2004 Oct 15;18(20):2469-73.

23.   Lawson ND, Scheer N, Pham VN, Kim CH, Chitnis AB, Campos-Ortega JA, Weinstein BM. Notch signaling is required for arterial-venous differentiation during embryonic vascular development. Development2001 Oct;128(19):3675-83.

24.   Nichols SA, Dirks W, Pearse JS, King N. Early evolution of animal cell signaling and adhesion genes. Proc Natl Acad Sci U S A2006 Aug 15;103(33):12451-6.

25.   King N, Westbrook MJ, Young SL, Kuo A, Abedin M, Chapman J, Fairclough S, Hellsten U, Isogai Y, Letunic I, Marr M, Pincus D, Putnam N, Rokas A, Wright KJ, Zuzow R, Dirks W, Good M, Goodstein D, Lemons D, Li W, Lyons JB, Morris A, Nichols S, Richter DJ, Salamov A, Sequencing JG, Bork P, Lim WA, Manning G, Miller WT, McGinnis W, Shapiro H, Tjian R, Grigoriev IV, Rokhsar D. The genome of the choanoflagellate Monosiga brevicollis and the origin of metazoans. Nature2008 Feb 14;451(7180):783-8.

26.   Bray SJ. Notch signalling: a simple pathway becomes complex. Nat Rev Mol Cell Biol2006 Sep;7(9):678-89.

27.   Zhong TP, Childs S, Leu JP, Fishman MC. Gridlock signalling pathway fashions the first embryonic artery. Nature2001 Nov 8;414(6860):216-20.

28.   Lawson ND, Weinstein BM. Arteries and veins: making a difference with zebrafish. Nat Rev Genet2002 Sep;3(9):674-82.

29.   Villa N, Walker L, Lindsell CE, Gasson J, Iruela-Arispe ML, Weinmaster G. Vascular expression of Notch pathway receptors and ligands is restricted to arterial vessels. Mech Dev2001 Oct;108(1-2):161-4.

30.   Krebs LT, Xue Y, Norton CR, Shutter JR, Maguire M, Sundberg JP, Gallahan D, Closson V, Kitajewski J, Callahan R, Smith GH, Stark KL, Gridley T. Notch signaling is essential for vascular morphogenesis in mice. Genes Dev2000 Jun 1;14(11):1343-52.

31.   Duarte A, Hirashima M, Benedito R, Trindade A, Diniz P, Bekman E, Costa L, Henrique D, Rossant J. Dosage-sensitive requirement for mouse Dll4 in artery development. Genes Dev2004 Oct 15;18(20):2474-8.

32.   Gale NW, Dominguez MG, Noguera I, Pan L, Hughes V, Valenzuela DM, Murphy AJ, Adams NC, Lin HC, Holash J, Thurston G, Yancopoulos GD. Haploinsufficiency of delta-like 4 ligand results in embryonic lethality due to major defects in arterial and vascular development. Proc Natl Acad Sci U S A2004 Nov 9;101(45):15949-54.

33.   Fischer A, Schumacher N, Maier M, Sendtner M, Gessler M. The Notch target genes Hey1 and Hey2 are required for embryonic vascular development. Genes Dev2004 Apr 15;18(8):901-11.

34.   Trindade A, Kumar SR, Scehnet JS, Lopes-da-Costa L, Becker J, Jiang W, Liu R, Gill PS, Duarte A. Overexpression of delta-like 4 induces arterialization and attenuates vessel formation in developing mouse embryos. Blood2008 Sep 1;112(5):1720-9.

35.   Lanner F, Sohl M, Farnebo F. Functional arterial and venous fate is determined by graded VEGF signaling and notch status during embryonic stem cell differentiation. Arterioscler Thromb Vasc Biol2007 Mar;27(3):487-93.

36.   Mukouyama YS, Shin D, Britsch S, Taniguchi M, Anderson DJ. Sensory nerves determine the pattern of arterial differentiation and blood vessel branching in the skin. Cell2002 Jun 14;109(6):693-705.

37.   Liu ZJ, Shirakawa T, Li Y, Soma A, Oka M, Dotto GP, Fairman RM, Velazquez OC, Herlyn M. Regulation of Notch1 and Dll4 by vascular endothelial growth factor in arterial endothelial cells: implications for modulating arteriogenesis and angiogenesis. Mol Cell Biol2003 Jan;23(1):14-25.

38.   Lobov IB, Renard RA, Papadopoulos N, Gale NW, Thurston G, Yancopoulos GD, Wiegand SJ. Delta-like ligand 4 (Dll4) is induced by VEGF as a negative regulator of angiogenic sprouting. Proc Natl Acad Sci U S A2007 Feb 27;104(9):3219-24.

39.   Visconti RP, Richardson CD, Sato TN. Orchestration of angiogenesis and arteriovenous contribution by angiopoietins and vascular endothelial growth factor (VEGF). Proc Natl Acad Sci U S A2002 Jun 11;99(12):8219-24.

40.   Lawson ND, Mugford JW, Diamond BA, Weinstein BM. phospholipase C gamma-1 is required downstream of vascular endothelial growth factor during arterial development. Genes Dev2003 Jun 1;17(11):1346-51.

41.   Hong CC, Peterson QP, Hong JY, Peterson RT. Artery/vein specification is governed by opposing phosphatidylinositol-3 kinase and MAP kinase/ERK signaling. Curr Biol2006 Jul 11;16(13):1366-72.

42.   Seo S, Fujita H, Nakano A, Kang M, Duarte A, Kume T. The forkhead transcription factors, Foxc1 and Foxc2, are required for arterial specification and lymphatic sprouting during vascular development. Dev Biol2006 Jun 15;294(2):458-70.

43.   Hayashi H, Kume T. Foxc transcription factors directly regulate Dll4 and Hey2 expression by interacting with the VEGF-Notch signaling pathways in endothelial cells. PLoS One2008;3(6):e2401.

44.   You LR, Lin FJ, Lee CT, DeMayo FJ, Tsai MJ, Tsai SY. Suppression of Notch signalling by the COUP-TFII transcription factor regulates vein identity. Nature2005 May 5;435(7038):98-104.

45.   Pereira FA, Qiu Y, Zhou G, Tsai MJ, Tsai SY. The orphan nuclear receptor COUP-TFII is required for angiogenesis and heart development. Genes Dev1999 Apr 15;13(8):1037-49.

46.   le Noble F, Moyon D, Pardanaud L, Yuan L, Djonov V, Matthijsen R, Breant C, Fleury V, Eichmann A. Flow regulates arterial-venous differentiation in the chick embryo yolk sac. Development2004 Jan;131(2):361-75.

47.   Wang HU, Chen ZF, Anderson DJ. Molecular distinction and angiogenic interaction between embryonic arteries and veins revealed by ephrin-B2 and its receptor Eph-B4. Cell1998 May 29;93(5):741-53.

48.   Flanagan JG, Vanderhaeghen P. The ephrins and Eph receptors in neural development. Annu Rev Neurosci1998;21:309-45.

49.   Wang HU, Anderson DJ. Eph family transmembrane ligands can mediate repulsive guidance of trunk neural crest migration and motor axon outgrowth. Neuron1997 Mar;18(3):383-96.

50.   Hamada K, Oike Y, Ito Y, Maekawa H, Miyata K, Shimomura T, Suda T. Distinct roles of ephrin-B2 forward and EphB4 reverse signaling in endothelial cells. Arterioscler Thromb Vasc Biol2003 Feb 1;23(2):190-7.

51.   Fuller T, Korff T, Kilian A, Dandekar G, Augustin HG. Forward EphB4 signaling in endothelial cells controls cellular repulsion and segregation from ephrinB2 positive cells. J Cell Sci2003 Jun 15;116(Pt 12):2461-70.

52.   Cowan CA, Yokoyama N, Saxena A, Chumley MJ, Silvany RE, Baker LA, Srivastava D, Henkemeyer M. Ephrin-B2 reverse signaling is required for axon pathfinding and cardiac valve formation but not early vascular development. Dev Biol2004 Jul 15;271(2):263-71.

53.   Janes PW, Saha N, Barton WA, Kolev MV, Wimmer-Kleikamp SH, Nievergall E, Blobel CP, Himanen JP, Lackmann M, Nikolov DB. Adam meets Eph: an ADAM substrate recognition module acts as a molecular switch for ephrin cleavage in trans. Cell2005 Oct 21;123(2):291-304.

54.   Egea J, Klein R. Bidirectional Eph-ephrin signaling during axon guidance. Trends Cell Biol2007 May;17(5):230-8.

55.   Noren NK, Pasquale EB. Eph receptor-ephrin bidirectional signals that target Ras and Rho proteins. Cell Signal2004 Jun;16(6):655-66.

56.   Jorgensen C, Sherman A, Chen GI, Pasculescu A, Poliakov A, Hsiung M, Larsen B, Wilkinson DG, Linding R, Pawson T. Cell-specific information processing in segregating populations of Eph receptor ephrin-expressing cells. Science2009 Dec 11;326(5959):1502-9.

57.	Herbert SP, Huisken J, Kim TN, Feldman ME, Houseman BT, Wang RA, Shokat KM, Stainier DY. Arterial-venous segregation by selective cell sprouting: an alternative mode of blood vessel formation. Science2009 Oct 9;326(5950):294-8.

58.	Swift MR, Weinstein BM. Arterial-venous specification during development. Circ Res2009 Mar 13;104(5):576-88.

59.	Vikkula M, Boon LM, Carraway KL, 3rd, Calvert JT, Diamonti AJ, Goumnerov B, Pasyk KA, Marchuk DA, Warman ML, Cantley LC, Mulliken JB, Olsen BR. Vascular dysmorphogenesis caused by an activating mutation in the receptor tyrosine kinase TIE2. Cell1996 Dec 27;87(7):1181-90.

60.	Zhou X, Hampel H, Thiele H, Gorlin RJ, Hennekam RC, Parisi M, Winter RM, Eng C. Association of germline mutation in the PTEN tumour suppressor gene and Proteus and Proteus-like syndromes. Lancet2001 Jul 21;358(9277):210-1.

61.	Limaye N, Wouters V, Uebelhoer M, Tuominen M, Wirkkala R, Mulliken JB, Eklund L, Boon LM, Vikkula M. Somatic mutations in angiopoietin receptor gene TEK cause solitary and multiple sporadic venous malformations. Nat Genet2009 Jan;41(1):118-24.

62.	Limaye N, Boon LM, Vikkula M. From germline towards somatic mutations in the pathophysiology of vascular anomalies. Hum Mol Genet2009 Apr 15;18(R1):R65-74.

63.	Weng AP, Ferrando AA, Lee W, Morris JPt, Silverman LB, Sanchez-Irizarry C, Blacklow SC, Look AT, Aster JC. Activating mutations of NOTCH1 in human T cell acute lymphoblastic leukemia. Science2004 Oct 8;306(5694):269-71.

64.	Matsuoka S, Oike Y, Onoyama I, Iwama A, Arai F, Takubo K, Mashimo Y, Oguro H, Nitta E, Ito K, Miyamoto K, Yoshiwara H, Hosokawa K, Nakamura Y, Gomei Y, Iwasaki H, Hayashi Y, Matsuzaki Y, Nakayama K, Ikeda Y, Hata A, Chiba S, Nakayama KI, Suda T. Fbxw7 acts as a critical fail-safe against premature loss of hematopoietic stem cells and development of T-ALL. Genes Dev2008 Apr 15;22(8):986-91.

65.	Yan M, Callahan CA, Beyer JC, Allamneni KP, Zhang G, Ridgway JB, Niessen K, Plowman GD. Chronic DLL4 blockade induces vascular neoplasms. Nature Feb 11;463(7282):E6-7.

66.	Ridgway J, Zhang G, Wu Y, Stawicki S, Liang WC, Chanthery Y, Kowalski J, Watts RJ, Callahan C, Kasman I, Singh M, Chien M, Tan C, Hongo JA, de Sauvage F, Plowman G, Yan M. Inhibition of Dll4 signalling inhibits tumour growth by deregulating angiogenesis. Nature2006 Dec 21;444(7122):1083-7.

67.	Noguera-Troise I, Daly C, Papadopoulos NJ, Coetzee S, Boland P, Gale NW, Lin HC, Yancopoulos GD, Thurston G. Blockade of Dll4 inhibits tumour growth by promoting non-productive angiogenesis. Nature2006 Dec 21;444(7122):1032-7.

68.	De Strooper B, Annaert W, Cupers P, Saftig P, Craessaerts K, Mumm JS, Schroeter EH, Schrijvers V, Wolfe MS, Ray WJ, Goate A, Kopan R. A presenilin-1-dependent gamma-secretase-like protease mediates release of Notch intracellular domain. Nature1999 Apr 8;398(6727):518-22.

69.	Serneels L, Van Biervliet J, Craessaerts K, Dejaegere T, Horre K, Van Houtvin T, Esselmann H, Paul S, Schafer MK, Berezovska O, Hyman BT, Sprangers B, Sciot R, Moons L, Jucker M, Yang Z, May PC, Karran E, Wiltfang J, D'Hooge R, De Strooper B. gamma-Secretase heterogeneity in the Aph1 subunit: relevance for Alzheimer's disease. Science2009 May 1;324(5927):639-42.

70.   Moellering RE, Cornejo M, Davis TN, Del Bianco C, Aster JC, Blacklow SC, Kung AL, Gilliland DG, Verdine GL, Bradner JE. Direct inhibition of the NOTCH transcription factor complex. Nature2009 Nov 12;462(7270):182-8.

71.   Seki T, Yun J, Oh SP. Arterial endothelium-specific activin receptor-like kinase 1 expression suggests its role in arterialization and vascular remodeling. Circ Res2003 Oct 3;93(7):682-9.

72.   Jonker L, Arthur HM. Endoglin expression in early development is associated with vasculogenesis and angiogenesis. Mech Dev2002 Jan;110(1-2):193-6.

73.   Kulkarni SV, Gish G, van der Geer P, Henkemeyer M, Pawson T. Role of p120 Ras-GAP in directed cell movement. J Cell Biol2000 Apr 17;149(2):457-70.

74.   Kim I, Ryu YS, Kwak HJ, Ahn SY, Oh JL, Yancopoulos GD, Gale NW, Koh GY. EphB ligand, ephrinB2, suppresses the VEGF- and angiopoietin 1-induced Ras/mitogen-activated protein kinase pathway in venous endothelial cells. Faseb J2002 Jul;16(9):1126-8.

75.   Henkemeyer M, Rossi DJ, Holmyard DP, Puri MC, Mbamalu G, Harpal K, Shih TS, Jacks T, Pawson T. Vascular system defects and neuronal apoptosis in mice lacking ras GTPase-activating protein. Nature1995 Oct 26;377(6551):695-701.

76.   Kunath T, Gish G, Lickert H, Jones N, Pawson T, Rossant J. Transgenic RNA interference in ES cell-derived embryos recapitulates a genetic null phenotype. Nat Biotechnol2003 May;21(5):559-61.

77.   Xia G, Kumar SR, Masood R, Zhu S, Reddy R, Krasnoperov V, Quinn DI, Henshall SM, Sutherland RL, Pinski JK, Daneshmand S, Buscarini M, Stein JP, Zhong C, Broek D, Roy-Burman P, Gill PS. EphB4 expression and biological significance in prostate cancer. Cancer Res2005 Jun 1;65(11):4623-32.

78.   Kudo FA, Muto A, Maloney SP, Pimiento JM, Bergaya S, Fitzgerald TN, Westvik TS, Frattini JC, Breuer CK, Cha CH, Nishibe T, Tellides G, Sessa WC, Dardik A. Venous identity is lost but arterial identity is not gained during vein graft adaptation. Arterioscler Thromb Vasc Biol2007 Jul;27(7):1562-71.

Publishing Agreement

It is the policy of the University to encourage the distribution of all theses, dissertations, and manuscripts. Copies of all UCSF theses, dissertations, and manuscripts will be routed to the library via the Graduate Division. The library will make all theses, dissertations, and manuscripts accessible to the public and will preserve these to the best of their abilities, in perpetuity.

Please sign the following statement:

I hereby grant permission to the Graduate Division of the University of California, San Francisco to release copies of my thesis, dissertation, or manuscript to the Campus Library to provide access and preservation, in whole or in part, in perpetuity.

_____
Author Signature

_1/11/2011_
Date